Zeitschrift: IABSE reports of the working commissions = Rapports des commissions de travail AIPC = IVBH Berichte der Arbeitskommissionen

Band: 6 (1970)

Rubrik: Prepared discussion

II

Effect of Aggregate Properties on the Strength and Deformation of Concrete

L'influence des caractéristiques des agrégats sur la résistance à la compression et à la déformation du béton

Der Einfluß der Eigenschaften der Zuschlagstoffe auf die Druckfestigkeit und die Formänderung des Betons

PICHAI NIMITYONGSKUL R.B.L. SMITH
Asian Institute of Technology
Thailand

Introduction

The effect of aggregate properties on the strength and deformation of concrete is of particular importance in prestressed concrete, since it influences the ultimate flexural capacity, the loss of prestress, and the camber and deflection of members. It also has implications for continuous reinforced concrete structures as it affects the distribution of moments and the rotation capacity of members. Previous work by Troxell, Raphael and Davis[1], Kaplan[2], and Kordina[3] has investigated the effect of aggregate properties on deformation and strength independently. In this study a direct comparison is made, the influence on workability is taken into account, and comparative tests of prestressed concrete beams are reported.

Details of Investigations

a) In the first series[4,5], compressive strength and sustained loading tests were carried out on concrete made from four types of aggregate available in Thailand. These were limestone, sandstone, andesite, and gravel. The selection was based on availability in Thailand, extent of use and uniformity of supply. Natural river sand was used as fine aggregate and the cement was Type I Normal Portland (Elephant Brand) manufactured by the Siam Cement Co. The mix proportions by weight for all specimens were: water-cement ratio 0.5; aggregate-cement ratio 4.0; sand-aggregate ratio 2/3. In order to allow a precise determination of the water content of the mixes, the aggregate was used throughout these tests in an initially dry condition. Nine 150 x 300 mm. cylinders of each mix were tested at 28 days for compressive strength. In the creep tests, 100 x 300 mm. cylinder specimens were loaded at an age of 40 days over a period of 40 days at stresses of 6.9 and 13.8 N/mm^2 under conditions of 21°C and 70% R.H. Deformations were measured along three 200 mm. gauge lengths at 120° about the axis by means of a Demec gauge. The results of these tests are summarised in Table I and Fig. 1.

Table I

Type of Aggregate	Source	Density of Concrete (gm/cc)	Cylinder Strength (N/mm^2)	Aggregate Absorption Capacity (%)	Slump* (mm)
Limestone	Rajburi	2.40	35.1	0.63	89
Sandstone	Korat	2.32	39.2	4.52	13
Andesite	Saraburi	2.42	37.6	1.46	76
Gravel	Rajburi	2.37	34.1	1.33	200

*Measured on Standard 300 mm. slump cone.

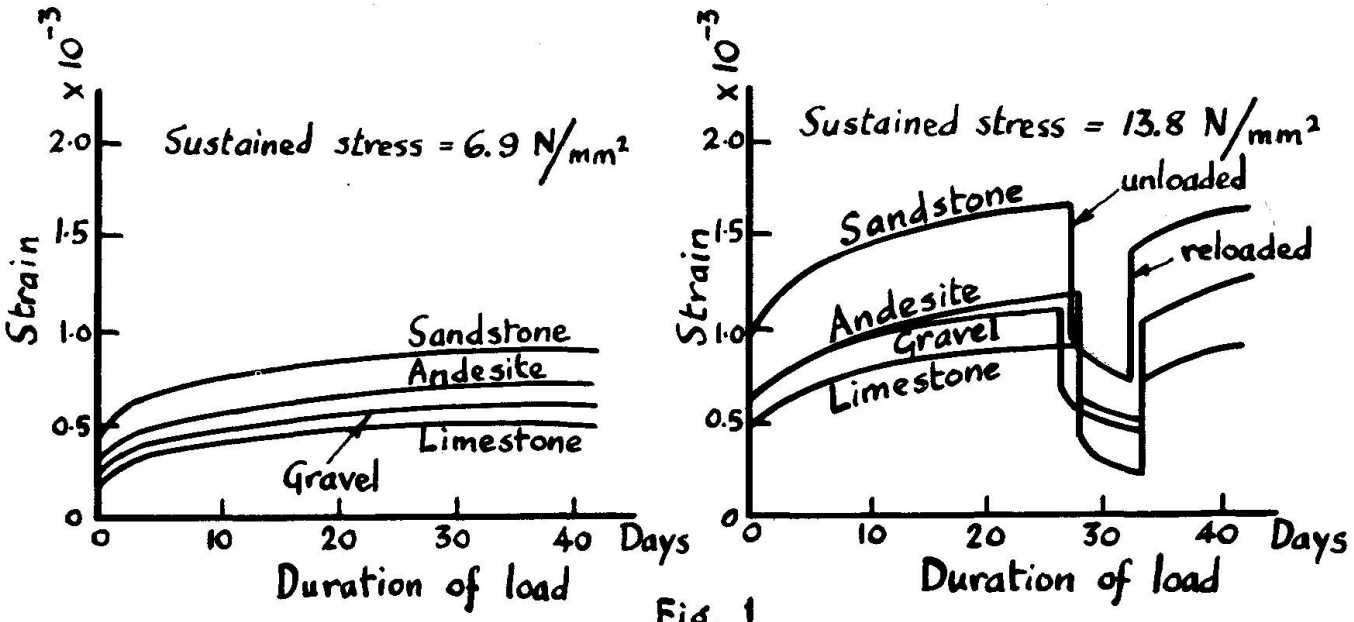

Fig. 1

b) The remaining tests were concerned with the two aggregates giving the most marked contrast in the first series, i.e. limestone and sandstone. As a preliminary, mixes of aggregate ratio as before but with four different water cement ratios were prepared using the above two aggregates, and the resulting workability and compressive strength at 7 days were investigated as given in Table II. From these tests the effect of the high absorption capacity of the sandstone is evident in reducing the effective water-cement ratio of the matrix, with consequent increase of strength and reduction of workability. From this work it was possible to design mixes for the second series of relative strength and deformation tests which had the same workability and mix proportions for limestone and sandstone aggregates but differing water-cement ratios to allow for this.

c) The second series of tests was carried out in a similar manner to that in a), except that only limestone and sandstone aggregates were used, with water-cement ratios of 0.375 and 0.475 respectively, and four different stress levels were used for the creep tests. The compression tests and the start of the sustained load tests were at an age of 7 days. The results are summarised in Table III and Fig. 2.

Table II

W/C	Aggregate	Slump	Compacting Factor	VB secs.	Density gm/cc	Comp.strength $N/_{mm^2}$
0.50	Limestone	89	0.965	2	2.44	31.5
	Sandstone	13	0.827	7	2.29	33.2
0.40	Limestone	70	0.950	3	2.46	36.5
	Sandstone	8	0.824	8	2.32	37.3
0.35	Limestone	0	0.750	12	2.47	47.2
	Sandstone	0	0.694	75	2.33	48.9
0.325	Limestone	0	0.700	30	2.49	40.8
	Sandstone	0	0.684	180	2.22	19.5

Table III

Type of Aggregate	Density of Concrete (gm/cc)	Cylinder Strength (N/mm^2)	Compacting Factor	VB secs.	Aggregate Absorption Capacity (%)	Specific Gravity
Limestone	2.45	39.8	0.73	10	0.80	2.65
Sandstone	2.32	43.0	0.73	10	4.38	2.275

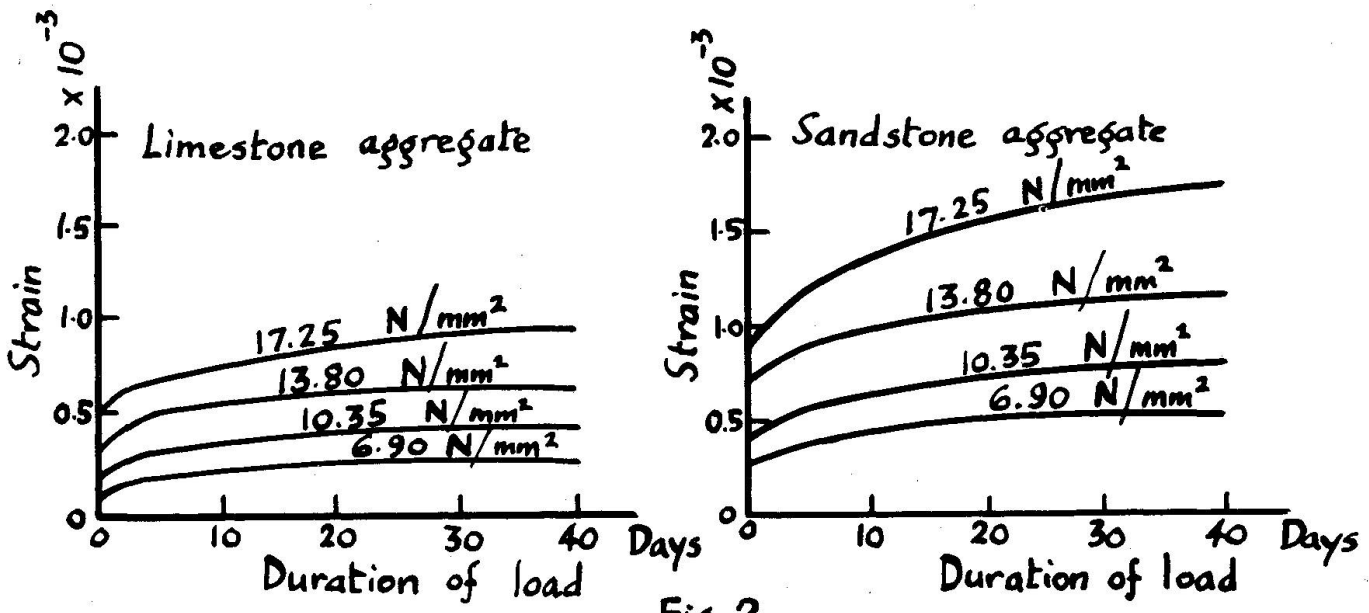

Fig. 2

d) In addition, six pretensioned concrete beams of which three contained limestone, and three sandstone, aggregates were tested for camber and ultimate flexural capacity. The beams were cast in long-line pairs so that initial prestress was identical for the members of each pair. Prestress was transferred at 7 days, and the camber was measured for 3 days before loading test. The cross-section of the beams was 127 x 178 mm; overall length 3 m. The prestressing force was applied by nine 5 mm indented wires, initially stressed to 1100 N/mm^2 whose resultant acted 60 mm from the bottom of the section. The effective span under center point loading was 2.44 m.

A summary of test results is given in Table IV and load deflection curves for the beams are plotted in Fig. 3. For beam pairs 2 and 3, 150 x 300 mm cylinder specimens of the concrete were subjected to compressive strain measurement to failure using Demec reading at 120° as for the creep specimens. The results are shown in Fig. 4.

Table IV

Beam Mark	1L	1S	2L	2S	3L	3S
Concrete Strength at 10 days, N/mm^2	29.0	31.6	29.7	44.2	25.6	40.0
Camber on release, mm	2.3	3.3	1.8	2.8	2.5	3.2
Camber 3 days after release mm	2.5	4.1	2.9	3.6	3.4	4.2
Ultimate center point load, kN	33.4	39.0	31.8	41.6	30.5	40.5
Ultimate moment at failure cross section, M_T, kNm	18.6	20.8	17.8	23.3	17.1	22.6
Calculated ultimate moment* M_u, kNm	18.5	18.9	18.5	21.6	17.1	20.4
Ratio M_T/M_u	1.01	1.10	0.96	1.08	1.00	1.11

*Based on Hognestad et al.[6]

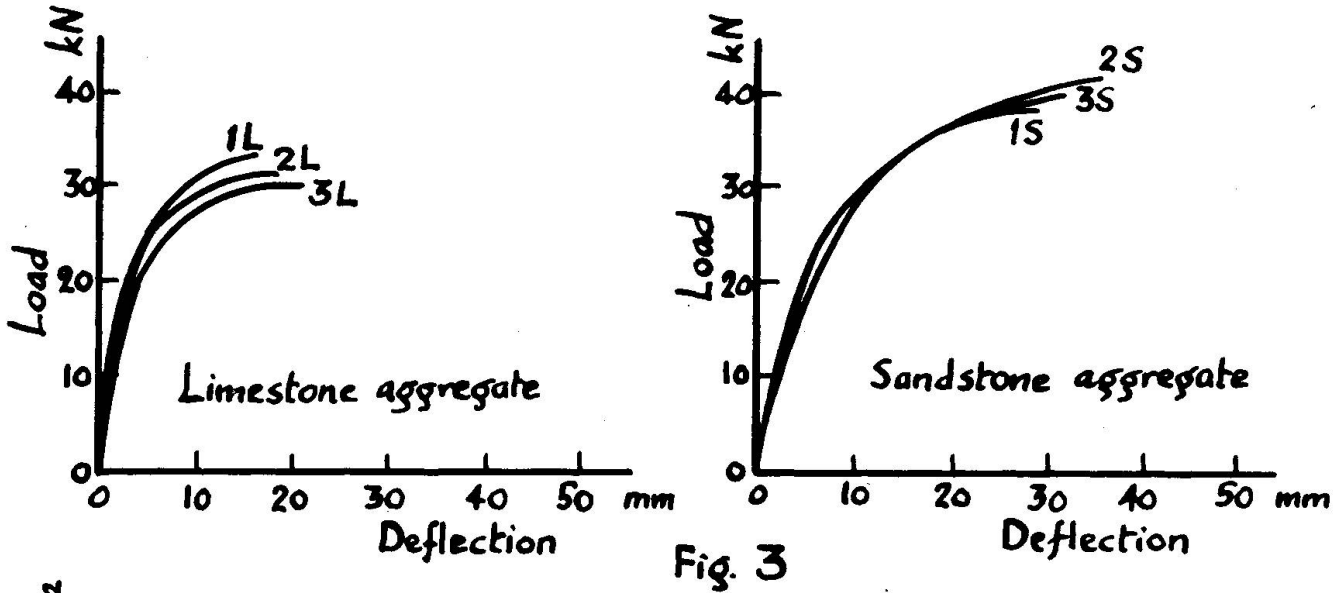

Fig. 3

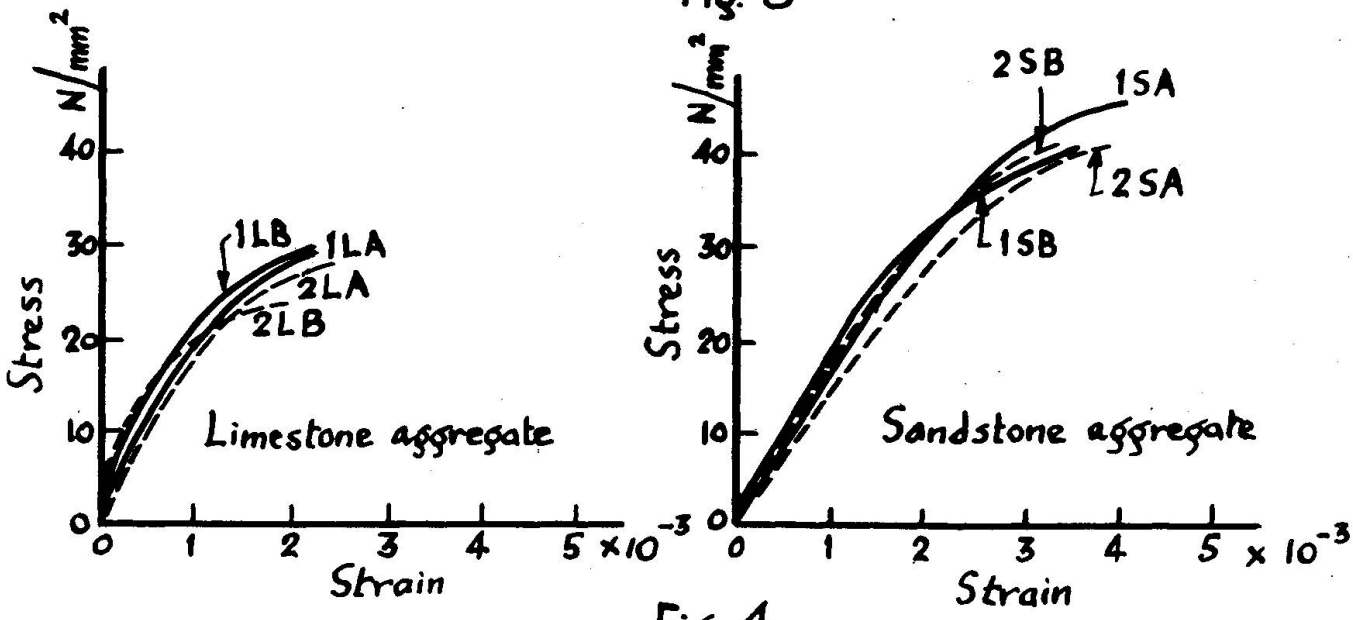

Fig. 4

e) Tests on slender reinforced concrete columns subjected to load eccentric about the major axis, which were performed by Tharasak,[7] included three pairs of specimens in which the effects of limestone and sandstone aggregates were compared. The results for these tests, given in Table V, indicate the reduction in flexural rigidity B_1 about the minor axis, corresponding to the lower effective modulus, for the columns made with sandstone aggregate concrete, although there is little difference in the calculated ultimate load P_u (ignoring the effects of slenderness) based on the concrete compressive strength. All the columns represented in the Table failed by lateral buckling at loads less than P_u and also less than the theoretical buckling load P_{c1}, about the minor axis, calculated from the values given.

Detailed analysis is presented in a report on the complete test series,[8] and it is only intended here to draw attention to the reduced failure loads of the sandstone aggregate columns of series 2 compared with their limestone companions. From this it follows that in the estimation of the strength of structures affected by slenderness, it is not safe to base the effective modulus value on the compressive strength, which was also the case for the camber deflections of the prestressed beams reported above.

Table V

Specimen details: overall length 2.08 m
Cross-section: overall depth 254 mm
" breadth 76 mm (Series 1)
" " 51 mm (Series 2)

Specimen Mark	(Series 1) 11	12	(Series 2) 21	22	23	24
Aggregate type	L	S	L	S	L	S
Concrete Strength (N/mm^2)	30.3	30.4	30.7	28.8	26.2	31.2
Load eccentricity (mm)	203	203	203	203	254	254
Flexural rigidity B_1 ($kNmm^2$)	647	612	169	132	218	172
Calc. buckling load P_{c1} (kN)	592	535	154	121	204	157
Calc. ult. load P_u (kN)	208	209	163	159	130	134
Test load P_t (kN)	182	187	109	91	88	67

Discussion

The following table gives a comparison of the effective moduli for short and long term loading from tests (a) and (c) with the values proposed by some design codes of practice. The values E_i are based on the instantaneous deformation under the stress level of 13.8 N/mm^2, and E_t on the creep (i.e., total deformation minus shrinkage) at 28 days after commencement of test. The draft British Standard Code[9] and the new ACI proposals[10,11] give good agreement with the results for limestone aggregate concrete, but for other aggregates, particularly sandstone, the test results give substantially lower effective moduli values, whilst the calculated values are marginally increased or unchanged. Both codes refer to the possibility that certain types of aggregates may give deformations greater than predicted by the formulae without giving any specific guidance. It is hoped that this paper will be regarded as providing some data, but further evidence is required to enable a more comprehensive equation to be developed.

Test	Aggregate	Test Results		B.S. Code 1959		ACI 318-63 Proposed Revision 1970		CP 115 1959
		E_i kN/mm^2	E_t kN/mm^2	E_c kN/mm^2	E_{ct} kN/mm^2	E_c kN/mm^2	E_{ct} kN/mm^2	E_c kN/mm^2
Ser. I	Limestone	29.3	11.9	29.8	7.9	29.8	11.9	36.0
	Sandstone	16.4	7.0	31.5	8.3	30.0	12.0	38.2
	Andesite	23.4	9.3	30.8	8.1	31.6	12.6	37.4
	Gravel	22.6	9.6	29.5	7.8	28.8	11.5	35.2
Ser.II	Limestone	36.0	18.2	31.8	9.1	32.9	13.2	38.6
	Sandstone	19.4	11.5	33.0	11.0	31.5	12.6	40.6

In the tests of prestressed concrete beams, the relative cambers and deflections are as expected, and the high ultimate load of the sandstone aggregate beam is caused not only by the concrete strength but more significantly by its high ultimate strain capacity. This has important implications in the study of moment-rotation capacity of continuous structures and in stability problems as in the test of reinforced concrete slender columns.

REFERENCES

1. Troxell, G.E., Raphael, J.M., and Davis, R.E., "Long-Time Creep and Shrinkage of Plain and Reinforced Concrete," Proceedings, ASTM, pp. 1101-1120, 1958.

2. Kaplan, M.F., "Flexural and Compressive Strength of Concrete as Affected by the Properties of Coarse Aggregate," Proceedings ACI, v. 55, pp. 1193-1207, 1959.

3. Kordina, K., "Experiments on the Influence of the Mineralogical Character of Aggregate on the Creep of Concrete," Rilem Bulletin, no. 6, pp. 7-22, 1960.

4. Nimityongskul, P., "Effect of Aggregate Properties on the Elasticity and Creep of Concrete," Thesis No. 271, Asian Institute of Technology, 1969.

5. Nimityongskul, P. and Smith, R.B.L., "Effect of Aggregate Properties on the Relative Strength, Elasticity, and Creep of Concrete," IABSE Seminar on Problems of Prestressing, Madras, India, January 1970.

6. Hognestad, Hansen, and McHenry, "Concrete Stress Distribution in Ultimate Strength Design," ACI Journal, December 1955.

7. Tharasak, Pramoth, "Lateral Instability of Reinforced Concrete Columns Under Combined Bending and Axial Load," Thesis No. 304, Asian Institute of Technology, 1970.

8. Tharasak, Pramoth and Smith, R.B.L. "Lateral instability of slender reinforced concrete columns under combined bending moment and axial force." Paper submitted for publication.

9. British Standards Institution, "Draft BS Code of Practice for the Structural Use of Concrete," 1969.

10. Proposed Revision of ACI 318-63, "Building Code Requirements for Reinforced Concrete," ACI Journal, 1970.

11. ACI Committee 435, "Deflections of Reinforced Concrete Flexural Members," Proceedings, ACI, v. 63, pp. 637 - 662, 1966.

SUMMARY

The effect of variation in the physical properties of coarse aggregate between commonly used types as exemplified by limestone, sandstone and others, on the compressive strength and deformation of concrete under sustained loading, was

studied (a) by keeping all other quantities constant and (b) by adjustment of the water-cement ratio to give constant workability. The results are of significance in the design of prestressed concrete and of continuous beams and slender compression members in reinforced concrete.

RESUME

On a étudié l'influence des propriétés physiques des agrégats de grandes dimensions par rapport aux agrégats couramment utilisés (p. ex. le calcaire ou le grès) sur la résistance à la compression et sur les déformations du béton soumis à une charge constante, (a) sans varier les autres proportions, (b) en adaptant le rapport eau-ciment pour obtenir la consistence habituelle. Ces résultats sont importants pour le calcul du béton précontraint, des poutres continues et des colonnes élancées comprimées en béton armé.

ZUSAMMENFASSUNG

Der Einfluss der Veränderung der physikalischen Eigenschaften der Zuschlagstoffe zwischen gewöhnlichen Sorten (zum Beispiel Kalkstein und Sandstein) auf die Druckfestigkeit und die Formänderung des Betons unter ständiger Belastung wurde untersucht: (a) durch Konstanthalten aller anderen Mengenverhältnisse und (b) durch Berichtigung des Wasserzementfaktors. Die Ergebnisse sind wichtig für die Berechnung des Vorspannbetons und der durchlaufenden Balken sowie der schlanken Säulen aus Stahlbeton.

II

Prestressing of Edge Members in Long Buildings to Restrain Shrinkage, Creep and Temperature Changes

Précontrainte des poutres latérales des bâtiments de grande dimensions, pour réduire les effets du retrait, du fluage et de la température

Vorspannung von Randbalken in langen Gebäuden, um Schwinden, Kriechen und Temperaturspannungen entgegen zu wirken

JAN BOBROWSKI PAUL W. ABELES
Senior Partner and Consultant respectively of
Jan Bobrowski and Partners,
Consulting Engineers
London

1. GENERAL CONSIDERATIONS

It is well known that temperature changes, shrinkage and creep greatly affect cracking of long reinforced concrete buildings. The development of such cracks cannot be completely excluded without prestressing, though it can be minimised when contraction and expansion joints are provided. This may be further improved by the provision of rigid columns suitably spaced and heavy reinforcement so that all theoretical secondary stresses are taken up by the frame construction. Obviously, even in such a case the development of fine cracks cannot be avoided altogether in non-prestressed constructions, although Rogers[1] claims that "after nine years of operation the structure is virtually crackless". This relates to a bakery at which very large temperature variations apply, and for a length of 520 ft. (158.5 m.) no joints were provided except for the roof. Temperature variations of $\pm$ 60°F ($\pm$ 33°C) were considered in addition to a temperature drop of 15°F (8.4°C) which had to be taken up by the stiffness of the framework, the bending moments of the columns being increased by 200%. As already stated, it is quite impossible to obtain a completely crackless reinforced concrete construction in spite of heavy reinforcement, as the development of fine hair cracks cannot be prevented except by the provision of an effective prestress. The avoidance of cracking becomes more important when precast outer surfaces (usually exposed, even polished) are used which badly show any cracking.

The first mentioned author designed in 1957[2] a construction at which 80 m (240 ft.) long edge beams of a six-storey building were to be prestressed. This related to single-bay composite floors containing precast prestressed beams. Although the thickness of the in-situ concrete was reduced to a minimum it formed in each floor together with the beams and edge members a large monolithic area over the entire building without interior columns and without any expansion or construction joints. The main purpose of prestressing was to avoid cracking. Particulars are described in Section 2.

The magnitude of the prestressing force to offset such tensile stresses which would cause visible cracking would be very large if the losses due to the rigidity of long buildings were fully taken into account. This would be greatly reduced if the prestressing of edge beams could be carried out at the cold period after which only a small further contraction would apply. This is, how-

ever, normally impracticable. In practice, the most unfavourable conditions must be taken into account. If e.g. a temperature difference of $\pm$ 27° (15°C) is considered together with an equal amount of shrinkage, this would amount to a contraction, corresponding to a compressive strain of 30 x 10^{-5}, if a temperature strain of 10^{-5} per 1°C temperature difference is taken into account. For a modulus of elasticity of E_c = 4.5 x 10^6 psi (3.5 x 10^5 kp/cm^2)*, a tensile stress of 1350 psi (94.5 kp/cm^2) would occur, though heating of the interior introduces further complications. If a tensile stress of, say, 600 psi (42 kp/cm^2) is assumed as permissible to avoid visible cracks, it would still be necessary to ensure an effective precompression of 750 psi (52.5 kp/cm^2). However, a considerably larger prestressing force would have to be applied at both ends of long edge beams if an effective prestress of the above nature were to be obtained at the centre of the building. The first named author decided on the magnitude of prestress at the first construction, discussed in Section 2, on an arbitrary basis for an average prestress of the edge members of 460 psi (32 kp/cm^2). This has proved quite satisfactory. Appreciable compressive stresses are introduced towards the centre of long outer members at temperature rise, when normal elongation is prevented by the rigidity of the construction and thus it may be assumed that the prestress, effective near the ends, is gradually transferred to the centre.

Leonhardt[3] suggests the provision of a limited prestress and states that an average compressive stress of 5-15 kp/cm^2 (70-210 psi) should be sufficient. However, even for such an insignificant minimum effective prestress appreciable prestressing forces would have to be applied at the ends to overcome the losses due to rigidity. In the example shown by Leonhardt, it would be interesting to know how large a prestressing force had to be applied at the ends to overcome the friction of the 71 m (232 ft) long wall (fig. 3)

Obviously the provision of a partially prestressed construction is quite satisfactory, either according to Class 2 of FIP-CEB at which visible cracks do not occur (e.g. with a permissible tensile stress as mentioned before); or a construction according to type (ii), as described by the second author in 1950[4] and at the 8th AIBS Congress 1968[5], which was also included in the "First Report on Prestressed Concrete" of the Institution of Structural Engineers 1951. This type (ii) (which unfortunately has been completely ignored in the FIP-CEB classification) presents a fully prestressed construction under normal loading with the possibility that fine hair cracks may develop occasionally under temporary extreme loading; this applies in the present circumstances to severe frost. These cracks would, however, be completely closed under ordinary conditions.

The experience with the first buildings (see Section 2) was very satisfactory in as much as cracks were not noticed and a contraction at the ends of the building of a magnitude of $\frac{1}{2}$ in. (12.5 mm) was noticed when the building was not heated in winter. This indicates that the prestressing force was overcoming the rigidity of the framework. The firm of Consulting Engineers, Jan Bobrowski and Partners, has continued with the provision of prestressing edge beams of long multi-storey buildings. In order to ascertain this, it was considered important to carry out strain measurements. This was first done at a parking garage in Bristol[6] at which photo-elastic stress meters were embedded in the concrete (see Section 3). In another parking garage in Reading the longitudinal non-prestressed, central beam was interrupted by transverse ramps, and in the roof transverse cracks developed which stopped at a distance of about 6 ft. (1.8 m) from the prestressed edge beams, as described in Section 4. Cracking was avoided altogether at another garage in Reading at which also the longitudinal centre beams were prestressed. In another building, at present under construction (Section 5), vibrating wire strain gauges are being embedded in the concrete which should enable the authors to study the gradual develop-

* The stresses are given in psi (lbf/in^2) and in kp/cm^2 (kgf/cm^2) rather than in N/mm^2 which fortunately has not yet been introduced internationally.

ment of prestress in the edge beams and the influences of temperature changes; there being thermo couples provided which allow the measurements of the temperature inside the concrete. It is hoped that a more detailed report after temperature movement during the two coming winters can be presented at the Amsterdam Congress 1972.

Finally it is pointed out that the design should allow great flexibility in longitudinal direction while still ensuring full stability of the building. Such a solution has been embodied in a design for a proposed building at which some of the rigid corner supports are on rollers.

2. WATSON HOUSE, FULHAM, LONDON

As described in paper[2], there are two 6-storey wings (see cross-section Fig. 1), 15 m (51 ft) wide and 30 m (96 ft) high. The 0.6 m (2 ft) deep floors are of composite design, comprising precast pretensioned beams spanning the entire width and an in-situ concrete topping placed on prefabricated concrete shuttering between them. The edge members in each floor (detail A of Fig. 1, as seen in Fig. 2) were prestressed. They are of composite nature, the lower part being precast with pretensioned tendons, the upper part cast in-situ at the same time as the topping to the main floor deck. The precast part which carries the dead weight of the floor contains a chase in which one of the two 19-wire strands 1 1/8 in. (28.7 mm) dia. was placed, the other being located in a duct of the upper part. The minimum breaking force of these was 362 x 10^3 lbs (162 x 10^3 kp) the initial prestressing force being 70% of this value and an average effective force of 60% (allowing 40% losses) has been considered, resulting in an average effective prestress of 460 psi (32 kp/cm^2), as indicated in Fig. 3, which shows the various stress conditions. Slender reinforced concrete columns supported the beams. Though this design was only experimental it has proved to be quite satisfactory and, as already stated, shortening of approximately 1/2 in. (12.2 mm) occurred at each end over a length of 80 m (260 ft). This would correspond to a temperature reduction (including shrinkage) of 33°C (59°F).

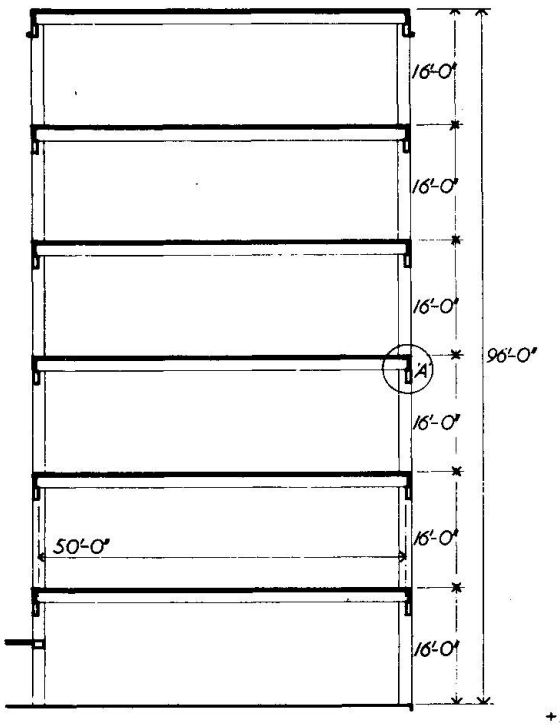

CROSS SECTION OF WATSON HOUSE.

FIG. 1

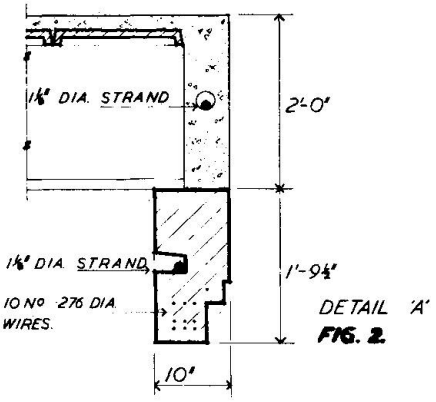

DETAIL 'A'

FIG. 2.

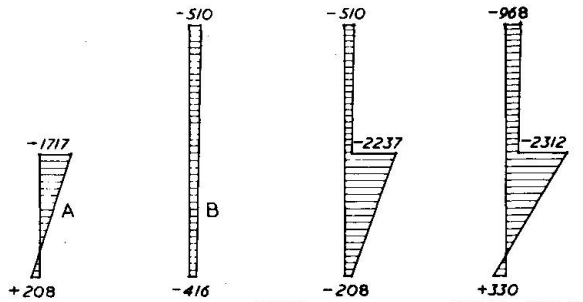

FIG. 3

3. CAR PARK AT THE UNICORN HOTEL, BRISTOL

This and the following two car parks, described in Section 4, are based on similar designs inasmuch as precast structural diamond frame wall units formed the outer walls, whereas precast reinforced concrete frames were used for the central spines, the first two car parks containing one central spine and the third car park having two such constructions. In each case long span, composite floors were used similar to the building described before. This is, in the author's view, advantageous from the production point of view because of the reduced number of columns and it is often also more economical. The composite floors were propped in all the designs, which with inverted T units greatly improves the economy.

Fig. 4 shows the elevation of the car park adjacent to the Unicorn Hotel, Bristol. The main element in the external walls is the precast "double diamond" unit, mentioned before, which incorporated an integral ring beam, as indicated in Fig. 5. Each upper ring beam contains five post-tensioned tendons of 1 1/8 in. (28.5 mm) dia. At the first floor level there are six such tendons provided. Each of the tendons was tensioned to 70% of its strength. The precast "double diamond" units have steel shoes with locating studs, which were removed before stressing. There was little friction at prestressing since the steel shoes were lubricated with graphite and only afterwards connected by welding. Finally they were protected by a 1 in. (25.4 mm) thick layer of Pyrok (a cementitious gypsum mixture). A relatively high prestress was introduced in the precast concrete, since prestressing was carried out, before the in-situ concrete was added.

The floor construction, already described, is seen in Fig. 7. External support at ground level is obtained by five V-shaped members 40 ft. (12 m)

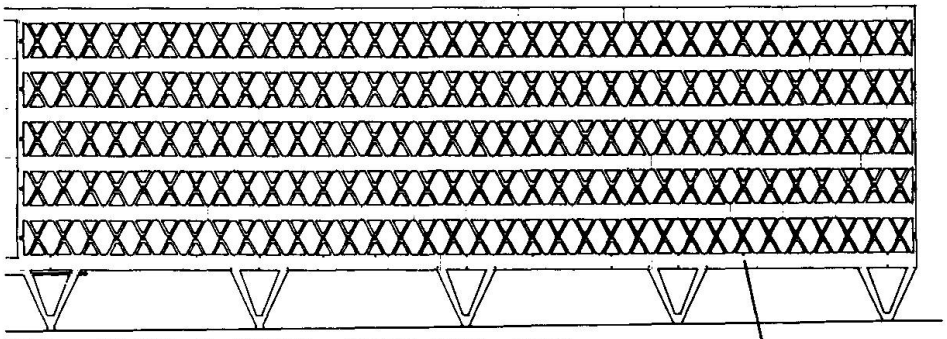

FIG. 4. ELEVATION OF CARPARK – UNICORN HOTEL, BRISTOL

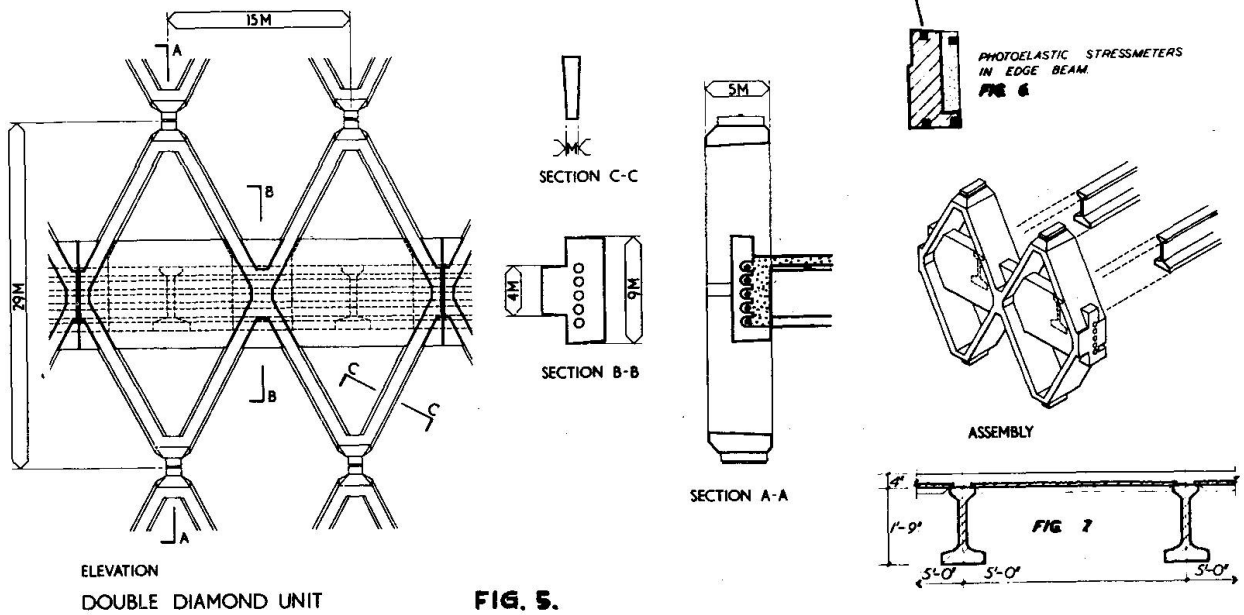

ELEVATION
DOUBLE DIAMOND UNIT

FIG. 5.

apart each carrying approximately 1,700,000 lbf (770,000 kgf); each arm containing three tendons of 12 wires 0.276 in. (7 mm) dia., anchored in the foundation pile cap and carried through the first floor ring beam. Post-tensioning of these V-shaped supports was carried out after completion of the first floor. All external structural elements are of white concrete with Capstone aggregate.

This system is highly statically indeterminate and was designed by the first named author by analogy to rigid walls and anchorage zones which allowed dimensioning of the "double diamond" element. It was subsequently checked by Professor Z.S. Makowski and Professor J.R. Hussey, who developed a computer programme based on statical indeterminacy of 362, as stated in paper[6], requiring 990 simultaneous equations. The building was self supporting during erection, and each stage was analysed separately.

In view of the complexity of the design it was decided to check the actual stresses by means of photo-elastic stress meters. These are bi-axial glass gauges which, when bonded to the material subsequently subjected to stress, allow the magnitude and directions of the applied principal strains to be obtained from photo-elastic fringe patterns visible on the gauge if it is observed with polarised light. Fifty such stress meters, produced by Horstman Ltd., Bath, England, were embedded in diagonal and horizontal precast concrete and in-situ concrete members at first and second floor levels and two at the bases of "V-shaped" columns. Principal particulars of positioning are shown in Fig. 6. This construction was built in 1965 and the stresses were assessed for the fully erected building under dead load only, based on the strains from the photo-elastic cylindrical plugs. The stresses obtained for the bases of the "V-columns" agreed very well with the calculated values. Most of the compressive stresses, obtained from the stress-plugs inserted in precast concrete, are in some agreement with the calculated stresses. Some are as close as 94% of the calculated values, others fall down to 60%, whereas in two cases the difference is even greater. This seems to indicate that there were secondary stresses and/or friction influences at prestressing, in spite of the provision of sliding. Most of the stress plugs inserted in the in-situ concrete did not function satisfactorily, probably in consequence of imperfect bond. A number of plugs did either not work at all or gave unreliable results particularly when in tension. It is claimed by the manufacturer of the stress plugs that, in the meantime, improvements have been made which should give better results in future.

In March and August 1970 further strain measurements were made. The temperature in March was + 42°F (+5.5°C) and in August + 68°F (20°C) respectively. A number of stress meters indicated variations in the stress level at several points along the length of the girder, relevant to the ambient temperature of concrete.

Generally the stress meters located in the compressive zone of the beam, near the supports, reflected the restrained expansion of the girder by the definite increase in the compressive stress.

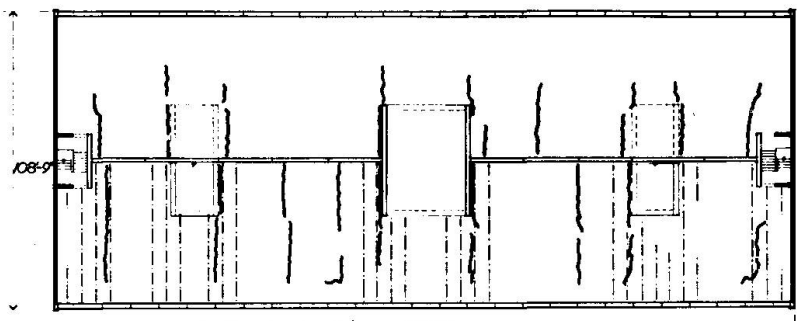

FIG. 8.

4. CAR PARK, YIELD HALL, READING

The construction of this car park is similar to that in Bristol, except that instead of the V-shaped columns, single columns were provided at 5 ft. (1.50 m) centres. Moreover, in this two-bay building of similar width to the Bristol design, the arrangement of the ramps was different and the centre spine beam was interrupted. As already stated in Section 1, transverse cracks developed in the roof construction, as indicated in Fig. 8. These cracks extended across the building and terminated at a distance of about 6 ft. (1.8 m) from the prestressed edge beams. This clearly shows the efficacy of prestressing of the selected construction. The car park was completed in 1966.

Based on this experience the centre beams of a second car park in Reading, having three bays, were prestressed. Otherwise, the construction is in principle the same. This building, which was completed in 1968, does not show any transverse cracks.

5. OFFICE BUILDING, WESTMINSTER, LONDON, 1970

This is a four-storey building, 192 ft. (58 m) long and 108 ft. (32.8 m) wide, as seen in the photograph, Fig. 9, whereas Fig. 10 shows a typical plan. There are two staircases at the ends and the walls enclosing them are provided with sliding joints to facilitate prestressing in longitudinal direction. The external walls are precast, and all surfaces have exposed polished concrete. The precast ground floor columns have cantilevers and are 12 ft. (3.6 m) apart. They are separated from each other, as indicated in the picture, Fig. 9. The columns are connected with the upper floors by reinforcement so placed as to give minimum stiffness in longitudinal direction, but appreciable stiffness transversely. The upper floors contain precast load bearing box frames which are connected to the edge beams to achieve a similar effect to that at first floor. The floor construction is similar to that of the previous buildings with the difference that the prestressed beams of 21 in. (0.53 m) depth are 4 ft. (1.2 m) apart. There are two outer bays of approximately 50 ft. (15 m) span. Along the spine, precast reinforced concrete H-frames are provided 20 ft. (6 m) apart. Cross-section of the edge beams are seen in Fig. 11: "A" refers to a normal case at which the in-situ slab is connected with the edge beam. It contains two tendons, each of them comprising two cable of four No. 0.6 in. (15.3 mm) dia. strands. Section "C" refers to a part adjacent to the staircase (where a strain gauge has been placed) without slab, whereas the horizontal Section "B" indicates that the joints between adjacent precast parts remains open for 6 in. (15 mm), which means that the prestress at the joints is greater than within the edge beam of relatively large section. This design had been completed before the car parks at Reading became operational, however, it was still possible to incorporate the post-tensioning of the transverse edge beams in full appreciation of its advantages clearly demonstrated in these car parks described in the preceding section.

Since such a design is very complex with regard to determining the inherent rigidity, causing loss of prestressing, more reliable strain measurements were introduced to investigate the development of the prestress in the various edge beams and to study the effects of temperature changes.

Vibrating strain gauges were embedded in the edge beams; generally, three gauges were provided at each edge beam (one approximately at the centre and one each about 20 ft. away from the ends). At the roof two more strain gauges are being provided at the two longitudinal edge beams at intermediate positions. These gauges were developed by the Building Research Station and are manufactured by Deakin Instrumentation Ltd., Walton-on-Thames. The type is a pretensioned transducer and allows measurements of internal slowly varying strains (e.g. due to temperature change) in the concrete. The gauges and the measuring equipment, including that for determining the internal temperatures by means of thermo couples, were provided by the Building Research Station, which is co-

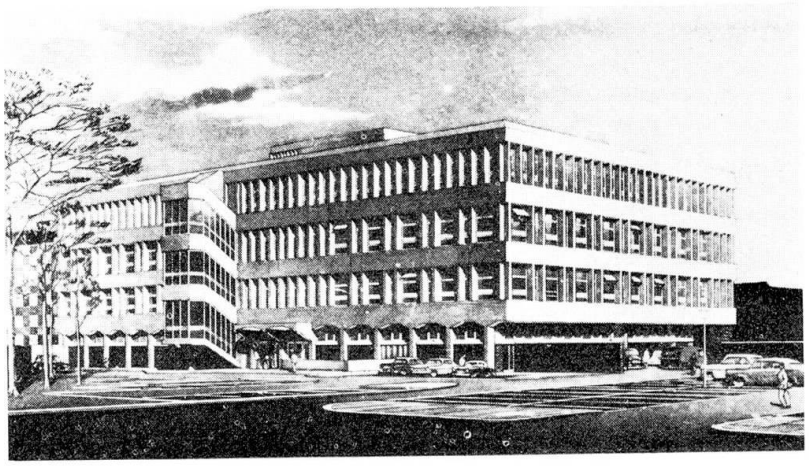

FIG·9

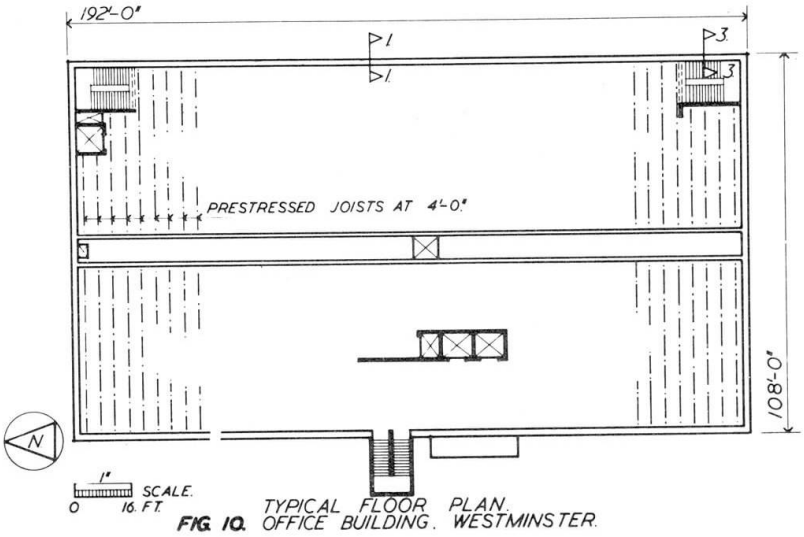

FIG. 10. TYPICAL FLOOR PLAN. OFFICE BUILDING. WESTMINSTER.

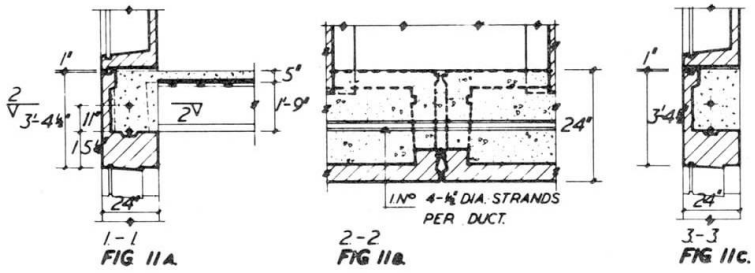

FIG 11A FIG 11B FIG 11C.

operating in these investigations, and the assistance of Mr D.W. Bryden-Smith is gratefully acknowledged.

At the time of writing this paper, a limited number of measurements only have been made: however, they have already revealed some interesting results. For example, in the east facade edge beam of the ground floor, the gauges at 21 ft distance from the ends showed after prestressing compressive strains of 26 x 10^{-6} and 41 x 10^{-6} respectively, whereas near the centre the strain was only 15 x 10^{-6}. The difference near the two ends can be explained by the fact that the second strain relates to a rectangular section ("C" in Fig. 11) whereas at the first ("A" in Fig. 11) the slab of the floor co-operates and takes up a part of the prestress. These strains would correspond to respective stresses of 117 and 184 psi (i.e. 8 and 12.9 kp/cm^2) at the ends and 67 psi (4.7 kp/cm^2) at the centre for E_{83} = 4.5 x 10^6 psi (315 x 10^3 kp/cm^2). The nominal compressive stresses for the entire cross section of the longitudinal edge beams was at prestressing 270 psi (19 kp/cm^2) at the ends. It should be noted that the edge beams carrying the ground floor were propped at the time which must have contributed to the losses, and it will be interesting to ascertain the changes after removal of the props, and of course proper allowance will also have to be made for proportion of prestress taken by heavy reinforcing bars in the first floor beams which is particularly concentrated towards the corners of the building. A later measurement at higher temperature shows an appreciable increase in the compressive strain at the centre, elongation being hindered by columns.

6. CONCLUSIONS

Experience described in the foregoing, has shown that the development of cracks in long multi-storey buildings without expansion and/or contraction joints can be satisfactorily controlled by prestressing. This is preferably applied to longitudinal edge beams and, in wide buildings, to longitudinal spine beams and transverse edge beams. Provisions should be made to allow con-

traction of the beams during prestressing to ensure compatibility between design assumption and actual behaviour of the building construction. The maximum advantages are possible if only precast parts of edge beams are prestressed, as in the car parks described above, before in-situ concrete is added. Moreover, if the precast edge beams are made of lightweight concrete their efficiency could be almost doubled in view of its lower Young's Modulus, thus using to advantage what is normally regarded as an inherent drawback of lightweight concrete.

REFERENCES

1. P. Rogers: "Temperature Changes on Reinforced Frame of Bakery Structure", Presented at the 1970 Annual Convention, ACI, New York, April 11-17.
2. A. J. Leggett and J. Bobrowski: "New Premises for the North Thames Gas Board, Fulham", Paper No. 6486, Proc. Inst. of Civ. Eng., Vol. 20, September 1961, pp. 85-106.
3. F. Leonhardt: "Konstruktive Massnahmen zur Verringerung schädlicher Einflüsse von Kriechen, Schwinden und Temperature", IABSE Symposium Madrid, 1970, p. 148.
4. P. W. Abeles: "Further Notes on Principles and Design of Prestressed Concrete", Civ. Eng. & Publ. Works, Vol. 45, July and Oct. 1950, pp. 443-445, pp. 657-662.
5. P. W. Abeles: "The Practical Application of Partial Prestressing", IABSE, 8th Congress, New York, Prepared Discussion IVb, pp. 913-924.
6. J. Bobrowski, J.S. Bernatek and B.K. Bardhan-Roy: "Use of Photo-elastic Stressmeters in the Unicorn Hotel Car Park, Prince Street, Bristol, to be published.

SUMMARY

In this paper the advantage of prestressing edge beams of long multistorey buildings are discussed so as to avoid cracking due to contraction. This includes description of five examples. Specific considerations are necessary at the design stage to permit longitudinal deformation at prestressing in order to reduce the losses of prestress due to rigidity of the building. Strain measurements at two of the buildings are briefly described, which are necessary to clarify the great complexity of the problem.

ZUSAMMENFASSUNG

In dem vorliegenden Artikel werden die Vorteile von Vorspannung langer Randbalken in mehrstöckigen Gebäuden, um Rissbildung infolge Verkürzung zu verhindern, diskutiert und 5 Beispiele beschrieben. Besondere Ueberlegungen beim Entwurf sind nötig, um Verluste der Vorspannkraft infolge der Steifheit der Konstruktion zu verhindern. Dehnungsmessungen an zwei der Gebäude werden kurz beschrieben, die nötig sind, um die Kompliziertheit des Problems klarzulegen.

RESUME

On expose dans le présent article les avantages de la précontrainte des poutres latérales dans les bâtiments à plusieurs étages, dans le but d'éviter la formation des fissures dues à la contraction. On décrit ensuite 5 exemples. Certaines considérations sont nécessaires au stade du projet, afin de permettre les déformations longitudinales provoquées par la précontrainte, qui doivent réduire les pertes dues à la rigidité de la structure. On présente rapidement les mesures d'allongement sur deux des bâtiments, ceci pour essayer de clarifier ce problème complexe.

II

Strength Characteristics of Reinforced Concrete Columns under Sustained Loading

Influence d'un effort permanent sur la résistance des colonnes en béton armé

Tragfähigkeitseigenschaften von Stahlbeton-Stützen unter Dauerlast

JOSTEIN HELLESLAND ROGER GREEN
The University of Waterloo
Canada

1. Introduction

The problem of creep instability of eccentrically loaded reinforced concrete columns become increasingly important with the use of more slender columns in building and bridge structures. Most of the available analytical (usually qualitative only) and experimental studies are aimed at determining the maximum load a column can sustain for an indefinite period of time. Less attention has been paid to the equally important problem of the influence of a sustained loading period on the residual strength or load carrying capacity (P_{u2}, Fig. 1) as obtained in a short time test following a sustained load period. Some experimental and analytical results pertaining to this problem are available [1, 2, 3, 4, 5, 8].

The present study is analytical and was undertaken to gain further insight into strength characteristics of columns under sustained loading (Fig. 1) and hopefully to provide a basis for rational design procedures for reinforced concrete columns under such load actions. The columns considered are unrestrained and loaded at constant end eccentricities (Fig. 2). The cross section is rectangular and symmetrically reinforced (Fig. 3). Further, only bending in one plane is considered.

2. Analysis

2.1 General

Only the main features of the rather involved rheological model and the analytical procedure employed are outlined in the following. More detailed information is available elsewhere [7].

Concrete is considered to be nonlinear visco-elastic material with time variant material properties, and also exhibiting shrinkage. The instantaneous or shorttime stress strain diagram is approximated by an expomential relationship, Fig. 4, in which unloading and reloading take place along a path given by the 'modulus of elasticity', $E_o = E_o\ (f''_c, \varepsilon_e)$. The effects on modulus of elasticity and concrete strength (f''_c) of hydration (beneficial effects) and of high sustained stresses (detrimental effects, noted previously by Rüsch [9]), are considered through a nondimensional 'strength variation

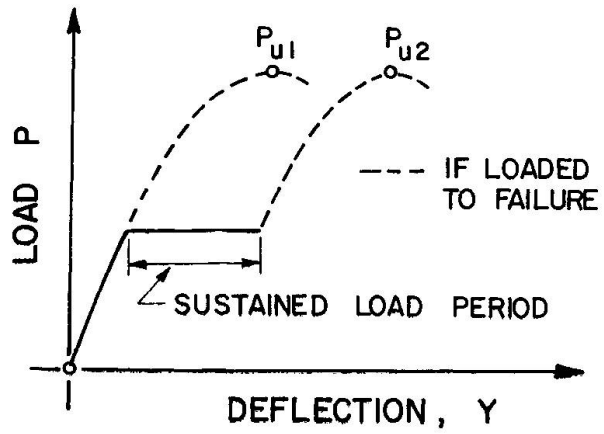

Fig. 1

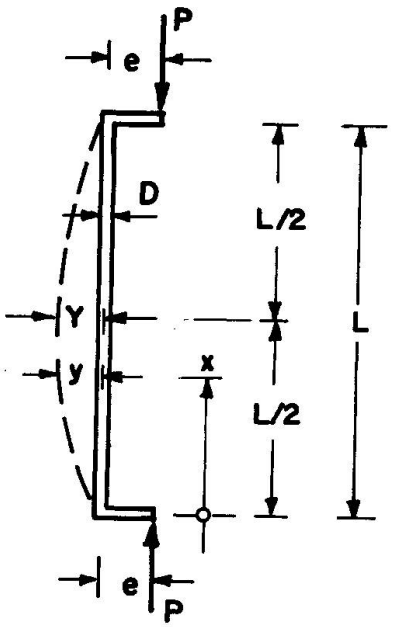

Fig. 2

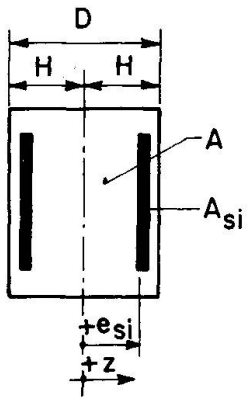

Fig. 3

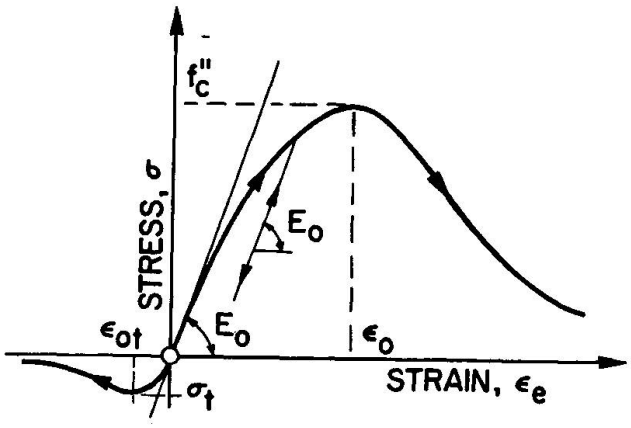

Fig. 4

function', θ. The adverse effects are taken a function of the stress intensity and the time over which the stress is maintained. Only stresses in excess of 70 per cent of the standard short time strength (at the time considered in the stress history) are assumed to have adverse effects on the strength. The strength variation model may be applied to any stress history, constant or variable.

The creep strains are accounted for by associating the specific creep (creep per unit stress as obtained at low stress levels) with a creep non-linearity function, dependent upon stress level and time (through the strength variation θ), and chosen so as to represent the large creep strains at high stress levels and stresses on the descending branch of the stress-strain diagram. Micro cracking beyond that taking place in a standard 2-minute test, is considered a part of the creep strain. The 'rate of creep' method is used to predict creep under variable stresses.

Predictions using the rheological model compare favourably with experimental results [9, 10] of plain concrete in uniform compression.

2.2 Problem Formulation

The equation of state representing the rheological model is (with all arguments deleted for convenience),

$$\dot{\varepsilon} = \dot{\varepsilon}_e + \dot{\varepsilon}_c + \dot{\varepsilon}_{sh} \tag{1}$$

where ε, ε_e, ε_c and ε_{sh} are total, instantaneous, creep and shrinkage strains respectively. Dots indicate differentiation with respect to time.

The equilibrium equations governing the quasi-static problem become

$$\dot{P} = \int_A \dot{\sigma}(z,x,t)dA + \sum_{i=1}^{2} \dot{\sigma}_{si}(x,t)A_{si} \tag{2}$$

$$P\,(y(x,t) + e) + P\dot{y}(x,t) = \int_A \dot{\sigma}(z,x,t)z\ dA + \sum_{i=1}^{2} \dot{\sigma}_{si}(x,t)e_{si}A_{si} \tag{3}$$

Here σ and σ_{si} are the concrete and steel stress respectively, the load rate $\dot{P}$ has a given value and coordinates y, x and z are defined in Figs. 2 and 3. Navier-Bernoulli's hypotheses is assumed for total strains,

$$\phi\ (x,t) = \frac{\dot{\varepsilon}(z,x,t) - \dot{\varepsilon}(z=0,x,t)}{z} \tag{4}$$

where ϕ is the curvature.

Eqs. 1 through 4 are reduced, in a similar fashion previously employed by Mauch [6], to a set of linear equations in discrete stress rates over the column midheight section. They may be written in matrix form as

$$[F]\ [\dot{\sigma}] = [U] \tag{5}$$

Small displacements were assumed ($(y'')^2 \ll 1$) and further no 'slip' in the interface concrete-steel. The integral terms were approximated by Simpson's rule and half a sine wave was assumed for the deflected shape (one point collocation). Eq. 5 was solved, on an IBM 360/75 digital computer, as a propagation problem in time using Euler's extrapolation formulae to yield both the short time and sustained load response. A set of initial conditions were obtained from a static analysis at a small load value. The preloading strains (induced by shrinkage prior to loading) were included in that analysis. Instability, indicated by negative deflection rate, was checked after each propagation step.

Predictions using the analysis compare favourably with experimental results [3, 7].

3. Numerical results

3.1 Input Data

The input data include a concrete strength at initial loading of $f_c'' = 4600$ psi (324 kg/cm^2) at an instantaneous strain $\varepsilon_o = 0.00225$ (Fig. 4). The corresponding values in tension were taken $\sigma_t = 0.05\ f_c''$ and $\varepsilon_{ot} = 0.1\ \varepsilon_o$. The ideally elasto-plastic steel considered had a yield stress of $f_y = 59000$ psi (4150 kg/cm^2) and a modulus of elasticity $E_s = 30.6 \times 10^6$ psi (2.15×10^6 kg/cm^2). The steel is placed at a distance of 0.325D from the centroid. The creep magnitudes chosen yield a creep coefficient (ratio of limiting creep to initial instantaneous strain) of approximately 2.5 at low stress levels.

The complete set of input data for the material laws are available [7].

3.2 Load Carrying Capacities

The variables considered were
- end eccentricity of applied load (e/D = 0.1 and 0.4),
- slenderness of the column (L/D = 15 and 30),
- steel percentage (p = 1.26 and 3.54 per cent),
- concrete age at initial loading (t_o = 14 and 56 days),
- sustained load period (t_s = 131 and 3000 days) and
- sustained load intensity (P_s).

The influence on a column's load carrying capacity of intensity and duration of a sustained load is illustrated, for some of the columns investigated, in Figs. 5 through 8. The load capacity, P_{u2} (Fig. 1), after a sustained load period, t_s, is plotted versus the corresponding sustained load, P_s. The coordinates are nondimensionalized with respect to the short time capacity, P_{u1}, at initial loading. The curves are limited to the right by the line $P_{u2} = P_s$, i.e. by the case of creep instability taking place under the constant load P_s. The change in P_{u2} with increasing t_s at $P_s = 0.0$ is mainly due to the continued hydration alone (effects of preloading strains are negligible).

Hydration effects, causing a concrete strength increase, may, depending upon column geometry, yield a considerable increase in load carrying capacity (P_{u2}) at low and intermediate load levels. On the other hand, a significant decrease in load carrying capacity results at high sustained load levels, this being mainly due to the large deflection increase at these load levels (see Fig 10). This decrease is, for all columns except those becoming unstable at low stress levels (e/D = 0.1, L/D = 30), further accentuated by adverse effects to the concrete strength from high sustained stress levels at the most strained portions of the column section.

With larger steel percentage, more stress transfer (due to creep and shrinkage) from concrete to steel takes place. High concrete stresses thus prevail for shorter periods of time with adverse effects to P_{u2} becoming less pronounced.

It was found [7], for the columns investigated, that the ratio of the sustained load capacity, defined as the load that causes creep instability at $t_s = \infty$ (here approximated by t_s = 3000 days), to P_{u1} decreases with increasing slenderness, increases with increasing end eccentricity, decreases with decreasing steel percentage, and is not significantly influenced by the age of loading.

4. Design Considerations

4.1 Safety Aspects

The load capacity, P_{u2}, of a column was found to vary with time under a given sustained load. Design procedures may be based on the lower bound values, $P_{u\,min}$ (Schematically illustrated in Fig. 9) and related to the allowable service loads by a set of load factors, A and B, such that

$$P_{u\,min} = A\,P_D + B\,P_L \qquad (6)$$

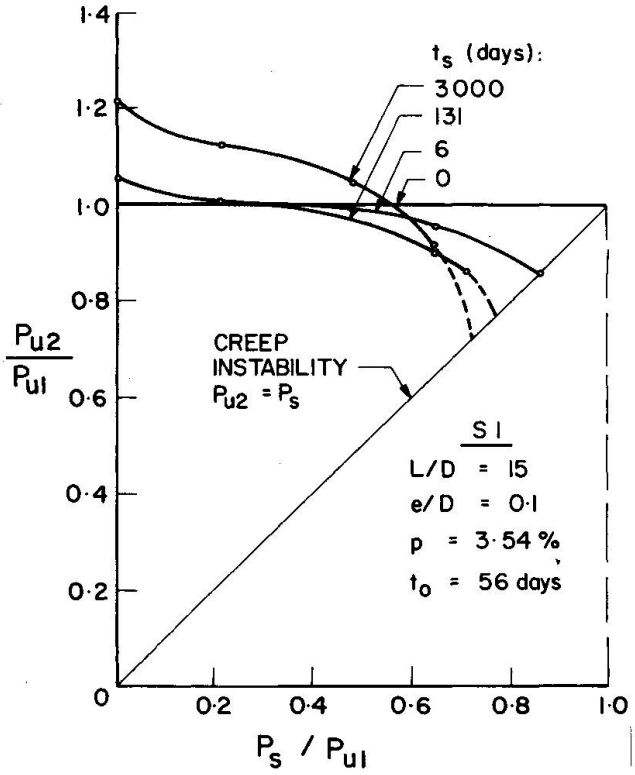

Fig. 5

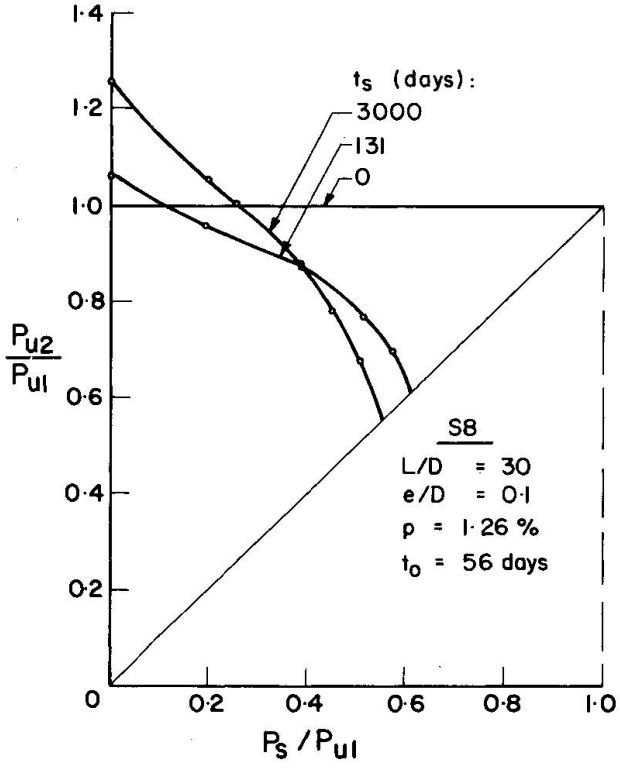

Fig. 6

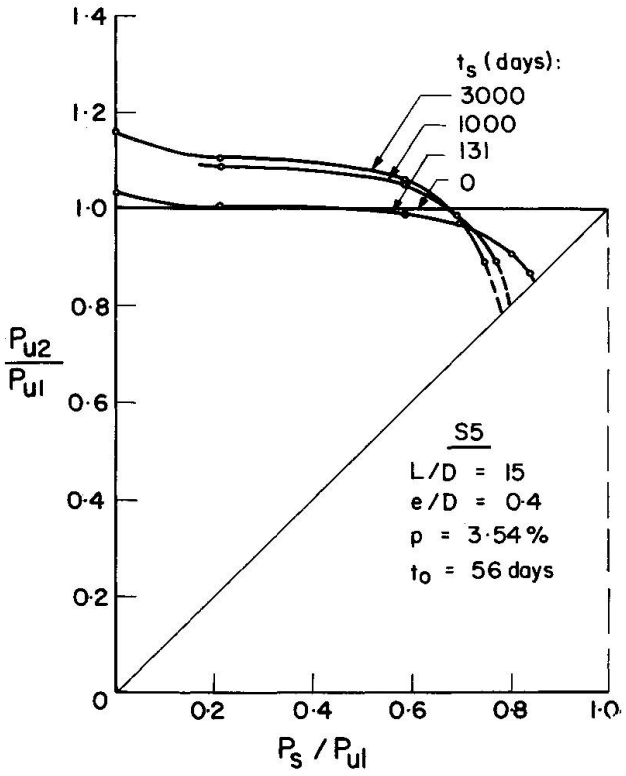

Fig. 7

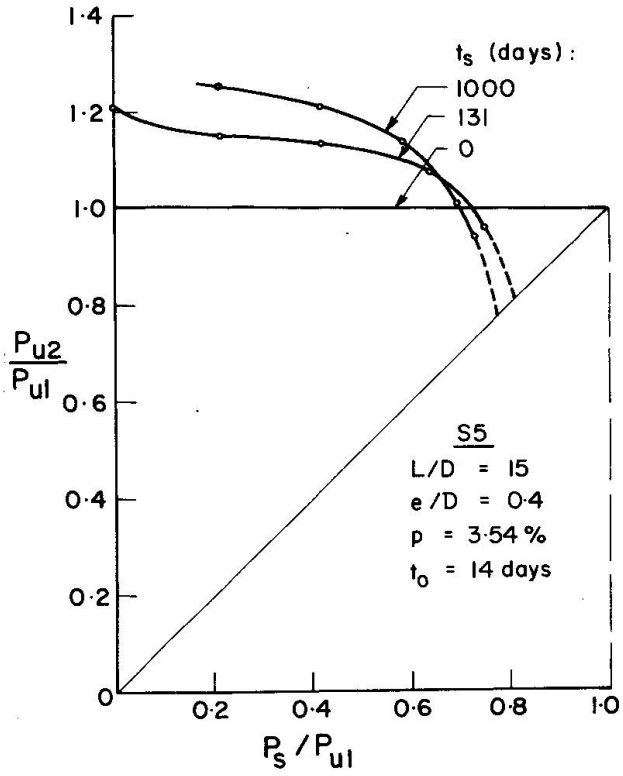

Fig. 8

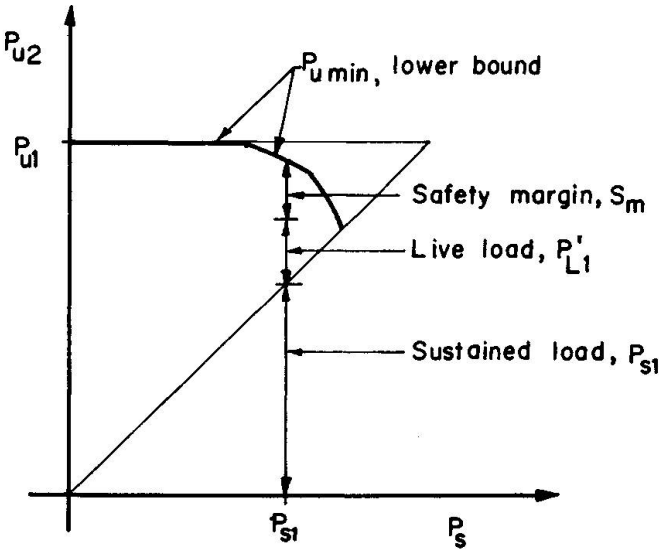

Fig. 9

where P_D is the dead load and P_L the live load.

These load factors, or more conveniently an 'overall load factor' (LF),

$$LF = P_{u\,min} / (P_D + P_L) \qquad (7)$$

can be examined in terms of a set of given 'nominal' factors, a and b, related to the short time capacity by

$$P_{u1} = aP_D + bP_L \qquad (8)$$

A 'nominal overall load factor' is obtained by replacing $P_{u\,min}$ with P_{u1} in Eq. 7.

If a typical building structure is considered with the dead load equal to the live load ($P_L = P_D$) and with half the live load essentially permanently applied throughout the life of the building, the total sustained load beomes $P_s = P_D + P_L/2 = 0.48\ P_{u1}$ (Eq. 8), with load factors a = 1.4 and b = 1.7 suggested in the proposed revision of ACI 318-63 [11]. With $P_s = 0.48\ P_{u1}$ and the column in Fig. 6 as an example, $P_{u\,min}$ becomes $0.73\ P_{u1}$ (at t_s =3000 days) and the overall load factor 1.14 (Eq. 7). This represents a 26 per cent reduction of the nominal overall load factor of 1.55.

In long span bridges the dead load is the predominant load. Using a live load of 6 per cent of the dead load, the dead load becomes $P_D = 0.60\ P_{u1}$, Eq. 8, with a=1.5 and b=2.5 (AASHO load factors [12]). For the column in Fig. 6, failure (creep instability) takes place under this dead load only at about t_s = 131 days. Thus while the nominal overall load factor is 1.56, the one based on $P_{u\,min}$ is below unity. Thus, the load factors used above may not be sufficient for the sustained loading case of this slender column. Comparison with the other columns investigated [7] indicates that all the columns but those very slender (L/D = 30) and with small end eccentricities (e/D = 0.1) would remain stable under the allowable loads, although with actual load factors smaller than the nominal ones.

These examples reinforce the need for careful consideration of sustained load effects in column design.

4.2 Serviceability and Aesthetic Aspects

It may be desirable, both from serviceability requirements and aesthetic viewpoints, to limit the column deflection to an amount at which it is not particularly apparent to the eye. Deflections in excess of about L/360 to L/300 are noticeable.

Typical results showing sustained loads versus the corresponding midheight deflections after various time periods are given in Fig. 10. A deflection of L/360 is indicated.

It was found, for all the columns investigated, that a sustained load $P_s \geq 0.48\ P_{u1}$ resulted in deflections at t_s = 3000 days in excess of L/360. Thus, deflection limitations rather than safety aspects may tend to become a design criterion for this class of columns.

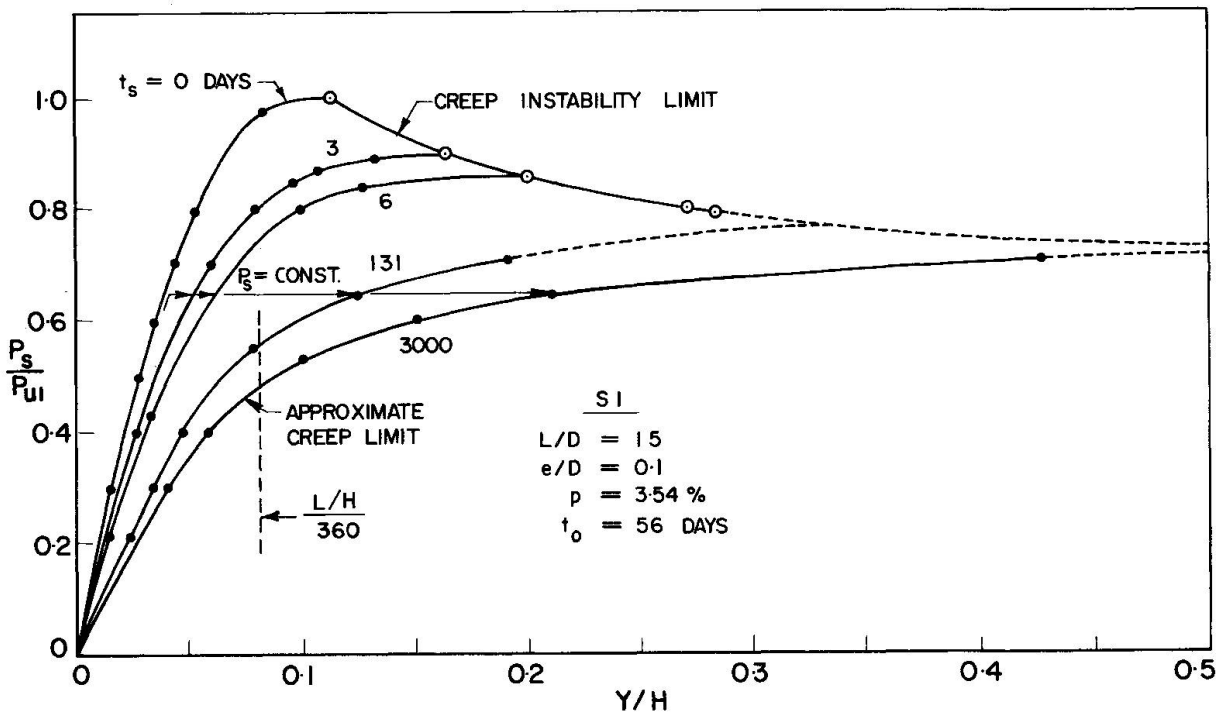

Fig. 10

5. Conclusions

Perhaps the principal conclusion to be drawn from this study is that the load carrying capacity of a column may be significantly reduced under sustained overload conditions and also under service loads for some combinations of end eccentricities and slenderness ratios.

Indications were further obtained that present design provisions in terms of load factors, may not provide adequate safety for very slender columns (L/D = 30) with relatively small end eccentricities (e/D = 0.1). It should be noted, however, that columns in actual structures are usually subjected to more favourable boundary conditions than those considered here (unrestrained). End restraints provided by beams and footings will usually allow a gradual moment transfer from the column to the restraining elements during the sustained loading period.

Lastly, serviceability and aesthetic considerations, seeking to limit deflections, may call for smaller service loads than those obtained from load capacity considerations.

ACKNOWLEDGEMENT

This investigation forms a part of a doctoral dissertation of the first author. The support provided by the National Research Council of Canada and the Computing Centre at the University of Waterloo is acknowledged.

REFERENCES

1. VIEST, I.M., ELSTNER, R.C. and HOGNESTAD, E., ''Sustained Load Strength of Eccentrically Loaded Short Reinforced Concrete Columns'', Journ. A.C.I. Proc. Vol. 54, No. 9, March 1956.

2. RAMU, P., GRENACHER, M., BAUMAN, M. and THÜRLIMANN, B., ''Versuche an gelenkig gelagerten Stahlbeton-stützen unter Dauerlast'', Bericht Nr. 6418-1, Institut für Baustatik, ETH, Zürich, May 1969.

3. HELLESLAND, J. and GREEN, R., ''Sustained and Cyclic Load Behavior of Reinforced Concrete Columns'', A.S.C.E. National Structural Engineering Meeting, Portland, Oregon, April 1970.

4. BREEN, J.E. and FERGUSON, P.M., ''The Restrained Long Column as a Part of a Rectangular Frame'', Journ. A.C.I., Proc. Vol. 61, No. 5, May 1964.

5. FURLONG, R.W. and FERGUSON, P.M., ''Tests of Frames with Columns in Single Curvature'', Symposium on Reinforced Concrete Columns, A.C.I. Publication SP-13.

6. MAUCH,S., and HOLLEY, M.J., ''Creep Buckling of Slender Columns'', Journ. A.S.C.E., Vol. 89, No. ST4, 1963, pp. 451-481.

7. HELLESLAND, J. '' A Study into the Sustained and Cyclic Load Behaviour of Reinforced Concrete Columns'', A Doctoral Dissertation presented to the University of Waterloo, Waterloo, Ontario, Canada, 1970.

8. MANUEL, R.F. and MacGREGOR, J.G., ''Analysis of Restrained Reinforced Concrete Columns under Sustained Load'', Journ. A.C.I., Jan. 1967.

9. RÜSCH, H., ''Researches towards a General Flexual Theory for Structural Concrete'', Journ. A.C.I., Proc. Vol. 57, No. 1, July 1960, pp. 1-28.

10. RASCH,C., ''Spannungs - Dehnungs - Linien des Betons und Spannungsverteilung in der Biegedruckzone bei kostanter Dehngeschwindigkeit,'' Deutscher Ausschuss für Stahlbeton, Heft 154, Sept. 1962, Berlin.

11. A.C.I. COMMITTEE 318, ''Proposed Revision of A.C.I. 318-63: Building Code Requirements for Reinforced Concrete'', Journ. A.C.I., Proc. V. 67, No. 2, Febr. 1970.

12. AASHO, ''Standard Specifications for Highway Bridges'', The American Association of State Highway Officials, 1965.

SUMMARY

This study has been concerned mainly with the influences of a sustained load on a column's load carrying capacity. Attention was restricted to unrestrained, eccentrically loaded columns. Most emphasis was placed on the column strength characteristics at low and intermediate load levels. The limiting case of loads causing creep instability at the end of the time periods considered was also obtained, however.

It was found that the load carrying capacity may be significantly reduced under sustained overloads, and also under sustained service loads for slender columns with small end eccentricities.

RESUME

Dans cette étude, les auteurs examinent l'influence d'un effort permanent sur la résistance des colonnes en béton armé. Ils examinent seulement les colonnes libres soumises à des charges excentriques. On détermine les caractéristiques de la résistance des colonnes soumises à des efforts réduits ou moyens et on obtient les valeurs des charges dont le fluage du béton entraîne l'instabilité au bout d'un certain temps.

L'étude montre la réduction considérable de la résistance des colonnes soumises à des excès de charges permanentes, et des colonnes élancées soumises à des charges de service légèrement excentriques.

ZUSAMMENFASSUNG

Die vorstehende Studie gilt hauptsächlich dem Einfluss der Dauerlast auf die Tragfähigkeit einer Säule, wobei die Betrachtungen auf freie exzentrisch belastete Säulen beschränkt waren. Das Hauptgewicht wurde auf die Aenderung der Tragfähigkeit zufolge geringer und mittlerer Dauerlasten gelegt. Ebenso wurde der Grenzfall der Belastungen bestimmt, welche Kriech-Instabilität am Ende des betrachteten Zeitintervalles bewirkten.

Als Ergebnis konnte festgestellt werden, dass die Tragfähigkeit durch Dauerlasten über dem zulässigen Lastwert beträchtlich reduziert wird; dies gilt auch für schlanke Säulen mit kleiner End-Exzentrizität unter geringer Dauerlast, wie etwa übliche Gebrauchsbeanspruchung.

Leere Seite
Blank page
Page vide

Das Kriechen betrachtet von der Seite der Bauplanung

Creep as a Factor in the Design of Structures

Le fluage au point de vue de la conception des constructions

E. ÉLIÁS
Budapest
Ungarn

Die Ursachen des Kriechens, die Einflüsse der Baustoff- und Umgebungseigenschaften werden von den Versuchsanstalten laufend untersucht. Der Ingenieur, der ein Bauwerk zu entwerfen hat, kann jedoch diese Untersuchungsergebnisse kaum unmittelbar anwenden, da jene keine solche Hinweise sind, die in die Berechnung der Wirkungen des Kriechens auf eine Beton- oder Stahlbetonkonstruktion einsetzbar währen. Die Versuche geben nämlich - zwecks der Vergleichbarkeit - die rheologischen Eigenschaften von verhältnismässig kleiner und einfacher Probekörper an, von denen der unmittelbare Übergang zu den grossen und verwickelten Konstruktionen unmöglich ist.

Es ist deshalb Notwendig, dass die Bauplanung für ihren Bedarf, auf Grund der Laborversuche, ein Modell konstruire, das die tatsächlichen Verhältnisse womöglich gut wiederspiegelt, ohne jedoch solche rechentechnische Schwierigkeiten zu bereiten, deren Überwindung durch die erreichten oder erreichbaren Vorteile nicht gerechtfertigt werden können.

Unserer Ansicht nach, können die wesentlichen und die weniger wichtigen Eigenschaften, dessen Berücksichtigung bzw. Vernachlässigung für zweckmässig scheint, wie nachstehend zusammengefasst werden.

1. Es besteht zwischen den Spannungen und den Verzerrungen die Boltzmann'sche Linearität.
2. Die belibenden - plastischen - Verformungen die unmittelbar nach der Belastung auftreten, können vernachlassigt werden.
3. Der Wert des Elastizitätsmoduls ist zeitunabhängig.
4. Die Kriechverformung strebt mit abnehmender Geschwindigkeit

- monoton zunehmend - einem Endwert zu.

5. Bei der Entlastung kann die sogenannte Erholung vernachlässigt werden.
6. Die obererwähnten Bedingungen bringen es mit sich, dass der Beton kein "Gedächtnis" hat. Das bedeutet, dass der zeitliche Ablauf der Formänderung von dem momentanen Spannungszustand abhängig ist, und die Art und Weise der vorangegangenen Belastungen keinen Einfluss hat. Nach völliger Entlastung hat der Betonkörper nur bleibende Formänderungen und es treten keine nachträgliche Bewegungen mehr auf.
7. Das Kriechen ist irreversibel. Unter dem Einfluss von zeitunabhängigen Zwangsverformungen nehmen die Spannungen allmählich bis zu einem nicht verschwindenden Endwert ab.
8. Die Kriechfähigkeit des Betons nimt mit der Zeit ab.

So einfach auch die oben angeführten Bedingungen sind, werden doch einige davon bestritten.

Bei der Entlastung des Betons zeigt sich eine gut wahrnehmbare Erholung, damit ist die "Gedächtnissfreiheit" wiederlegt und das Kriechen ist deshalb teilweise reversibel.

Eine Kriechfunktion - das Verhältniss der Kriechverformung zu der elastischen Verformung - lässt sich im Allgemeinem durch eine zweiparametrige Funktion ausdrücken.

$\varphi(t,\tau)$ τ Zeitpunkt der Belastung

t Zeitpunkt der Verformung

Es wird verlangt dass $\varphi(t,t) = 0$

Wenn man die angeführten Bedingungen annimmt gestaltet sich die Kriechfunktion

$$\varphi(t,\tau) = \varphi(t) - \varphi(\tau)$$

und für die kleinen Veränderungen gilt die Dischinger'sche Differentialgleichung:

$$d\varepsilon = \frac{1}{E}\left[d\sigma + \sigma d\varphi\right]$$

Wenn man aber die Teorie den Versuchen besser anpassen will, muss man eine mehr verwickelte Form nehmen etwa

$$\varphi(t,\tau) = k(\tau) f(t-\tau)$$

und es lässt sich für die kleinen Veränderungen keine Differenti-

algleichung mehr anschreiben.

Im ersten Falle führen die Kriechaufgaben auf Differentialgleichungen, die zum Beispiel durch die Laplace'schen Transformation sehr bequem behandelt werden können.

Im zweiten Falle führen die selben Aufgaben auf Integralgleichungen und die rechentechnischen Schwierigkeiten werden kaum erträglich.

Die sorgfältige Feststellung einer Kriechfunktion anhand einer Reihe von Messungen an vorhandenen Probekörper ist an sich schon eine schwierige Sache. In der Bauplanung müssen aber die Kriecheigenschaften des Betons vorhergesagt werden, und diese Vorhersage ist noch immer, und bleibt trotz der sorgfältigsten Laborversuche noch lange mit groben Fehlern behaftet. Es besteht also die Frage, ob eine feinausgebildete Teorie mit einer Riesenrechenaufwand bei diesen Umständen gerechtfertigt angesehen werden darf.

Der Dischinger'schen Differentialgleichung entspricht kein strenges Naturgesetz. Sie ist halb Erfahrung und halb Zweckmässigkeit. Wenn man sie, und ihre Folgerungen nnimmt, ist sie wiederspruchsfrei und man benötigt keine weiteren Ansätzen.

Ich meine sie wird noch lange umentbehrlich sein, und gute Dinste leisten.

Es wurde öfters versucht, die elastischen und Kriechvorgänge des Betons durch ein viskoelastisches Modell darzustellen, es kann jedoch nachgewiesen werden, dass ein Modell, das die obenerwähnten Bedingungen erfüllt, aus zeitunabhängigen rheologischen Elementen nicht zusammenstellbar ist.

Wenn jedoch gelingt es aus zeitabhängigen Elementen ein Modell, des Betonkriehens, das die Kriecherscheinungen treu wiedergibt, zusammenzubasteln, das beweist nichts mehr als die ungeheuere Anpassungsfähigkeit der Teorie der Rheologie und ist nur ein Eingehen der Tatsache, dass die Kriechteorie zur Zeit noch eine vorwiegend fenomenologische Wissenschaft ist.

ZUSAMMENFASSUNG

Bei der Modellbildung der Kriecherscheinungen ist es zweckmässig, die nach der Entlastung entstehende Erholung zu vernachlässigen. Diese Annahme bringt es

mit sich, dass der Beton kein Gedächtnis hat, und die Kriechformänderungen völlig irreversibel sind. Dadurch kann die Lösung der Kriechaufgaben auf Differentialgleichungen zurückgeführt werden, was rechentechnisch sehr vorteilhaft ist.

SUMMARY

In the development of creep models it is useful to neglect the phenomenon of creep recovery, which occurs after unloading. This assumption implies that concrete has no memory and that the deformations caused by creep are completely irreversible. In this way the solution of creep problems can be reduced to the form of differential equations, which is quite suitable from the point of view of computation.

RESUME

Au cours de la construction des modèles de fluage, il semble raisonnable de négliger le phénomène de recouvrance du fluage survenant après la suppression de la charge. Cette simplification implique que le béton n'a pas de mémoire et que les déformations causées par le fluage sont complètement irréversibles. Par conséquent, la solution des problèmes de fluage peut être réduite à celle des équations différentielles, ce qui est favorable pour le calcul.

II

Die Berücksichtigung des unterschiedlichen Kriechens bei den "Viaducs de la Plaine du Rhône"

Influence of Differential Creep in the Construction of the "Viaducs de la Plaine du Rhône"

Prise en considération du fluage différentiel dans la construction des "Viaducs de la Plaine du Rhône"

BENNO BERNARDI
Zürich, Schweiz

1. Einleitung

Die "Autoroute du Léman" führt am obern Ende des Genfersees bei Villeneuve in einer Höhe von 7 - 18 m über die Rhoneebene. Die geotechnisch sehr ungünstigen Untergrundverhältnisse machten hier die Ueberbrückung durch die "Viaducs de la Plaine du Rhône" mit einer Gesamtlänge von 1170 m' erforderlich. Es handelt sich um zwei in der Querrichtung durchgehend getrennte Bauwerke mit einer Breite von je 13.20 m. In der Längsrichtung sind in einem Abstand von ca. 400 m Bewegungsfugen angeordnet. Somit ergeben sich 2 x 3 = 6 Brücken mit einer Grundrissfläche von total ca. 31'000 m2 - eines der grössten Brückenbauwerke in der Schweiz.

Die "Viaducs de la Plaine du Rhône" wurden auf Grund eines Submissionswettbewerbes vergeben. Unter den 39 Angeboten war dasjenige der Firma Losinger am preisgünstigsten und stellte den Bauherrn sowohl in bautechnischer wie ästhetischer Hinsicht zufrieden.

Bei der Projektierung war die Wirtschaftlichkeit ein primäres Anliegen. Dieselbe wird wesentlich bestimmt durch die Baumethode und die Grösse der Spannweiten. Auf der Grundlage von Vergleichsuntersuchungen wurde eine vorfabrizierte Spannbetonkonstruktion für den Ueberbau gewählt. Bei Berücksichtigung der Fundation ergab sich in Funktion der Spannweite ein Kostenminimum für L = 26 - 30 m. Die gewählte Spannweite von L = 29.8 m kann über die ganze Brückenlänge konstant durchgenommen werden und ergibt zudem eine günstige Einteilung im Grundriss, wobei alle vorgeschriebenen Lichtraumprofile eingehalten werden.

2. Brückenüberbau

Der voll vorfabrizierte Brückenüberbau besteht aus 2 Elementtypen Längsträger und Fahrbahnplatten, und zwar pro Feld aus 3 Längs-

trägern und 6 grossformatigen, konstant 22 cm starken Fahrbahnplattenelementen mit den Grundrissabmessungen von 945 x 615 cm.

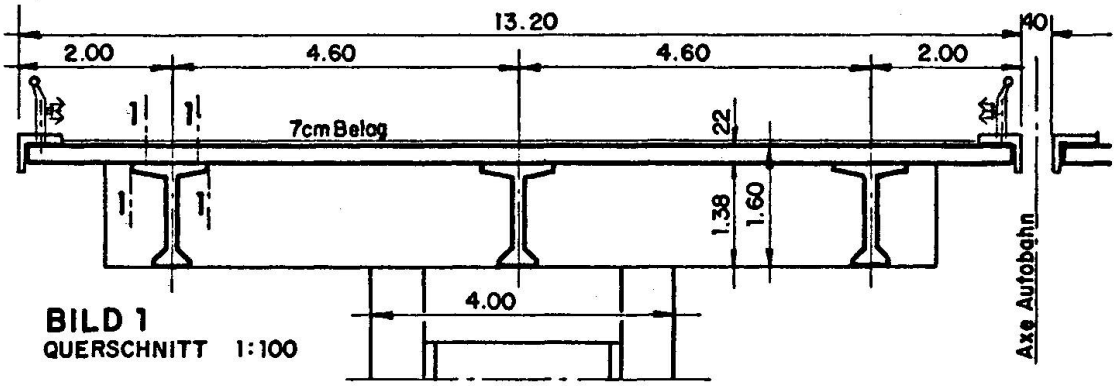

BILD 1
QUERSCHNITT 1:100

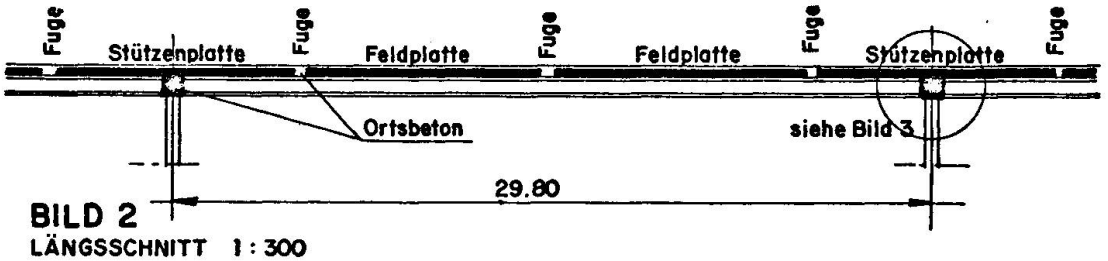

BILD 2
LÄNGSSCHNITT 1:300

Diese Elemente erstrecken sich auf die halbe Fahrbahnbreite und sind im Bauzustand statisch bestimmt auf dem Obergurt des Mittel- und eines Randlängsträgers gelagert. Die Länge der Elemente von 9.45 m wurde so gewählt, dass sich pro Brückenfeld nur drei Querfugen in der Fahrbahnplatte ergeben; diejenige in Brückenmitte befindet sich in der Druckzone, die beiden andern etwa im Momentennullpunkt des Durchlaufträgers. Die Fahrbahnplattenelemente sind somit so angeordnet, dass sich im Stützenschnitt keine Querfuge befindet.

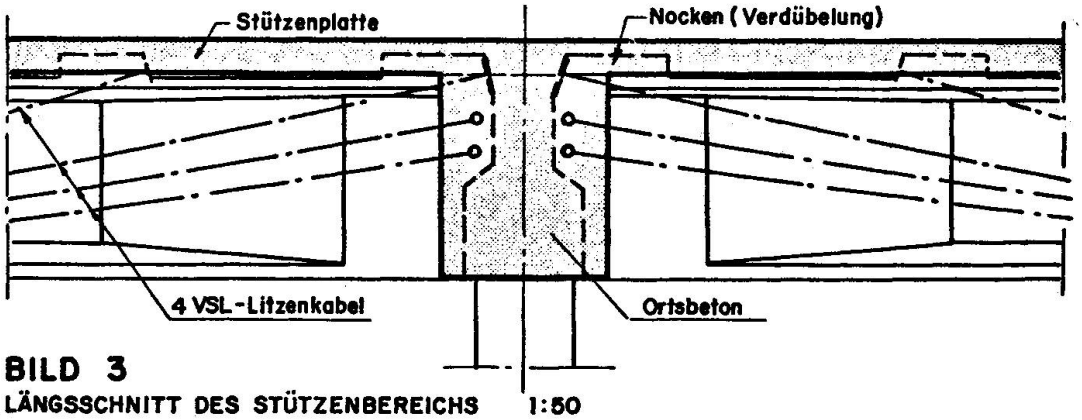

BILD 3
LÄNGSSCHNITT DES STÜTZENBEREICHS 1:50

Die 2 Platten im Stützenschnitt erhalten zudem vor der Verlegung eine zugbandartige Vorspannung in Brückenlängsrichtung. Die Fahrbahnplatte ist in Querrichtung nicht vorgespannt.

Durch den Verguss der Längs- und Querfugen sowie der Ortsbetonquerträger in den Stützenschnitten entsteht eine monolithisch wirkende Verbundkonstruktion: 3-stegiger Plattenbalken (ohne Feldquerträger) und in Längsrichtung fugenlos durchlaufende Brücken über 12 Felder (Länge 357.60 m), bezw. 15 Felder (Länge 447 m).

3. Die Auswirkungen des unterschiedlichen Kriechens

3.1 Der Kriechvorgang

Im Bauzustand (t = o) sind die Längsträger als einfache Balken statisch bestimmt aufgelagert und stark vorgespannt. Die Fahrbahnplatten dagegen sind nicht (im Feld) bezw. nur leicht (über den Stützen) vorgespannt und wirken vorerst nicht im Verbund.

Durch den Verguss der Fugen sowie des Ortsbetonquerträgers wird im Zeitpunkt t1 einerseits der Verbundquerschnitt (3-stegiger Plattenbalken) und anderseits in Brückenlängsrichtung der statisch unbestimmte Durchlaufträger hergestellt.

Die stark verschiedenen Beanspruchungen der benachbarten Fasern unterkant Fahrbahnplatte und oberkant Längsträger bedingen ein unterschiedliches Betonkriechen. Diese Kriechverformungen können sich nicht frei auswirken, sondern es tritt eine gegenseitige Behinderung auf. Dadurch wird in der Fuge zwischen der Fahrbahnplatte und den Längsträgern stufenweise eine Umlagerungskraft aufgebaut, die den Längsträger entlastet (exzentrischer Zug) und die Fahrbahnplatte unter Druck setzt. Diese Umlagerungskräfte sind im Gleichgewicht und ergeben einen Eigenspannungszustand am Verbundquerschnitt; sie bewirken jedoch gleichzeitig Verformungen in Längsrichtung und erzeugen somit statisch unbestimmte Zwängungsmomente am Durchlaufträger. Diese Zwängungsmomente sind prinzipiell zu unterscheiden von jenen, die durch die Vorspannung verursacht werden und schon im Zeitpunkt t = o auftreten ("Parasitärmomente").

3.2 Die statische Berechnung

Die theoretische Lösung der Kriechumlagerung wird gefunden durch die Formulierung der Formänderungsbedingungen des Verbundquerschnittes, wonach in jedem Zeitpunkt t in jedem Querschnitt die Verformungen des untern Randes der Fahrbahnplatte und des obern Randes des Längsträgers gleich sein müssen.

Für die praktische Berechnung machten wir die folgenden Vereinfachungen: als statisches System wird anstelle der durchlaufenden Verbundkonstruktion ein ebenes Stabwerk gewählt (Veerendeelträger).

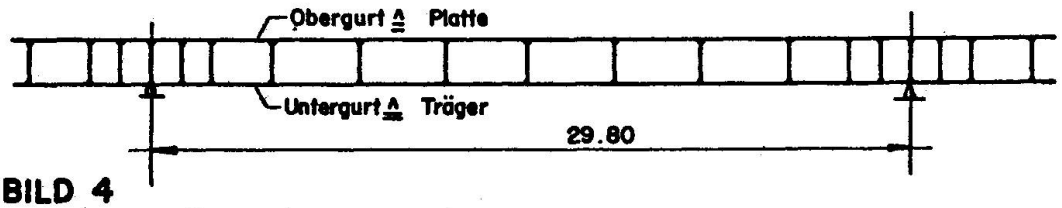

BILD 4
VEERENDEELTRÄGER : SYSTEMSKIZZE

Die Kriechberechnung wird als Stufenverfahren aufgebaut, indem der ganze Kriechbereich in einzelne Kriechintervalle zerlegt wird, wobei innerhalb eines Intervalls die Umlagerungsspannungen linear mit dem Kriechen anwachsen.

Beim Veerendeelträger werden dem Untergurt die Querschnittswerte des Längsträgers und dem Obergurt diejenigen der Fahrbahnplatte zugewiesen. Die biegesteif angeschlossenen Vertikalstäbe entsprechen dem Steg des Verbundquerschnittes. Für jeden Stab werden als Belastung die Normalkräfte und Momente mit den Kriechwerten des betreffenden Intervalles eingeführt. Hiefür wurde ein spezielles Programm entwickelt, wodurch die umfangreichen numerischen Berechnungen elektronisch durchgeführt werden konnten.

Die Kriechberechnungen wurden unter der Annahme einer Endkriechzahl von $\varphi 35 - \infty = 1.8$ sowohl für den Träger- wie den Fahrbahnplattenbeton durchgeführt. Beide Elemente wiesen im massgebenden Zeitpunkt des Ortsbetonvergusses der Fugen ein Erhärtungsalter des Betons von ca. 35 Tagen auf. Der Einfluss des unterschiedlichen Alters des Fugenbetons wurde vernachlässigt.

Die durch die Kriechumlagerungen verursachten statisch unbestimmten Zwängungsmomente ergeben sich aus den Auflagerreaktionen der vorstehend beschriebenen elektronischen Berechnungen.

3.3 Ergebnisse und Erkenntnisse

Aus dem Verlauf der Betonspannungen zufolge ständiger Belastung (g + V) je in einem charakteristischen Feld- und Stützenschnitt im Zeitpunkt t = o und t = ∞ ist der erhebliche Einfluss der Kriechumlagerungen ersichtlich. Im Feldschnitt ist es für die massgebende Betonspannung σ_u am untern Querschnittsrand günstig,

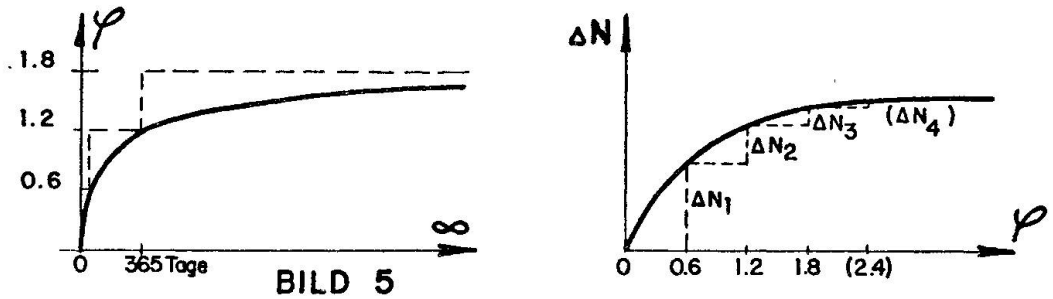

BILD 5
VERLAUF DES KRIECHENS UND DER UMLAGERUNGSKRAFT

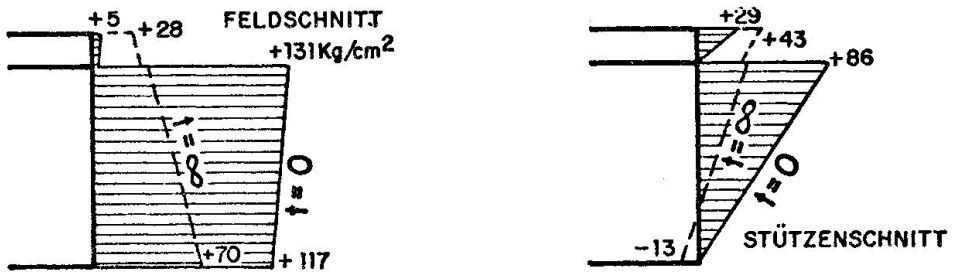

BILD 6
SPANNUNGSVERLAUF FÜR STÄNDIGE LASTEN BEI t=0 und t= ∞

dass die Umlagerungskraft als exzentrischer Zug oberkant Längsträger wirkt; damit wird für σ_u wegen dem negativen Zusatzmoment der zentrischen Zugspannung noch eine Druckspannung überlagert. - Im Stützenschnitt wird die initiale Druckvorspannung an der Fahrbahnplattenoberfläche durch das Kriechen vergrössert; dies ist für den Durchlaufträger im Bereich mit negativen Stützenmomenten infolge Verkehrslasten günstig, weil damit die Rissesicherheit verbessert und die Dauerhaftigkeit des Belages günstig beeinflusst wird.

Zur Ermittlung der Umlagerungskräfte wurde die Kriechkurve mit $\varphi_{35\,-\infty} = 1.8$ in 3 gleiche Intervalle mit $\Delta\varphi = 0.6$ unterteilt.

Tabelle 1: Entwicklung der Umlagerungskraft N in der Fuge zwischen Fahrbahnplatte und Längsträger in einem Feldschnitt.

	N_{Platte}	$N_{Träger}$	$\Sigma \Delta N$
t = o	57	1460	
ΔN_1 für $\Delta\varphi_1 = 0.6$	+ 467	- 467	467 ~ 61 %
nach 1. Schnitt	524	993	
ΔN_2 für $\Delta\varphi_2 = 0.6$	+ 208	- 208	675 ~ 88 %
nach 2. Schnitt	732	785	
ΔN_3 für $\Delta\varphi_3 = 0.6$	+ 92	- 92	767 ~100 %
nach 3. Schnitt	824	693	
ΔN_4 für $\Delta\varphi_4 = 0.6$*	+ 41	- 41	808 ~105 %
nach 4. Schnitt*	865	652	

* extrapoliert; N in Tonnen, + Druck

Aus der Tabelle No. 1 ist ersichtlich, dass das erste Kriechintervall schon 61 % der gesamten Umlagerung ausmacht, das zweite noch 27 % und das dritte nur noch 12 %. Die Berechnungen bei analogen Brückensystemen mit Spannweiten von 24 - 58 m zeigten ähnliche Ergebnisse. Daraus kann allgemein geschlossen werden, dass das anfängliche Kriechen die grössten Auswirkungen zeigt. Ein Grossteil der Kriechumlagerungen wird somit schon nach einem Jahr stattgefunden haben. - Eine fehlerhafte Einschätzung der Endkriechzahl hat einen relativ kleinen Einfluss; gegenüber der angenommenen Endkriechzahl von $\varphi = 1.8$ ergäbe eine solche von $\varphi = 2.4$ eine nur 5 % grössere und eine solche von $\varphi = 1.2$ eine lediglich 12 % kleinere Umlagerungskraft.

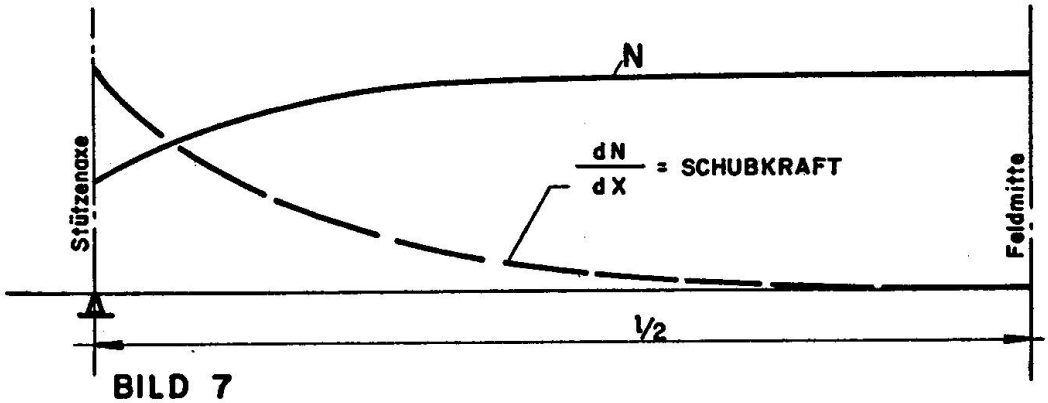

BILD 7
VERLAUF DER UMLAGERUNGSKRAFT

Im Bild 7 ist der Verlauf der endgültigen Umlagerungskraft N für das Innenfeld eines Durchlaufträgers mit unendlich vielen Spannweiten dargestellt. Die erste Ableitung der Umlagerungskraft $\frac{dN}{dx}$ ergibt die Verdübelungsbeanspruchung der Fuge zwischen Fahrbahnplatte und Längsträger. Aus dieser Verdübelungsbeanspruchung werden die schrägen Hauptzugspannungen zufolge der Kriechumlagerungen errechnet, welche im vorliegenden Fall im Stützenbereich und zwar für den Schnitt 1 - 1 (vergl. Bild 1) massgebend wurden.

3.4 Die Berücksichtigung beim Bruchsicherheitsnachweis

Für Konstruktionen, bei denen im Laufe der Bauausführung Systemwechsel vollzogen werden, ergeben sich Probleme beim Bruchsicherheitsnachweis. Bei den meisten Brückenbauten treten Systemwechsel auf, z.B. für Freivorbauten zuerst Kragarme, dann Durchlaufträger; für feldweise nach Taktverfahren hergestellte Brückenüberbauten etc. Im vorliegenden Fall lagerten die Fertigelemente im Bauzustand als einfache Balken statisch bestimmt; im Endzustand wirken sie als statisch unbestimmte Durchlaufträger.

Wird die Sicherheit des ganzen Bauwerks, die sogenannte Systemsicherheit nachgewiesen, so haben die Auswirkungen des Kriechens zufolge Systemwechsel keine Bedeutung; denn es entstehen lediglich Umlagerungen vom Feld- auf die Stützenschnitte; so ergibt z.B. eine Zusatzbelastung des Feldes eine entsprechende Entlastung der Stützenschnitte und umgekehrt. Es kann auch argumentiert werden, dass die Zwängungsbeanspruchungen zufolge Kriechumlagerungen, analog wie für die Wirkung ungleichmässiger Temperaturverteilungen, am Gesamtsystem für sich im Gleichgewicht sind; zudem würden diese Zwängungen im Bruchzustand durch die grossen plastischen Verformungen sowieso schrittweise abgebaut.

Anders verhält es sich, wenn die sogenannte Querschnittbruchsicherheit nachzuweisen ist. Nach den schweizerischen SIA-Normen No. 162 (1968) ist bei Spannbeton die Sicherheit gegen Biegebruch in jedem gefährdeten Querschnitt zu erbringen, wobei von den wie folgt vergrösserten, nach der Statik elastischer Systeme ermittelten Schnittkräften aus Hauptbelastungen des Gebrauchszustandes auszugehen ist:

$$M' = S_1 (Mg + p) + 0.8\, M_z$$

Eine ausreichende Bruchsicherheit ist vorhanden, wenn in jedem Schnitt die folgende Bedingung erfüllt ist:

$$M_{Br} \geq S_2 \cdot M' = s_1 \cdot S_2 (Mg + p) + 0.8 \cdot S_2 \cdot M_z$$

S_1 = Lastfaktor = 1.4

S_2 = Querschnittsfaktor = 1.3

$s_1 \cdot s_2 = 1.82$; $s_2 \cdot 0.8 = 1.04$

Mg = Biegemoment aus ständigen Lasten

Mp = Biegemoment unter Nutzlasten

Mz = Zwängungsmoment aus initialer Vorspannung (t = o)

Dieses Prinzip wurde für den vorliegenden Fall wie folgt erweitert: es wird unterschieden zwischen den Zwängungsmomenten zufolge Systemwechsel (einfache Balken → Durchlaufträger) und jenen, die durch die Herstellung des Verbundquerschnittes (Ortsbetonverguss der Fugen zwischen den Längsträgern und den Fahrbahnplattenelementen) entstanden sind. Der zuletzt genannte Anteil entspricht einem Eigenspannungszustand und wird beim Bruchsicherheitsnachweis nicht berücksichtigt. Der durch den Systemwechsel verursachte Anteil wird einerseits durch das Eigengewicht und anderseits durch die Vorspannung erzeugt; im Bruchsicherheitsnachweis werden die Wirkungen des Eigengewichts und der Vorspannung mit unterschiedlichen Sicherheitsbeiwerten von $S_1 = 1.4$ bzw. 0.8 berücksichtigt. Die Bruchsicherheit wurde somit wie folgt errechnet:

im Zeitpunkt t = o

im Feld $\quad M_{Br} \geq 1.3 \cdot 1.4 (Mg_1 + Mg_2 + Mp)$

über der Stütze $\quad M_{Br} \geq 1.3 \cdot 1.4 (Mg_2 + Mp)$

im Zeitpunkt $t = \infty$

im Feld $\quad M_{Br} \geq 1.3 \{1.4 (Mg_1 + Mg_2 + Mp + Mzg) + 0.8\, Mzv\}$

über der Stütze $\quad M_{Br} \geq 1.3 \{1.4 (Mg_2 + Mp + Mzg) + 0.8\, Mzv\}$

Mg_1 = Biegemoment infolge dem Eigengewichtsanteil, der im Bauzustand statisch bestimmt wirkt.

Mg_2 = Biegemoment infolge dem Eigengewichtsanteil, der am Durchlaufträger wirkt.

Mzg = Zwängungsmoment durch Systemwechsel, infolge Eigengewicht.

Mzv = Zwängungsmoment durch Systemwechsel, infolge der Vorspannung.

PS Es gibt Fälle, bei denen sich ungünstigere Werte ergeben, falls im Bruchsicherheitsnachweis die Wirkungen des Eigengewichts und der Vorspannung mit dem gleichen Sicherheitsbeiwert $S_1 = 0.8$ berücksichtigt werden.

3.5 Konstruktive Vorkehren

Den üblichen Schub- und Verbundbeanspruchungen infolge der Wirkungen von Querkraft und Torsion werden durch das Kriechen erhebliche Zusatzbeanspruchungen überlagert. Der monolithische Verbund zwischen den vorfabrizierten Längsträgern und Fahrbahnplattenelementen wird durch den Ortsbetonverguss der Längs- und Querfugen sowie der Stützenquerträger gewährleistet, sowie durch vorstehende Armierungen, die Aufrauhung der Flanschoberfläche der Längsträger und die speziellen Vertiefungen in der Stirnfläche der Fahrbahnplatten (Verzahnung). Die an den Trägerenden aus dem Flansch vorspringenden Nocken (vergl. Bild 3) wurden besonders zur Abtragung dieser Verdübelungsbeanspruchungen angeordnet; sie ermöglichen zudem die erwünschte möglichst hoch liegende Lage der Verankerungen der Vorspannkabel.

ZUSAMMENFASSUNG

Der Brückenüberbau der "Viaducs de la Plaine du Rhône" wird vollständig vorfabriziert. Die 78 Brückenfelder bestehen aus 2 Elementen konstanter Abmessung: den Längsträgern und den grossformatigen Fahrbahnplattenelementen. Durch ein neuartiges Verfahren ergibt sich im Endzustand eine monolithische bis zu 447 m lange und fugenlose Brücke.

Die unterschiedlichen Beanspruchungen der stark vorgespannten Längsträger im Gegensatz zu der nicht bzw. schwach vorgespannten Fahrbahnplatte verursachen ein unterschiedliches Kriechen und entsprechende Kräfteumlagerungen.

SUMMARY

The superstructure of the "Viaducs de la Plaine du Rhône" is entirely precast. The 78 spans are made of 2 units with constant dimensions: the longitudinal beams and the large size slab units. The new method results, in the final stage, in monolithic jointless bridges with a length up to 447 m.

The variations in stress in the longitudinal beams, which are highly prestressed, and in the slab, unprestressed or with very little prestress, produce a differential creep and consequently a redistribution of forces.

RESUME

La superstructure des "Viaducs de la Plaine du Rhône" est entièrement préfabriquée. Les 78 travées consistent en 2 éléments de dimensions constantes:les poutres longitudinales et les plaques de grand format pour la chaussée. La méthode originale utilisée permet d'obtenir, dans l'état final, des ponts monolithiques allant jusqu'à 447 m de longueur, sans aucun joint.

Les sollicitations différentes de la poutre longitudinale fortement précontrainte et de la chaussée non précontrainte ou relativement peu précontrainte, produisent un fluage différentiel et, par conséquent, une redistribution des forces.

II

BART Aerial Structures, Creep and Shrinkage Control Part I: Design

La structure aérienne du BART — Contrôle du fluage et du retrait
Partie I: Projet

BART Hochbahnstrecken — Kriech- und Schwindkontrolle
Teil I: Vorkehrungen

THOMAS R. KUESEL
Partner-Parsons, Brinckerhoff, Quade & Douglas
New York, USA

The San Francisco Bay Area Rapid Transit System, known as BART, comprises 75 miles of double-track construction. As shown on Fig. 1, one-third of this length is comprised of "Aerial Structures", including a single structure 10 miles long between Oakland and Hayward.

The typical aerial structure (Fig. 2) consists of twin precast, post-tensioned concrete box girders, each carrying a single track. The girders are supported on cast-in-place reinforced concrete piers. Simple span construction was chosen to simplify manufacture and erection of the girders, and an average span length of 70 feet was used to permit truck transportation from the casting yard to the site. Spans up to 98 feet long were used for street crossings, and required special permits and equipment to handle their 140-ton weight. The girders are connected by cast-in-place concrete closure strips, which also encase special earthquake anchorages. A uniform girder depth of 4'-0" was used for all spans to produce a "ribbon structure" architectural effect.

In order to eliminate the weight and cost of ballasted deck construction, as well as to secure a thin structure for architectural design, it was decided to fasten the running rails directly to the concrete deck. This made control of deformations of great importance, in order to provide a smooth-riding profile and to minimize future maintenance adjustments.

The history of concrete structures in the San Francisco area indicated that both shrinkage and creep would cause unacceptable deformations unless special precautions were taken. The predominant sources of concrete aggregates in the area are sandstones which form high-strength concrete, but with relatively large deformability.

Theoretical considerations indicated that limiting the free water content of the concrete mix would significantly reduce shrinkage, and using an

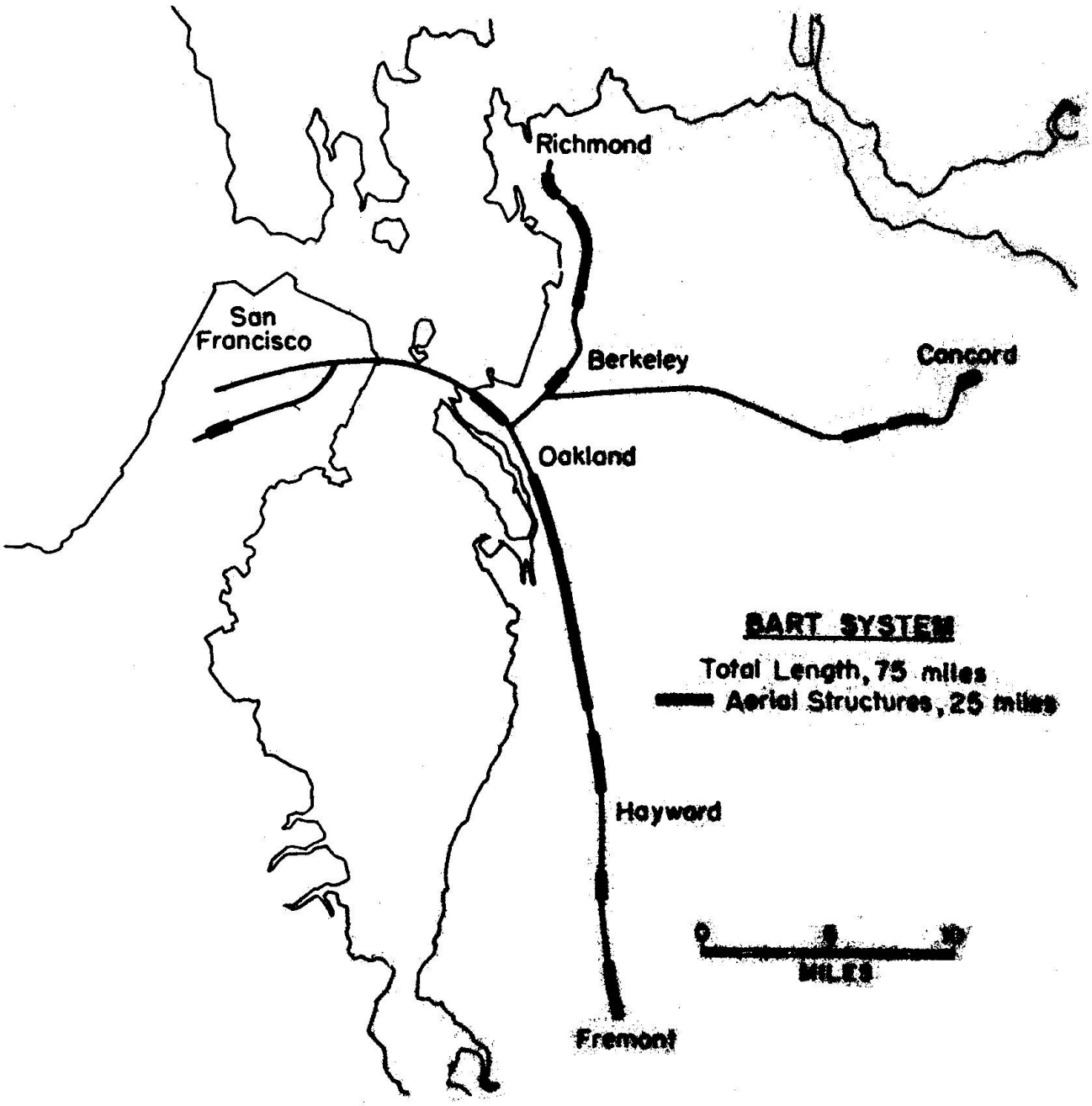

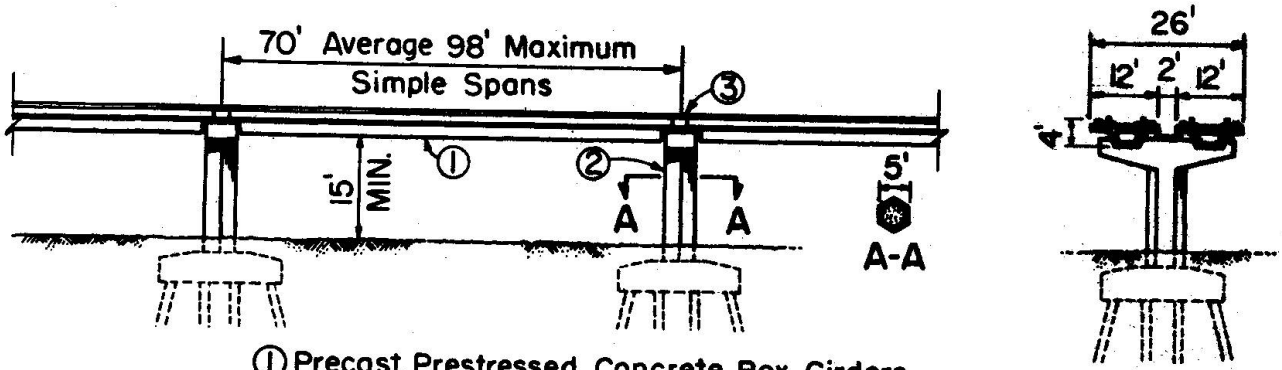

① Precast, Prestressed Concrete Box Girders
② Cast-in-place Reinforced Concrete Piers
③ Cast-in-place Concrete Closure Strip

BART AERIAL STRUCTURES
TYPICAL DETAILS

Fig. 2

aggregate with a high modulus of elasticity would reduce both shrinkage and creep. Since no accepted standards for these matters exist in the United States, it was necessary to devise special limitations and testing methods for the BART project. The aims were to screen out unacceptable materials without incurring excessive costs, and to set up performance tests that could be consistently repeated to provide a clear measure of acceptability.

The BART Standard Specifications for concrete include a limitation on free water content in pounds per cubic yard, with the allowable amount increasing with greater slump and smaller size aggregate. For the prestressed concrete box girders, both air-extraining and water-reducing admixtures were required. Both these ingredients promote workability of the mix, and this was recognized by further reducing the allowable free water content when admixtures were used.

The use of a large, well-equipped precasting yard was economically mandated by the size of the project – some 3,000 individual box girders comprising over 200,000 cubic yards of concrete. This implied careful layout of the prestressing tendons and the mild steel reinforcement in order to facilitate concrete placement, and efficient use of internal vibrators to ensure complete filling of the forms. In addition, the box girder webs were deliberately made a uniform 10 inches thick, and the bottom slab a uniform 8 inches thick, which exceeded the stress requirements, specifically to promote placement of the concrete.

By these means, the use of a relatively dry mix was secured despite the confined spaces inherent in a highly reinforced box girder section, with a great reduction in the free water content and resultant shrinkage. The actual mix used is shown in Table 1.

Table 1

BART SPECIAL CONCRETE

	Mix Proportions (Quantities)	
Material	1 Cubic Yard	1 Cubic Meter
Cement	699 pounds	415 kilograms
Water	298 pounds	177 kilograms
Fine Aggregate (1/4 inch max.)	1,163 pounds	691 kilograms
Coarse Aggregate (3/4 inch max.)	1,775 pounds	1,054 kilograms
Air-entraining admixture	9.0 fluid ounces	264 milliliters
Water-reducing admixture	1.49 pounds	850 grams

Beyond the general specification limits on proportions and on cleanness and soundness of materials, the construction contractors were permitted to select their own material sources and propose their own concrete mix. The proposed mix was tested against a control mix consisting of selected materials, with respect to compressive strength, modulus of elasticity, shrinkage, and

creep. Specimens of the proposed mix were required to be within certain percentages of the performance of the control specimens. (Details of the tests are given below in Part II.)

Setting the limits on relative performance requirements was a delicate matter. If the limits were set too high, all local material sources would be excluded and the premium costs for importing aggregate from distant sources would be excessive. If the limits were too low, many sources could be qualified, and the lowest cost (and probably poorest quality) material would be used, with resulting increased deformation and its associated problems.

By judicious accommodation between desirable and practical limits, two relatively economical local aggregate sources (one granite, and one basalt) were qualified, and several proposed sandstone aggregate sources were rejected. An interesting development was a proposal for an alternative design using light-weight concrete made with expanded shale aggregate. This design showed economic advantages and adequate strength, but was eventually rejected because the proposed mix was greatly deficient in creep resistance.

In addition to requiring special control of materials, the designers limited creep deformations by providing substantial amounts of nonprestressed mild steel reinforcement in the top slab, which resist any tendency toward upward bowing. The girder forms were also cambered downward by an amount calculated so that after elastic deformation under its own weight and that of track construction, plus an allowance for creep deformation, the girder would be approximately level. The calculation of creep allowance was based on the assumption that total creep deformation would be about three times the elastic deformation. Provision was made to adjust this allowance when experience had been obtained with the first girders cast using the approved concrete mix.

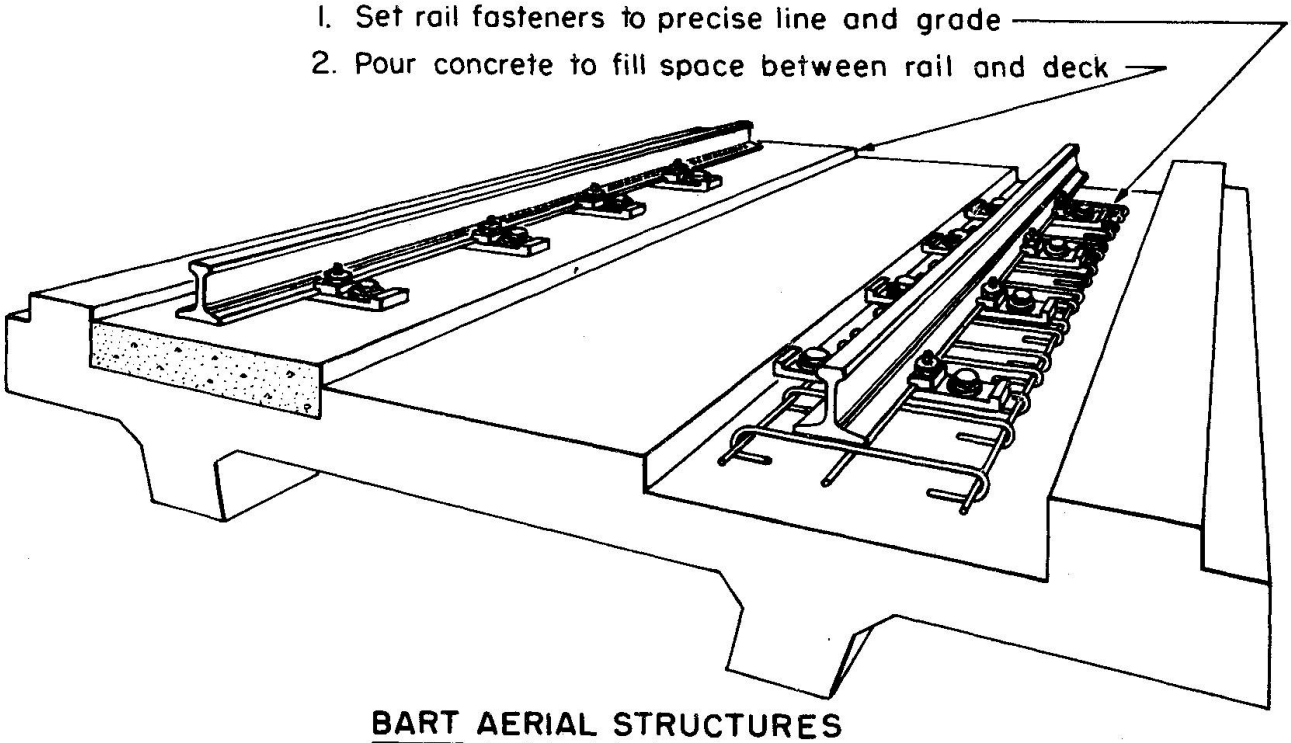

BART AERIAL STRUCTURES
"SECOND POUR" TRACK BED CONSTRUCTION

Fig. 3

Finally, it was recognized that despite controlled pre-casting, the practical tolerance in girder manufacture would exceed the allowable tolerance in rail profile. Accordingly, the running rails were independently set to final profile slightly above the concrete deck, as shown on Fig. 3, and the variable intervening space was filled with a "second pour" of concrete to take up any variations.

The cost of the BART shrinkage and creep control program, including premium charges for special aggregates and all costs associated with developing and carrying out the special testing program, was somewhat less than 2% of the cost of the girders using the special concrete, or about 1% of the total cost of the aerial structures.

SUMMARY

For 25 miles of the BART system, twin precast, prestressed box girders are made of concrete conforming to special creep and shrinkage tests. Reduction of water content and use of aggregates with high elastic modulus were primary control methods. Running rails were independently set to accurate profile, and then attached to the girders through a "second pour" of concrete. The cost of creep and shrinkage control was 1% of the total cost of the structures using special concrete.

RESUME

Sur quarante kilomètres, le système BART se compose de structures aériennes: poutres en caisson jumelées, préfabriquées en béton précontraint soumis à des essais de fluage et de retrait. Les premières méthodes de contrôle ont été la diminution de la teneur en eau, et l'utilisation des agrégats à module d'élasticité élevé. On a posé indépendamment les rails sur le profil exact; ensuite, ils ont été fixés aux poutres au moyen d'une deuxième coulée de béton. Le coût du contrôle du fluage et du retrait s'est élevé à 1% du coût total des structures utilisant le béton spécial.

ZUSAMMENFASSUNG

Für 40 Kilometer der BART Anlagen wurden doppelt vorgegossene, vorgespannte Kastenträger aus Beton hergestellt, die auf besondere Prüfungen für Kriechen und Schwinden abgestimmt waren. Die wesentlichsten Kontroll-Methoden waren Reduzierung des Wassergehaltes und Verwendung von Aggregaten mit hohem elastischem Modul. Die Schienen wurden unabhängig genau nach Profil gelegt und dann durch einen zweiten Betonguss mit den Trägern verankert. Die Kosten der Kontrolle über Kriechen und Schwinden bei Verwendung dieses Spezial-Betons beliefen sich auf ein Prozent der Gesamtkosten für das Bauwerk.

Leere Seite
Blank page
Page vide

II

BART Aerial Structures, Creep and Shrinkage Control
Part II: Laboratory Testing and Field Performance

La structure aérienne du BART — Contrôle du fluage et du retrait
Partie II: Essais de laboratoire et comportement sur le chantier

BART Hochbahnstrecken — Kriech- und Schwindkontrollen
Teil II: Materialprüfung im Labor und Leistungsfähigkeit des Bauwerks

KEITH D. BULL
Project Manager
Tudor Engineering Company
San Francisco, USA

The reliability and reproducibility of concrete tests have been questioned since their advent. Test procedures for determining shrinkage and creep characteristics have been used in the United States for many years. However, none of these procedures has attained a degree of acceptability comparable to the standard compressive strength test. In the United States this standard test is defined by the American Society for Testing and Materials as ASTM Designation C 39. The test is performed on a cylindrical specimen 6 inches in diameter by 12 inches high, and at an age of 28 days. The coefficient of variation of the results of this test is about 15 percent when applied to field produced specimens. The results of shrinkage and creep tests show considerably greater variation.

The most widely accepted shrinkage test in the United States is ASTM Designation C 157. This test was developed for use in a laboratory, and its application as a control test to field situations is questionable. In recent years the Division of Highways of the State of California has used a shrinkage test similar to ASTM C 157 as one test for the acceptability of set retarding, water reducing admixtures. The test is applied to determine the laboratory characteristics of a product. Once these have been determined, the product is accepted or rejected and no attempt is made to control its field performance. All of California's work is performed in their own laboratory using their own trained technicians. Such an ideal laboratory situation is enviable, but unrealistic for a private consultant to contemplate.

In the San Francisco area a number of shrinkage tests using a variety of test specifications and different sized specimens have become popular in the building industry. Most of these have been performed by privately owned laboratories. While the general quality of the work done by these laboratories has been good, the reproducibility of the shrinkage results produced by them has been notoriously poor. Part of the fault lies in the fact that large storage

facilities with controlled temperature and humidity are extremely expensive. In 1964 the only private facilities available were small make-shift boxes. In addition, no private laboratory had attempted a creep test.

Since BART was committed to using private testing laboratories, it was necessary to develop test procedures and also to stimulate the development of the laboratories to implement them. To accomplish this goal, it was necessary to develop a test which provided enough consistency so that it could be reproduced by several private laboratories. Also, the test had to be simple enough to be economically feasible and sophisticated enough to provide satisfactory results.

It was decided to use a comparison test rather than an absolute value test. That is, the results of the test mix, the concrete proposed by the contractor, were compared with those of a predetermined control mix. This procedure helped to eliminate the differences between the various laboratory facilities and their personnel. Unfortunately, it doubled the work and the cost of each test.

A specific aggregate source was used for the control mix. The aggregate is nearly pure quartz. It is rounded, river-run aggregate with a bulk specific gravity of 2.62, and an absorption capacity of 0.5 percent. The sand produced relative mortar strengths in excess of standard Ottawa sand mortar. Because of the unusually tight control at the source, gradation was maintained within plus or minus two percent with minor rescreening in the laboratory. The cement used was a blend of three local Portland Cements. The cement factor and slump were set at the same values as those of the test mix. Proportions for a typical 7.5-sack control mix with a 3.5-inch slump were as follows:

Material	Quantity
Cement	705 lb
Water	289 lb
Sand	1,342 lb
Coarse Aggregate	1,574 lb

It was decided that because of the time and costs involved in testing, testing would be limited to a qualification test at the beginning of the job and follow-up tests every six months. The specification called for comparisons of compressive strength, modulus of elasticity, shrinkage, and creep as follows:

Property	Performance of Test Mix versus Control Mix (Percent)
Compressive Strength:	
at end of curing cycle	95 minimum
at 28-day age	90 "

Property	Performance of Test Mix versus Control Mix (Percent)
Modulus of Elasticity:	
at end of curing cycle	95 minimum
at 28-day age	95 "
Shrinkage, 14 days after end of curing cycle	130 maximum
Creep, 28 days after end of curing cycle	110 maximum

The overall quality of the concrete, or Class, was specified by cement factor and slump. Provided that the mix was not changed, only standard compressive strength tests were required during construction. The tests for compressive strength and modulus of elasticity are standard ASTM tests and will not be discussed here.

The shrinkage test developed was patterned very closely after ASTM C 157. It specified prismatic specimens 3 inches by 3 inches by 11 inches long. Length changes were measured over the full 11-inch length. Three specimens were required for the reference mix and three for the test mix. The curing procedure used for the test specimens was that method proposed by the contractor for field use. Generally, the contractors used an 18-hour steam curing cycle consisting of 5 hours of set time, 11 hours of steam at 140 degrees Fahrenheit and 2 hours of cooling. The control mix was cured for seven days in a controlled atmosphere consisting of a relative humidity of 90 percent or greater and a temperature of 73.4 plus or minus 3 degrees Fahrenheit. The shrinkage of the control mix and test mix were compared at an age of 14 days after curing.

The creep test was developed with the help of Professor Milos Polivka at the University of California at Berkeley. It specified cylindrical specimens 6 inches in diameter by 16 inches high. Length changes were measured along three 10-inch gauge lines located 120 degrees from one another around the cylindrical surface. Six specimens were required for the reference mix and six for the test mix. Three specimens were to be loaded in the creep frame and the other three were to act as shrinkage adjustment specimens. The curing procedures were the same as those discussed under the shrinkage test. The specimens in the creep frame were subjected to compressive stress of 1,200 pounds per square inch. After adjustments for elastic strain and shrinkage strain, the creep strain of the control mix and test mix were compared at an age of 28 days after curing.

About 3,000 girders were cast for the job. The majority of these were produced by a single contractor at a precasting yard which was completely rebuilt for the job. The girders were cast in steel forms on a concrete bed.

The concrete was placed by a belt conveyor and vibrated internally and externally. The fresh concrete was steam-cured and the girders were stressed in place before storing at the yard. Stressing was done with 1-1/4-inch diameter high strength alloy steel rods. The girders were transported to the job by truck and placed by crane. Field control consisted of the compressive strength tests discussed previously and controlling the camber of the steel forms.

The camber of the forms was shown on the contract drawings for each girder. These camber dimensions were originally calculated on the basis of the properties of the control mix. After the first 100 girders had been placed in the field, a survey was made of the amount of camber in each girder. The survey indicated that the finished girder camber varied by plus or minus 3/4-inch from the average camber. It also showed that the average girder camber was approximately 1/2-inch greater than the calculated camber. Camber surveys made at different ages indicated that elastic and shrinkage strains were higher than anticipated while creep strains were lower. No attempt was made to explain the discrepancy between the calculated camber and observed camber, but the specified form camber was lowered to produce the desired finished product.

While it might be argued that the field control, mainly compression tests, did not constitute field control of the elastic and inelastic strain properties, the finished product results indicated otherwise. Before track was laid on the structure, a profile of the girders was made. On one four-mile section which was studied in detail, the mean difference between calculated and observed cambers was less than 1/8-inch while the standard deviation was less than 1/4-inch.

The resulting structure will provide a safe and comfortable surface for the passengers of the 1970's to travel throughout the San Francisco Bay Area at speeds of 80 miles per hour.

SUMMARY

The reliability of concrete testing has long been questioned. Test procedures for shrinkage and creep characteristics are usually too time consuming and expensive to apply to field applications. The field performance of the BART aerial structures provides evidence that the tests developed for BART were effective in solving these problems.

RESUME

On a longtemps discuté de la validité des essais sur le béton. Les procédés des essais de fluage et de retrait sont généralement trop longs et coûteux pour être utilisés sur le chantier. Le comportement sur place des poutres de la structure aérienne du "BART" prouve que les essais développés pour le "BART" ont résolu ces problèmes de manière efficace.

ZUSAMMENFASSUNG

Die Zuverlässigkeit von Betonprüfungen hat immer schon in Frage gestanden. Kriech- und Schwind-Untersuchungen für individuelle Betonbauwerke sind normalerweise zu zeitraubend und zu teuer. Die Leistungfähigkeit von BART's aufgestelzter Fahrbahn beweist, dass die speziell für BART entwickelten Prüfverfahren erfolgreich waren und dazu beigetragen haben, Kriech- und Schwind-Probleme vorteilhaft zu lösen.

Leere Seite
Blank page
Page vide

II

Effet du fluage et du retrait dans les constructions en béton partiellement précontraint

Auswirkung der Kriech- und Schwinderscheinungen in Bauten aus teilweise vorgespanntem Beton

Effect of Creep and Shrinkage in Partially Prestressed Concrete Structures

S. CHAIKES
Ingénieur-Conseil A.I.G.
Directeur du Bureau d'Etudes PRECO
Belgique

I. INTRODUCTION

Les pièces en béton précontraint intégral subissent à l'état permanent de fortes contraintes de compression, surtout dans les sections à grand rendement, ce qui entraine un fluage considérable et des déformations différées souvent indésirables. Dans bien des cas, celles-ci nuisent à l'aspect, provoquent des contre-flèches inégales dans les éléments juxtaposés et créent des perturbations dans les liaisons, de nature à entraver le développement du béton précontraint dans le bâtiment.

Ces fortes contraintes de compression présentent en outre un danger latent de microfissuration possible du béton lors de la précontrainte, pouvant entrainer dans les pièces ainsi affaiblies des contraintes de traction non négligeables, voire même une fissuration sous charges totales.

Dans d'autres cas, la fissuration de ce matériau, en principe non armé, par le retrait ou par le gradient thermique durant le durcissement et autres effets atmosphériques ou purement accidentels, comme un tassement d'appui avant la précontrainte, font en sorte que sous charges les fissures risquent de s'ouvrir pour un léger dépassement de ces charges si les pertes de précontrainte ou le frottement des câbles dépassent les prévisions du calcul.

La précontrainte partielle permet de remédier à cette situation. En effet, la précontrainte réduite atténue dans les proportions désirées la valeur du fluage et de la déformation différée, et l'armature ordinaire améliore les propriétés d'allongement du béton tant avant la précontrainte que sous charges et permet de résister aux effets atmosphériques et autres effets imprévisibles.

Ce dernier avantage diminue cependant en cas de forte concentration de l'armature ordinaire. En effet, celle-ci perturbe l'évolution du retrait d'abord et du fluage dû à la précontrainte ensuite. Le raccourcissement par le retrait moindre se solde par une contrainte de traction dans le béton tandis que le raccourcissement

par le fluage également moindre, se solde par une diminution de la compression du béton.

Il est donc essentiel de connaître avec une précision suffisante l'influence directe exercée par les deux armatures, de précontrainte et ordinaire, sur l'évolution du fluage et du retrait des pièces en béton partiellement précontraint pour pouvoir rendre cette solution intéressante par une utilisation équilibrée des deux armatures.

Dans cette communication, nous nous attacherons d'abord à évaluer les effets du fluage et du retrait en fonction des deux armatures pour tout le champ compris entre le béton précontraint intégral et le béton armé classique. Des formules pratiques permettront un calcul de ces effets d'après la compression induite dans les deux armatures.

L'intervention de ces effets dans la perte globale de précontrainte à la longue sera ainsi déterminée.

Ce calcul nous permettra ensuite de déterminer la zone du rendement optimum de la précontrainte, zone où les avantages procurés par l'armature ordinaire à concentration modérée sont prépondérants.

Ce faisant, nous aborderons le champ de la version dite "béton précontraint armé", procédé utilisé notamment pour de nombreux ouvrages d'art construits en Belgique. Conception de synthèse de la précontrainte et de l'armature, cette solution répond aux critères généraux de la Classe II du béton partiellement précontraint définis par le Comité Mixte F.I.P. - C.E.B.

Une comparaison des valeurs des effets du fluage et du retrait et de leurs conséquences pratiques pour des ouvrages d'art identiques réalisés en béton précontraint intégral, Classe I, et en béton précontraint armé clôturera l'exposé.

II. EFFET DU FLUAGE

L'effort de traction induit dans le béton par le fluage est égal à l'effort de compression induit dans les deux armatures, active (de précontrainte) et passive (ordinaire).

Dans l'hypothèse du fluage linéaire, cet effort peut être déterminé par l'expression suivante :

$$\Delta F_f = m_f \, \sigma'_{bt} \, A_t \, \beta_f \qquad (1)$$

avec $m_f = \varphi m_i$: coefficient d'équivalence acier-béton pour la déformation différée; φ étant le coefficient du fluage et $m_i = E_a / E_b$ le coefficient d'équivalence instantané.

σ'_{bt} : contrainte de compression initiale du béton sous charges permanentes au niveau du centre de gravité des deux armatures.

A_t : aire totale des deux armatures.

$\beta_f = \dfrac{1}{1 + K_t m_f \omega_t}$: degré d'induction < 1 de l'effort de compression dû au fluage dans les deux armatures.

$K_t = 1 + \frac{e_t^2}{i^2}$ étant le coefficient d'influence de l'excentricité résultante e_t des deux armatures à ce même niveau (fig. 1), i le rayon de giration et ω_t le pourcentage géométrique total des deux armatures.

Cet effort induit peut être transféré au centre de gravité de l'armature active. Il devra alors pour conserver le même effet à la fibre extrême, être majoré par un coefficient de transfert γ qui est le rapport des coefficients d'influence des excentricités de l'armature résultante et de l'armature active, à cette fibre extrême.

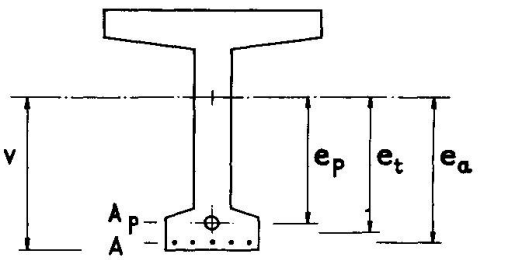

FIG.1

$$\Delta F_f \gamma = m_f \sigma'_{bt} A_t \beta_f \gamma \qquad (2)$$

$$\gamma = \frac{K_{tv}}{K_{pv}} \; ; \qquad K_{tv} = 1 + \frac{e_t v}{i^2} \; ; \qquad K_{pv} = 1 + \frac{e_p v}{i^2}$$

L'effort ainsi majoré, rapporté à la section de l'armature active A_p et à sa contrainte de traction initiale σ_{api} peut être considéré comme étant la perte de précontrainte par fluage, soit :

$$p_f = \frac{\Delta \sigma_{api}}{\sigma_{api}} = \frac{m_f \sigma'_{bt}}{\sigma_{api}} (1 + \alpha) \beta_f \gamma \qquad (3)$$

avec $\alpha = A / A_p$ rapport des aires des deux armatures.

Le premier terme du facteur $(1 + \alpha)$ est relatif à la perte directe dans l'armature de précontrainte, le deuxième terme est relatif à la perte indirecte dissipée dans l'armature passive.

Dans les cas courants des sections avec armature de précontrainte disposée au voisinage immédiat de l'armature ordinaire, le coefficient de transfert γ peut être pris égal à 1. La valeur de $m_f = \varphi m_i$ peut être prise égale à 2 x 5 = 10 pour les bons bétons.

III. EFFET DU RETRAIT

Pour les constructions post-contraintes, il faut distinguer :

1°- la phase avant la mise en précontrainte durant laquelle la présence de l'armature passive est seule à considérer.

2°- la phase après la mise en précontrainte où les deux armatures passive et active interviennent.

Ici également, l'effort de traction induit dans le béton par le retrait est égal à l'effort de compression induit dans les deux armatures active et passive.

Cet effort de compression peut être déterminé par l'expression suivante :

$$\Delta F_r = \Delta F_{r1} + \Delta F_{r2} = E_a A \varepsilon_{r1} \beta_{r1} + E_a A_t \varepsilon_{r2} \beta_{r2} \qquad (1)$$

avec ε_{r1} , ε_{r2} retraits correspondants du béton non armé et β_{r1} , β_{r2} degrés d'induction de l'effort de compression durant ces phases.

$$\varepsilon_{r1} + \varepsilon_{r2} = \varepsilon_r \quad : \text{retrait total.}$$

$$\beta_{r1} = \frac{1}{1 + K_a m_{r1} \omega_a} \quad ; \qquad \beta_{r2} = \frac{1}{1 + K_t m_{r2} \omega_t}$$

$$K_a = 1 + \frac{e_a^2}{i^2} \quad ; \qquad K_t = 1 + \frac{e_t^2}{i^2}$$

K_a et K_t étant les coefficients d'influence des excentricités de l'armature ordinaire et de l'armature résultante à leurs niveaux respectifs, m_{r1} , m_{r2} les coefficients d'équivalence moyens acier-béton et ω_a , ω_t les pourcentages géométriques correspondants durant ces phases.

Toutefois, vu la faible importance de l'effort de compression induit dans l'armature passive durant la première phase par rapport à l'effort induit dans les deux armatures durant la deuxième phase, on peut dans un but de simplification en cette matière, libérer le calcul de la sujétion aux deux phases, avec des valeurs de ε_{r1} , ε_{r2} m_{r1} et m_{r2} somme toutes assez aléatoires et effectuer le calcul en une phase comme si l'armature active était présente dès le début.

En procédant ainsi, on accepte un léger excès de sécurité, excès qui devient tout à fait négligeable pour la Classe III par exemple, où l'armature active est de plus en plus réduite par rapport à l'armature passive.

L'expression devient dès lors :

$$\Delta F_r = E_a A_t \varepsilon_r \beta_r \qquad (2)$$

avec $\beta_r = \frac{1}{1 + K_t m_r \omega_t}$: degré d'induction de l'effort de compression dû au retrait dans les deux armatures et m_r coefficient d'équivalence moyen acier-béton durant le retrait.

Cet effort de compression induit, transféré au centre de gravité de l'armature active tout en conservant le même effet à la fibre extrême et rapporté à sa section A_p et à sa contrainte de traction initiale σ_{api} peut être considéré comme la perte de précontrainte par retrait:

$$p_r = \frac{\Delta \sigma_{api}}{\sigma_{api}} = \frac{E_a \varepsilon_r}{\sigma_{api}} (1 + \alpha) \beta_r \gamma \qquad (3)$$

Ici également, comme pour le fluage, le coefficient de transfert γ peut très souvent être pris égal à 1.

La valeur de ε_r est à considérer en fonction de la composition et de la qualité du béton ainsi que du degré d'exposition à l'air. Dans les régions tempérées par exemple, ε_r est généralement de l'ordre de 0,25 mm/m pour les constructions exposées et de 0,40 mm/m pour les constructions protégées. m_r varie de 30 à 60 suivant la qualité du béton. Il est de l'ordre de 50 pour les bétons normaux.

IV. EXEMPLE D'APPLICATION

Ce calcul des pertes de précontrainte par fluage et retrait dans les constructions partiellement précontraintes, fonction de la concentration globale des deux armatures, permet de déterminer la zone du rendement optimum de la précontrainte et le choix d'une solution rationnelle.

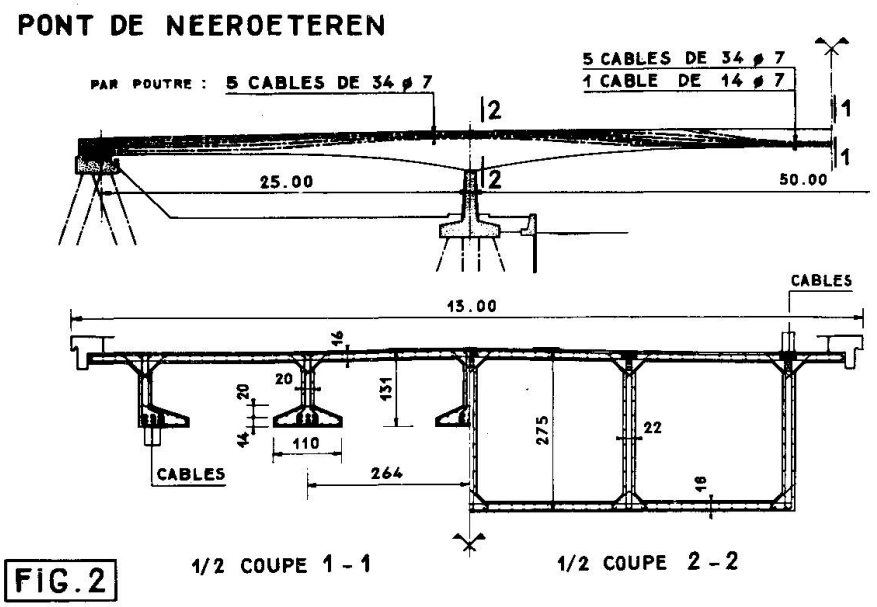

FIG.2

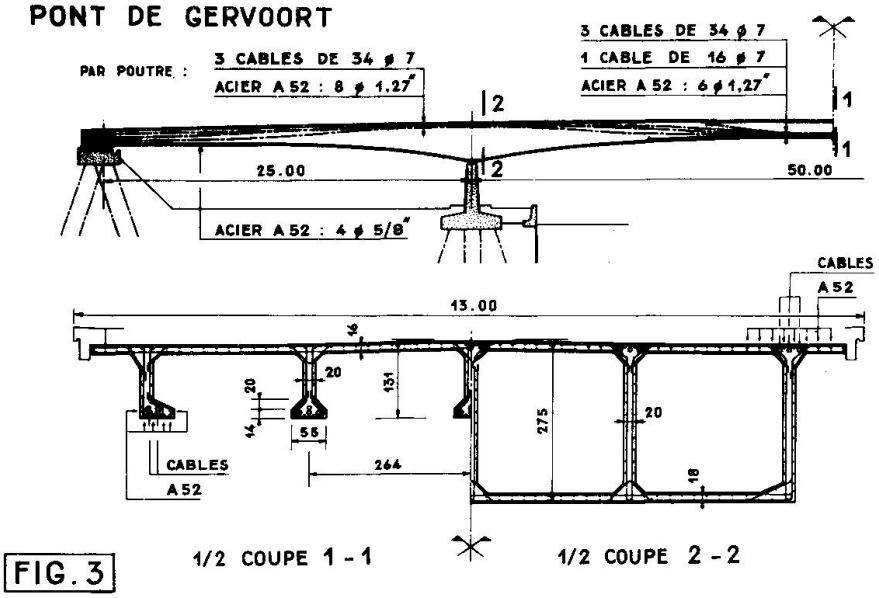

FIG.3

Nous allons l'illustrer à la lumière d'un exemple de deux ouvrages d'art identiques, réalisés l'un en béton précontraint intégral Classe I, l'autre en béton précontraint armé, conception de synthèse de la précontrainte et de l'armature répondant aux critères généraux de la Classe II.

La figure 2 montre le pont de Neeroeteren intégralement précontraint, à 3 travées continues de 50 et 2 x 25 m de longueur. Les poutres à semelle inférieure de 1 m 10 de largueur, forment caisson au voisinage des piles. La précontrainte se compose de 5 câbles de 34 Ø 7 continus plus 1 câble de 14 Ø 7 dans la section du milieu.

La figure 3 montre le pont de Gervoort partiellement précontraint de mêmes dimensions extérieures. La largeur de la semelle inférieure est de 55 cm seulement. La précontrainte se compose de 3 câbles de 34 Ø 7 continus plus 1 câble de 16 Ø 7 dans la même section, soit 36 % en moins, compensés par une armature passive de 6 Ø 1,27" A52.

L'indice de précontrainte i_{pr}, rapport de l'effort permanent de précontrainte à l'effort total des deux armatures, vaut ici 0,78 tandis que l'indice des charges permanentes i_{Mq}, rapport du moment permanent au moment total, est de 0,49 dans cette section.

La figure 4 donne le régime des contraintes dans la section.

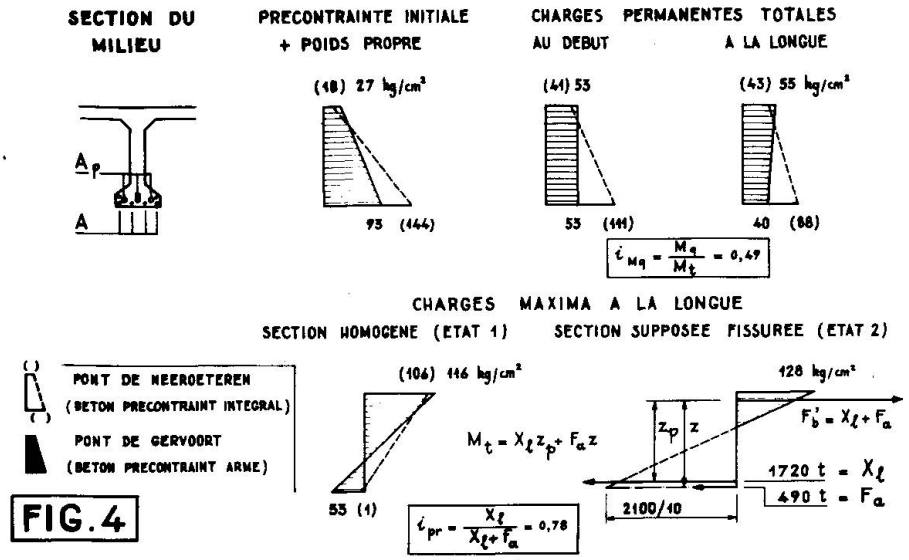

FIG.4

A la précontrainte, la compression à la fibre inférieure est de 144 kg/cm2 pour le pont intégralement précontraint contre 93 kg/cm2 pour le pont partiellement précontraint. La compression sous charges permanentes au début vaut respectivement 111 kg/cm2 et 53 kg/cm2. Elle est de 88 kg/cm2 et de 40 kg/cm2 à la longue.

Calcul des pertes de précontrainte :

Pont de Gervoort :

$B = 3,71\ m^2$; $I = 0,75\ m^4$; $v = 0,83\ m$; $A = 233\ cm^2$; $A_p = 227\ cm^2$ d'où $\alpha = \sim 1.$
$\omega_t = 0,0125$; $e_a = 0,76\ m$; $e_p = 0,72\ m$; $e_t = 0,74\ m$ d'où $K_t = 3,70$ et $\gamma = \sim 1.$
$m_f = 10$ d'où $\beta_f = 0,68$; $\sigma'_{bt} = 53\ kg/cm^2 = 0,53\ kg/mm^2$; $\sigma_{ap_i} = 85\ kg/mm^2$;
$E_a = 2 \times 10^4\ kg/mm^2$; $\varepsilon_r = 2,5 \times 10^{-4}$ et $m_r = 50$ d'où $\beta_r = 0,30$.

Soit
$$\rho_f = \frac{m_f\ \sigma'_{bt}}{\sigma_{ap_i}} (1 + \alpha)\ \beta_f\ \gamma = \frac{10 \times 0,53}{85} (1 + 1)\ 0,68 = 0,085$$
$$\rho_r = \frac{E_a\ \varepsilon_r}{\sigma_{ap_i}} (1 + \alpha)\ \beta_r\ \gamma = \frac{2 \times 10^4 \times 2,5 \times 10^{-4}}{85} (1 + 1)\ 0,3 = \frac{0,035}{0,120}$$

soit 12 % de perte dont 6 % de perte directe dans l'armature active et 6 % de perte dissipée dans l'armature passive.

Vu la valeur réduite de la contrainte de traction initiale σ_{ap_i} dans la section du milieu, par suite du frottement, par rapport à la résistance garantie R_g , la perte par relaxation de l'acier de précontrainte est voisine de zéro dans cette section. ($R_g = 150\ kg/mm^2$).

Pont de Neeroeteren :

$B = 4,15\ m^2$; $I = 0,95\ m^4$; $v = 0,74\ m$; $A_p = 354\ cm^2$; $\omega_p = 0,0085$; $\alpha = 0.$
$e_p = 0,65\ m$ d'où $K_p = 2,85$; $m_f = 10$ d'où $\beta_f = 0,80$; $\sigma_{ap_i} = 83\ kg/mm^2$;
$\sigma'_{bt} = 104\ kg/cm^2 = 1,04\ kg/mm^2$; $\varepsilon_r = 2,5 \times 10^{-4}$ et $m_r = 50$ d'où $\beta_r = 0,45.$

Soit
$$\rho_f = \frac{m_f\ \sigma'_{bt}}{\sigma_{ap_i}}\ \beta_f = \frac{10 \times 1,04}{83}\ 0,80 = 0,100$$
$$\rho_r = \frac{E_a\ \varepsilon_r}{\sigma_{ap_i}}\ \beta_r = \frac{2 \times 10^4 \times 2,5 \times 10^{-4}}{83} 0,45 = \frac{0,027}{0,127}$$

La figure 5 montre pour la même section la variation de la perte globale de précontrainte par fluage et retrait en fonction de la concentration totale des deux armatures et également en fonction de l'indice de précontrainte.

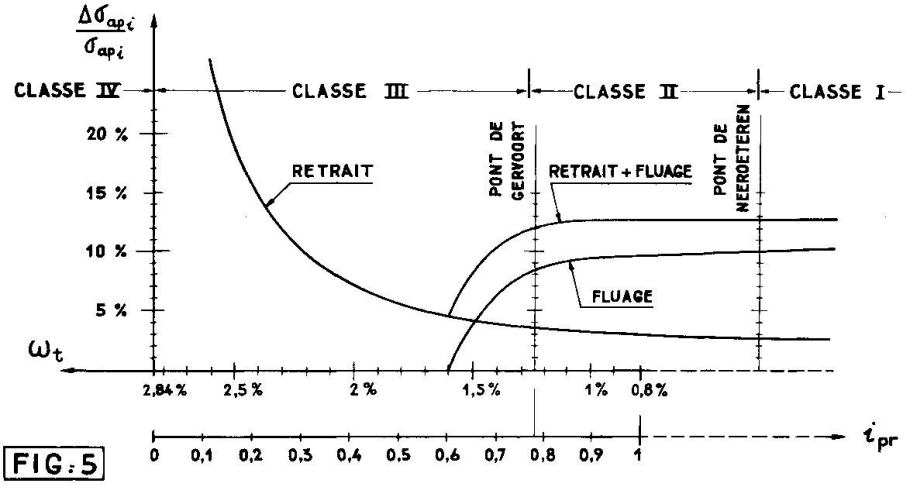

FIG:5

On voit que la perte par fluage diminue avec i_{pr} et s'annule en Classe III pour $i_{pr} = 0,6$, valeur correspondante à la décompression sous charges permanentes, tandis que la perte par retrait augmente rapidement à partir de ce moment et devient considérable avec l'augmentation de la concentration des armatures en Classe III.

Le choix d'un $i_{pr} > 0,6$ pour le pont partiellement précontraint est conditionné ici par les considérations de sécurité à la fissuration sous charges totales.

Remarquons que la perte directe par fluage et retrait dans l'armature de précontrainte est moitié moindre ici que pour le pont intégralement précontraint. La perte globale qui comprend la perte dissipée dans l'armature passive est du même ordre pour les deux ouvrages.

V. CONCLUSIONS

On aperçoit ainsi tout l'intérêt d'une précontrainte et d'une armature passive modérées. Avec l'élimination des effets nuisibles du fluage et du retrait, la solution équilibrée des deux armatures entraine des conséquences toutes favorables à la sécurité durant toutes les phases de sollicitation et notamment :

1) Avant la précontrainte : sécurité à la fissuration améliorée vis-à-vis des effets du retrait, des variations atmosphériques ou des sollicitations accidentelles, grâce à la présence de l'armature passive.
2) Lors de la précontrainte : sécurité quant au danger d'une microfissuration possible du béton par compression excessive, grâce à la précontrainte modérée.
3) Sous charges permanentes : sécurité accrue par l'absence d'un fluage et des déformations différées excessives.
4) Sous charges totales : sécurité à la fissuration mieux assurée grâce aux deux armatures par suite du bon comportement sous les trois phases précédentes et également en cas d'un léger dépassement des surcharges ou en cas de pertes de précontrainte ou de frottement des câbles supérieures aux prévisions.

BIBLIOGRAPHIE

S. CHAIKES :

Le béton précontraint armé.
IVème Congrès de la F.I.P. Rome 1962, Volumes 1 et 2.

Le béton partiellement précontraint,
Etude théorique, essais et réalisations.
Annales des Travaux Publics de Belgique, n° 2 - 1966.

Le béton précontraint armé,
Evolution dans la conception des structures précontraintes.
VIIIème Congrès de l'A.I.P.C. New-York 1968.

Ouvrages d'art remarquables en béton précontraint armé.
Annales des Travaux Publics de Belgique, n° 3 - 1969/70.

Comparaison d'ouvrages d'art identiques réalisés en béton précontraint intégral et en béton précontraint armé.
Contribution au VIème Congrès de la F.I.P. Prague 1970.

RESUME

L'auteur détermine l'effet du fluage et du retrait dans les constructions en béton partiellement précontraint à partir de la valeur de la compression induite par ces phénomènes dans l'armature de précontrainte et dans l'armature ordinaire.

Le calcul des pertes globales de précontrainte qui en résultent permet ensuite, à la lumière d'un exemple numérique d'ouvrages d'art réalisés, de déterminer la zone du rendement optimum de la précontrainte et le choix d'une solution rationnelle.

ZUSAMMENFASSUNG

Der Autor bestimmt die Auswirkung der Kriech- und Schwindeerscheinungen in Bauten aus teilweise vorgespanntem Beton auf der Grundlage des Kompressionswertes, der durch diese Erscheinung in der Vorspannbewehrung und in der normalen Bewehrung verursacht wird.

Die Berechnung der sich daraus ergebenden totalen Vorspannverluste erlaubt dann, mit Hilfe eines Zahlenbeispiels von bereits ausgeführten Bauten, die optimale Vorspannzone und die Wahl einer rationellen Lösung zu bestimmen.

SUMMARY

The author determines the effect of shrinkage and creep in partially prestressed concrete on the basis of the compression induced by these phenomena in the prestressing steel and in the ordinary reinforcement.

The calculation of the resulting total loss of prestress is then used, with the help of a numerical example from a completed structure, to determine the optimum efficiency range of prestress and the choice of a rational solution.

Das Konstruktionsprinzip der Flutbrücke der vierten Donaubrücke in Wien: Feldweiser Aufbau eines Durchlaufträgers

Design Principle used for the fourth Danube Bridge in Vienna:
Span-by-Span Construction of Continuous Girders

Le principe de construction du quatrième pont sur le Danube à Vienne:
Construction par travées d'une poutre continue

MANFRED WICKE
Dr.-Ing.
Wien, Oesterreich

Die vierte Donaubrücke liegt im Zuge der Nordostautobahn im Stadtbereich von Wien. Die Flutbrücke am linken Ufer umfaßt ca. 23.000 m2 Brückenfläche; sie gliedert sich in die Flutbrücke 1 und in die Flutbrücke 2 einschließlich der 4 Rampenbrücken.

Die Flutbrücke 1 ist ein Spannbetontragwerk von 6 x 51,20 m Stützweite und von im Mittel ca. 34,0 m Breite. Je Richtungsfahrbahn wurde ein dreistegiger Plattenbalkenquerschnitt von 3,60 m Konstruktionshöhe angeordnet. Die Flutbrücke 2 weist sieben Felder zu je 28,50 m Stützweite auf. Ihre Konstruktionshöhe beträgt 1,80 m. Der Querschnitt ist je nach Brückenbreite ein zwei- oder dreistegiger Plattenbalken. Im Bereich der abzweigenden Rampen ist eine untere Druckplatte angeordnet. Die Rampenbrücken sind wegen ihrer starken Krümmung im Grundriß als Hohlkastenquerschnitt ausgebildet. Ihre Spannweiten betragen im Mittel ca. 30,0 m. Alle Tragwerke sind in Längsrichtung nach dem Dywidag-Spannverfahren voll vorgespannt. Die Fahrbahnplatte, die Stege und die Querträger sind mit Rippentorstahl RT 50 schlaff bewehrt.

Bauherrin ist die Republik Österreich, vertreten durch das Bundesministerium für Bauten und Technik bzw. durch das Amt der Wiener Landesregierung. Projekt und Ausführung lagen in Händen der Arbeitsgemeinschaft Ing.Mayreder,Kraus & Co, Wien und Ed. Ast & Co, Graz.

Das Tragwerk wurde abschnittsweise auf Lehrgerüst hergestellt. Wegen der stark veränderlichen Brückenbreite schied der Einsatz eines Gerüstwagens aus. Die Wirtschaftlichkeit der Herstellung auf Lehrgerüst war auch in der geringen Höhe über dem Gelände von etwa 10–12 m begründet. Vergleichende Kostenberechnungen von seiten der Arbeitsvorbereitung ergaben einen wirtschaftlichen Vorteil bei Anordnung der Abschnittsfuge über den Pfeilern. Dies war unter anderem in dem geringeren Einsatz von Lehrgerüstmaterial über die ganze Baudauer begründet.

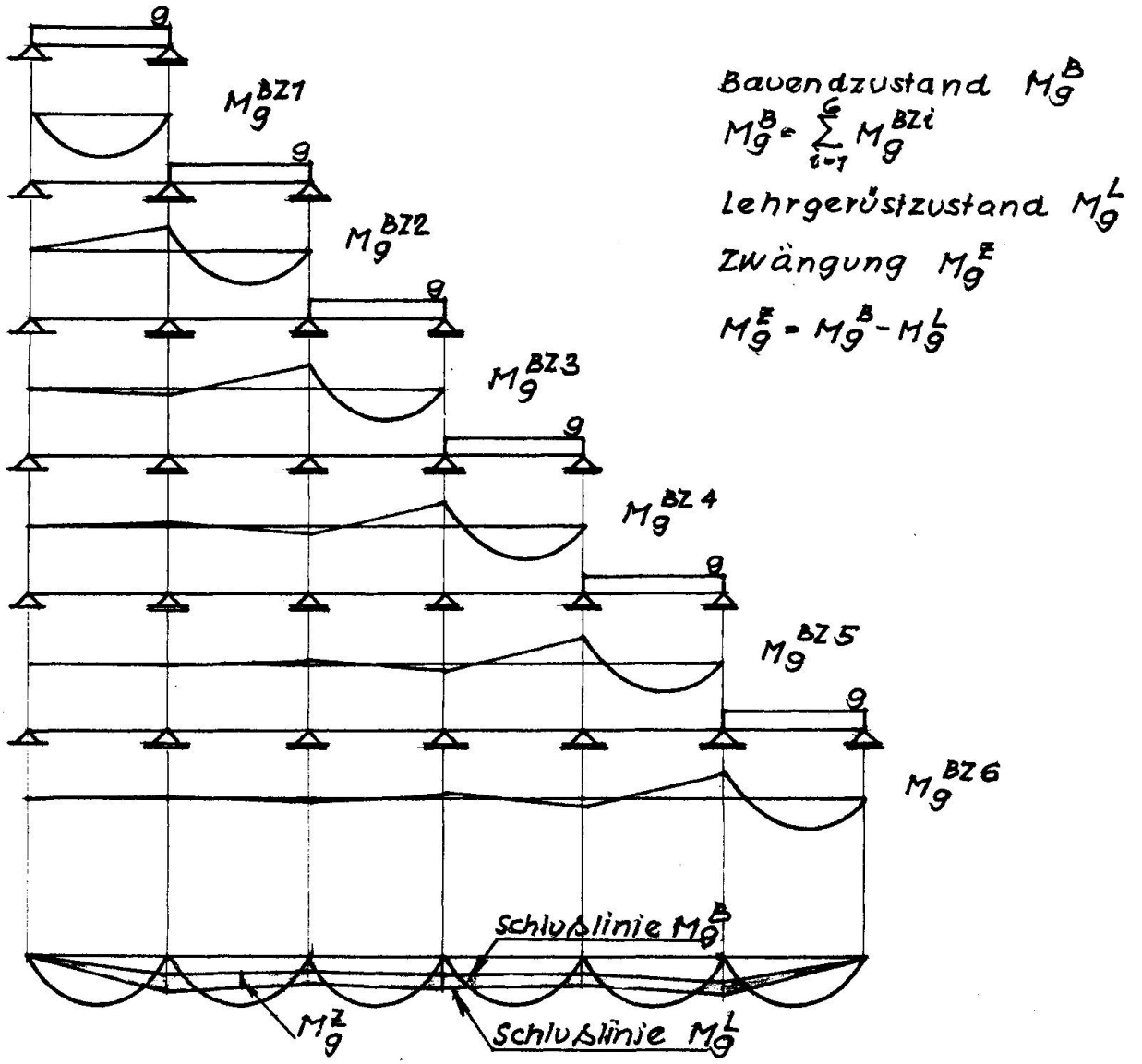

Bild 1 Aufbau der Eigengewichtsmomente an einem Sechsfeldträger mit J = const und g = const

Es war somit den Konstrukteuren die Aufgabe gestellt ein Konstruktionssystem für das Tragwerk zu finden, das den gewünschten feldweisen Bauvorgang ermöglichte. Eine mögliche Lösung wäre die Aneinanderreihung von Einfeldträgern gewesen. Dieses System schied aber aus, weil die Einsparungen beim Bauvorgang durch die Massenmehrungen im Tragwerk wieder verloren gegangen wären. Es kam daher nur ein durchlaufender Balken in Frage.

Beim Durchlaufträger besteht die Schwierigkeit darin, daß an der Arbeitsfuge, und damit im Stützenquerschnitt, zunächst kein Biegemoment auftritt, während im endgültigen System große Stützenmomente wirken. Verfolgt man den Aufbau der Eigengewichtsmomente (M_g^B) am Beispiel eines Sechsfeldträgers, so erkennt man, daß diese wesentlich kleiner sind als die zugehörigen Lehrgerüstmomente (M_g^L) am natürlichen System (siehe Bild 1)

Durch den Bauvorgang entsteht im fertigen Tragwerk eine Zwängung der Größe $M_g^Z = (M_g^B - M_g^L)$. Diese wird durch das Kriechvermögen des Tragwerkes abgebaut und weckt relativ große Kriechumlagerungen $M_g^\varphi = M_g^Z \, e^{-\varphi}$. Durch diese wird aber eine Unsicherheit in das Tragwerk getragen. Wenn man auch heute auf Grund verfeinerter analytischer Rechenverfahren den Einfluß des Kriechens sehr gut verfolgen kann, so bleiben trotzdem noch die Unsicherheiten in der Größe der Endkriechzahl φ und im zeitlichen Verlauf des Kriechens $\varphi = \varphi(t)$. Beide hängen von einer Anzahl von Parametern ab, die dem Konstrukteur zum Zeitpunkt der Berechnung noch nicht bekannt sind oder auf die er keinen Einfluß nehmen kann. Es ist daher ratsam ein Tragwerkssystem bei welchen das Kriechen einen großen Einfluß auf die Schnittgrößen hat zu vermeiden und sich möglichst unabhängig von der Größe des Kriechbeiwerts zu machen.

Wir haben bisher nur den Lastfall Eigengewicht (g) betrachtet und die Vorspannung (v) außer Acht gelassen. Es liegt nun der Gedanke nahe, in der stets vorhandenen gemeinsamen Wirkung der beiden Lastfälle g und v den Einfluß des Kriechens weitgehend auszuschalten. Wenn man bedenkt, daß durch die Arbeitsfuge an der Stütze zunächst dort kein Biegemoment auftritt ($M^B=0$), dann erscheint es sinnvoll, auch im Lehrgerüstzustand die Biegemomente an der Stütze null werden zu lassen ($M_L=0$). Wenn aber $M^L = M_g^L + M_v^L = 0$ sein soll, dann muß $M_v^L = - M_g^L$ werden.

Durch die Wahl einer geeigneten Spannstrangführung lassen sich aber tatsächlich Umlagerungsmomente wecken, die negativ gleich groß den Eigengewichtsstützenmomenten sind. Eine praktisch verwertbare Lösung erhält man, wenn man die Stützendrehwinkel α am Einzelfeld aus den beiden Lastfällen g und v entgegengesetzt gleich groß macht, wenn also gilt

$$\alpha_g = -\alpha_v$$

Für den vereinfachten Fall eines feldweise konstanten Trägheitsmomentes und eines konstanten Eigengewichtes sowie einer gleichbleibenden Vorspannkraft lassen sich die Bedingungen für eine derartige Spannstrangführung leicht angeben:

Lastfall Eigengewicht (g)

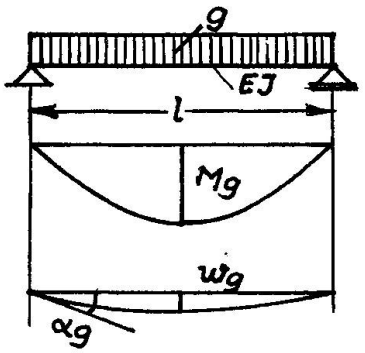

$$M_g = \frac{gl^2}{8}$$

$$EJ\alpha_g = \frac{gl^3}{24} = \frac{M_g l}{3}$$

Lastfall Vorspannung (v); parabolische Spannstrangführung

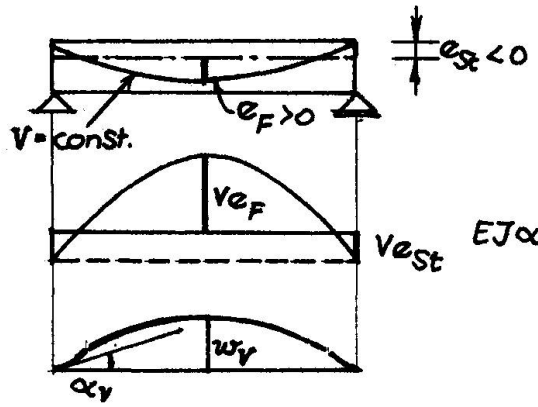

$$EJ\alpha_v = \frac{V.(e_F - e_{st}).l}{3} + \frac{V.e_{st}.l}{2}$$

$$= \frac{V.e_F.l}{3} + \frac{V.e_{st}.l}{6}$$

Die beiden Werte für αg und αv in die Bedingung $\alpha g = -\alpha v$ eingesetzt ergeben:

$$\frac{Mg.l}{3} = -\frac{V.eF.l}{3} + \frac{V.est.l}{6} \quad \text{oder} \quad -\frac{Mg}{V.eF} = 1 + \frac{est}{2eF}$$

Zu derselben Beziehung gelangt man, wenn man nicht vom freidrehbar gelagerten Balken als Grundsystem ausgeht, sondern den beiderseits starr eingespannten Balken wählt. Dann muß $M_v^{St} = - M_g^{St}$ werden.

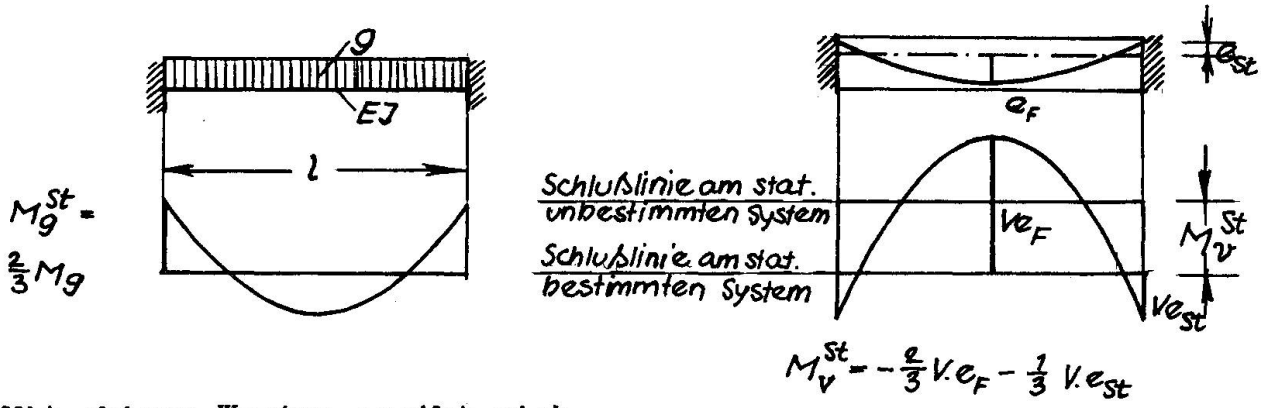

Mit obigen Werten ergibt sich

$$-\frac{2}{3} V.e_F - \frac{1}{3} V.e_{St} = +\frac{2}{3} M_g \quad \text{oder}$$

$$-\frac{Mg}{V.e_F} = 1 + \frac{e_{St}}{2e_F}$$

welcher Ausdruck mit dem oben abgeleiteten übereinstimmt.

In der Tabelle 1 sind für verschiedene Werte $\frac{e_{St}}{eF}$ zu zugehörigen Werte $-\frac{M_g}{Ve_F}$ eingetragen.

Tabelle 1

$-e_{St}/e_F$	0,0	0,1	0,2	0,3	0,4	0,5	0,6	0,7	0,8	0,9	1,0	2,0
$-M_g/Ve_F$	1,00	0,95	0,90	0,85	0,80	0,75	0,70	0,65	0,60	0,55	0,50	0,00

Bei einem Plattenbalkenquerschnitt liegt e_{St}/e_F zwischen - 0,2 bis - 0,4 und bei einem Hohlkastenquerschnitt zwischen - 0,5 und - 0,8.

Das Vorspannmoment in Feldmitte Ve_F muß aber einem Anteil des gesamten Lastmomentes $M_q = \frac{gl^2}{8} + M_{\Delta g} + \varphi M_p$ das Gleichgewicht halten. Setzt man für $M_q = - 1{,}2\ Ve_F$ dann ergibt sich für Plattenbalkenquerschnitte

$$M_g/M_q = 0{,}67 \ldots\ldots 0{,}75$$

und für Hohlkastenquerschnitte

$$M_g/M_q = 0{,}50 \ldots\ldots 0{,}62$$

Im Fall der Flutbrücke 1 betrug $M_g/M_q \sim 0{,}70$ und es konnte somit bei einem Plattenbalken eine geeignete Spannstrangführung gefunden werden.

Man sieht aber auch, daß durch den vorgegebenen kleinen Spielraum von M_g/M_q das Anwendungsgebiet des beschriebenen Konstruktionsprinzip eingeengt ist. Man kann den Bereich etwas erweitern, wenn man von der Forderung nach voller Vorspannung abgeht und beschränkte Vorspannung zuläßt, weil man dann etwas freizügiger in der Spannstrangführung wird.

Hat man die Bedingung $M_v^L = - M_g^L$ erfüllt in der Form, daß $\alpha_v = -\alpha_g$ gemacht wurde, dann hat jedes Einzelfeld unter dem Lastfall $(g + v)$ eine horizontal Tangente an der Stütze, $\alpha^{el}_{(g+v)} = 0$. Diese bleibt aber auch während des Kriechvorganges horizontal, was man direkt aus der Beziehung

$$\alpha^{\varphi}_{(g+v)} = \alpha^{el}_{(g+v)} \quad (1+\varphi) = 0$$

ablesen kann. Damit passen die benachbarten Felder auch nach dem Kriechen ohne Klaffung an der Stütze zusammen und es werden somit keine Kriechumlagerungen geweckt. Weiters erkennt man, daß während des gesamten Systemaufbaues keine Stützenmomente entstehen, da die Felder jeweils nahtlos aneinander passen.

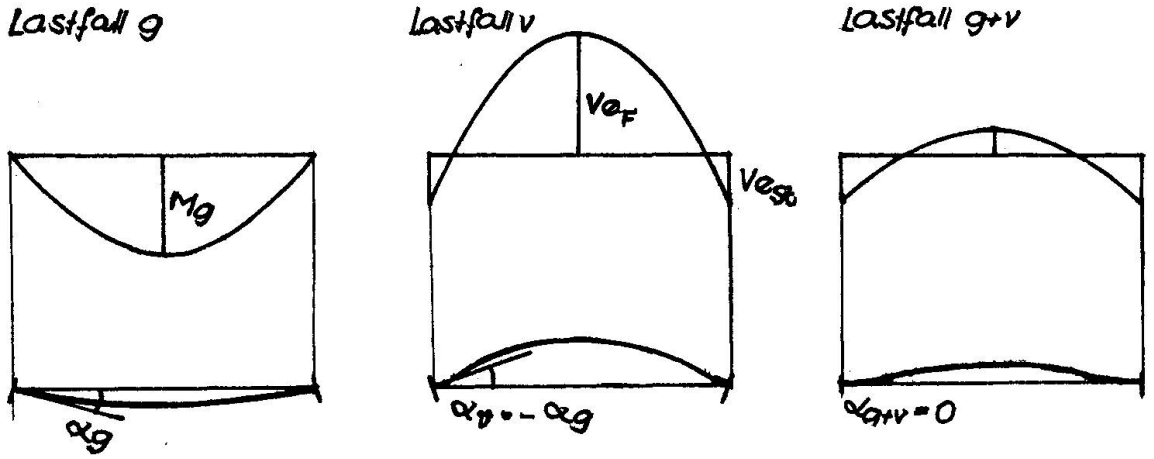

Die große Zwängung des Lastfalles Eigengewicht M_g^Z wird also durch eine entgegengesetzt gleich große des Lastfalles Vorspannung kompensiert

$$M_v^Z = - M_g^Z$$

Für den resultierenden Lastfall (g+v) stimmen somit Bauendzustand und Lehrgerüstzustand überein und es entstehen somit keine Kriechumlagerungen. Das Kriechen wirkt sich nur mehr über den Abfall der Vorspannkraft ΔV aus, und zwar in zwei verschiedenen Wirkungen.

Erstens entstehen die Schnittgrößen ΔV und $M_{\Delta V} = \Delta V.e$ am statisch bestimmten Grundsystem.
Zweitens weckt der Lastfall ΔV wiederum Umlagerungsmomente $M_{\Delta V}$ deren Größe unter der Voraussetzung eines über die Spanngliedlänge konstanten Spannkraftverlustes leicht angegeben werden kann.

$$M_{\Delta V} = - \frac{\Delta V}{V} \cdot M_v^L = \frac{\Delta V}{V} \cdot M_g^L$$

Diese Momente sind ein Bruchteil des Eigengewichtsstützenmomente und daher negativ und entlasten den Feldquerschnitt.

Beim Gebrauchsspannungsnachweis kann der Lastfall (g+v) in seiner Überlagerung in die Rechnung eingeführt werden und besteht aus der Aneinanderreihung der Freibalkenmomente der einzelnen Felder. Die Schnittgrößen der Lastfälle ständige Auflast (Δg) und Verkehrslast (φp) werden am durchlaufenden System ermittelt. Für den Lastfall Vorspannung kann man jedes Feld für sich getrennt betrachten, weil durch die horizontale Stützentangente keine Beeinflußung durch benachbarte Felder erfolgt. Die Spannstrangführung ist nach den Erfordernissen des Spannungsnachweises so zu wählen, daß sie der Bedingung $\alpha_v = - \alpha_g$ genügt.

Beim Bruchsicherheitsnachweis ist hingegen zu beachten, daß die Schnittmomente aus g und v mit unterschiedlicher Wertigkeit in die Berechnung eingehen. Aus diesem Grund müssen hiezu die Bauzustandsmomente und ihre Umlagerung in Richtung auf die Lehrgerüstmomente hin berechnet werden.

ZUSAMMENFASSUNG

Es wird ein Konstruktionsprinzip beschrieben, mit dessen Hilfe es möglich ist, einen vorgespannten Durchlaufträger feldweise herzustellen, ohne dass dadurch Kriechumlagerungen ausgelöst werden. Es gelingt dies durch Wahl einer Spannstrangführung, die Umlagerungsmomente weckt, die negativ gleich gross den Eigengewichtsstützenmomenten sind. Die Auswirkung des Kriechens wird damit auf den Einfluss des Spannkraftverlustes beschränkt.

SUMMARY

A design principle is described which permits the construction of a prestressed continuous beam in individual spans in such a way as to preclude the occurrence of any redistribution due to creep. This is accomplished by means of a tensioning strand arrangement resulting in moments of redistribution which are equal and opposite to the moments about the points of support resulting from the own weight of the structure. The effects of creep are thus restricted to the influence exerted by the loss of prestressing force.

RESUME

Description d'un principe de construction à l'aide duquel on peut construire par travées entières une poutre continue précontrainte sans provoquer de redistribution des efforts due au fluage. On y réussit en choisissant une position des câbles donnant naissance à des moments parasitaires correspondant négativement aux moments du poids propre sur les appuis. L'effet du fluage se trouve ainsi réduit à l'influence de la perte de précontrainte.

II

Effect of Creep on the Flexural Strength and Deformation of Concrete Beams

Influence du fluage sur la résistance et déformation en flexion des poutres en béton armé et précontraint

Einfluß des Kriechens auf die Biegefestigkeit und die Verformung von Stahlbetonträgern

A. HUBER R. RASIA
Institute of Applied Mechanics and Structures (IMAE)
Universidad Nacional de Rosario
Argentina

INTRODUCTION:

Some years ago the writers were engaged in an investigation of the effect of creep on the deformations and strength of statically determinate beams of reinforced concrete (1) and arrived at the conclusion that a previous creep history has little effect on the flexural strength. From limit analysis it can be inferred that this will also be true for continous beams. The same conclusion has been reported by Messrs. Ghosh and Cohn in the Preliminary Publication of this Symposium (2) .

A non-linear analysis program was used for solving the stresses in a rectangular concrete member by successive approximations. The effect of time dependant deformation was introduced by both the reduced modulus concept and by numerical integration of specific creep curves. The experimental program was limited in scope and included tests of aluminum reinforced resin models and simply reinforced concrete beams.

More recently the second author extended the method of solution to unsymmetrical double-T sections, typical of pre-stressed concrete (3) and had the opportunity to compare the theoretical solutions of long-time behaviour with the experimental data of the investigation under way at the Institut du Genie Civil of the University of Liege.

SECTION ANALYSIS:

The usual assumption of a linear strain distribution across the section is made while compressive and eventual tensile stresses in the viscoelastic material as well as in the reinforcement may follow arbitrary stress-strain laws (Fig. 1). Defining the

stress by their secant moduli and corresponding strains and combining equilibrium and compatibility equations a quadratic expression for the neutral axis position is obtained.

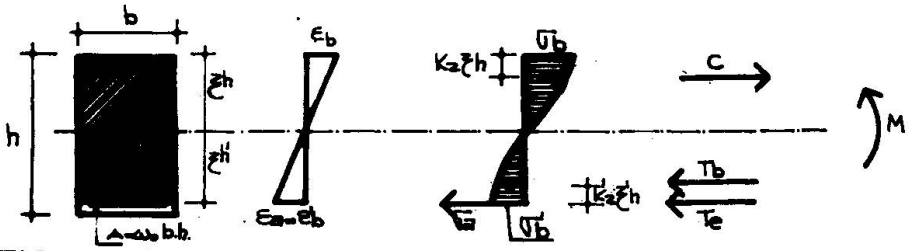

FIG. 1 STRAINS, STRESSES AND INTERNAL FORCES

The equations have general validity for any state of stress up to failure. The solution is obtained by a process of successive approximations. Moment-curvature relationships are also obtained. Special cases, as f. i. linear stress-strain laws, abscence of tensile stresses and combinations thereof are readily obtained. The failure moment is a limiting condition for which the strain-dependant coefficients take known values.

TIME DEPENDANT DEFORMATION:

For non-aging materials with linear creep and linear behaviour under instantaneous loading the stress-strain relation can be expressed by :

$$\varepsilon_b(t) = \sigma_b(t)\left[\frac{1}{E_b(t_o)} + \bar{\varepsilon}_o(t, \tau_o)\right] \qquad (1)$$

where $\bar{\varepsilon}_o(t,\tau_o)$ is the specific creep. The term between parenthesis can be interpreted as the inverse of a reduced modulus. Eq.(1) represents the first term of the exact solution of the problem by power series and constitutes in many cases of practical importance

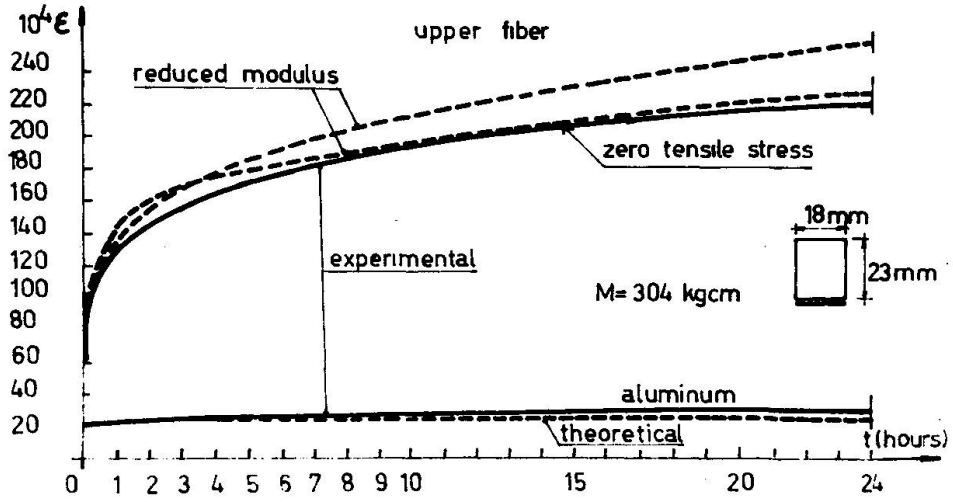

FIG.2 DEFORMATION-TIME RELATIONSHIP FOR ALUMINUN-REINFORCED EPOXY MODEL

a very good approximate solution (4). Introducing this reduced modulus in the equations of section analysis an approximate solution for the redistribution of stresses is obtained.

Fig. 2 shows the results of redistribution obtained with an aluminum reinforced resin model maintained under a constant moment and the comparison with reduced modulus solutions.

NUMERICAL SOLUTION:

For linear creep the strain increment can be expressed in function of the corresponding specific creep curves. From Fig. 3 the following expression is obtained:

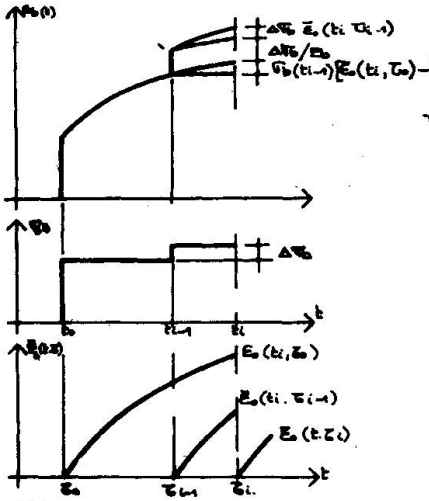

FIG. 3 FINITE VARIATION OF CREEP STRAIN

$$\Delta\varepsilon_b = \sigma_b(t_{i-1})\left[\bar{\varepsilon}_o(t_i,\tau_o) - \bar{\varepsilon}_o(t_{i-1},\tau_o) - \bar{\varepsilon}_o(t_i,\tau_{i-1}) - \frac{1}{E_b(t_{i-1})}\right] + \sigma_b(t_i)\left[\bar{\varepsilon}_o(t_i,\tau_{i-1}) + \frac{1}{E_b(t_i)}\right] =$$

$$= \sigma_b(t_{i-1})\, f_{i-1} + \sigma_b(t_i)\, f_i \qquad (2)$$

Substituting Eq. (2) into the equilibrium equations it is possible by iteration to obtain the unknown value of $\sigma_b(t_i)$ for each

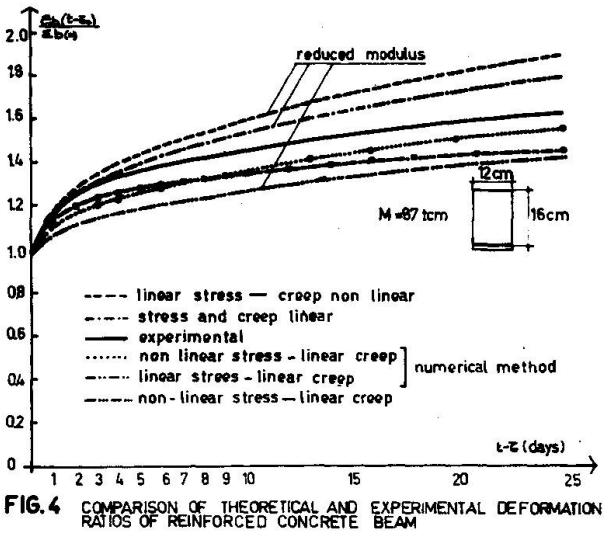

FIG. 4 COMPARISON OF THEORETICAL AND EXPERIMENTAL DEFORMATION RATIOS OF REINFORCED CONCRETE BEAM

time increment. This calculation is best performed by a computer. Fig. 4 shows the experimental and analytical results for a rectangular reinforced concrete beam, loaded at the age of 7 days just below its failure moment which was maintained constant for a period of 25 days when the beam was tested to failure.

ULTIMATE MOMENT OF A BEAM WITH PREVIOUS CREEP HISTORY:

In order to determine the failure moment of a reinforced concrete section with a previous creep history it can be assumed that at a certain instant, t, the deformations in both concrete and steel are known and that the applied moment is increased up to failure in a short period of time such that further creep deformation is excluded. Maintaining the hypothesis of linear strain distribution, failure will occur by limiting states of either concrete or steel reinforcement.

Designating the corresponding values of the limiting state by a horizontal bar, the following ratios of moments with and without a previous creep history are obtained:

$$\text{Failure by steel:} \quad \frac{\bar{M}r}{Mr} = \frac{1-\bar{k}_e\,\bar{\xi}}{1-k_2\,\xi} \qquad \text{(underreinforced)}$$

$$\text{Failure by concrete:} \quad \frac{\bar{M}r}{Mr} = \frac{\bar{\sigma}_a}{\sigma_a}\,\frac{1-\bar{k}_2\,\bar{\xi}}{1-k_2\,\xi} \qquad \text{(overreinforced)} \qquad (3)$$

where $\bar{\sigma}_a$ is the steel stress, inferior to its yield stress, but affected by the redistribution process. In order to evaluate the effect, comparative calculations were made for the test beam section with different assumptions for the form of the stress-strain relationship (linear, parabolic, rectangular) and for the ultimate strength of concrete with (146 and 195 Kg/cm^2) and without creep history (174 Kg/cm^2). It was found that even for extreme combinations the influence was only of the order of $\pm$ 10 %.

The results are not surprising since it is well known that the failure moment of underreinforced concrete sections is not influenced very much by even rather big concrete strength variations. It is also evident that an experimental determination would be virtually impossible because of inherent variations of material properties.

T-SECTIONS OF REINFORCED AND PRESTRESSED CONCRETE:

The calculations of creep deformations by the reduced modulus concept have been extended to double-T sections typical of prestressed concrete (Fig. 5) subjected to flexural moments applied in two stages.

The results of calculated deformations for zero prestress are shown in Fig. 6 and 7 by dashed lines for the maximum compressive

and tensile strain respectively. There is quite a good agreement between these calculated values and the experimental results (solid lines) of an investigation under way at the Institut du Genie Civil of the University of Liege.

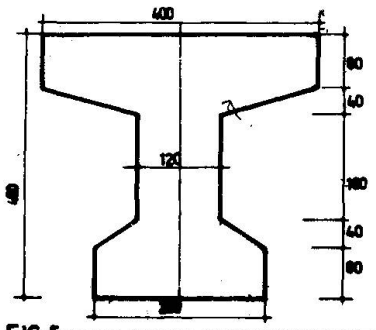

FIG. 5 CROSS SECTION CHARACTERISTICS OF TESTED BEAM (IN MM.)

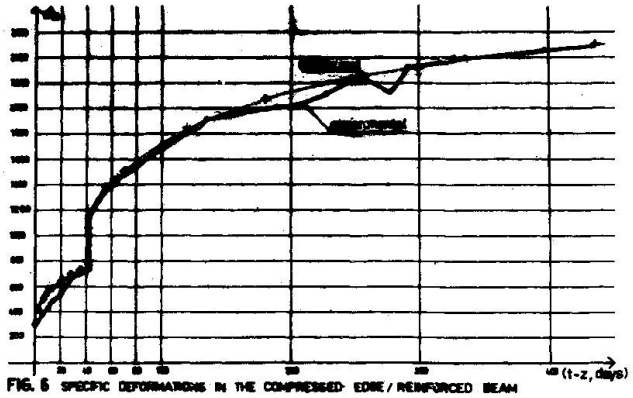

FIG. 6 SPECIFIC DEFORMATIONS IN THE COMPRESSED EDGE / REINFORCED BEAM

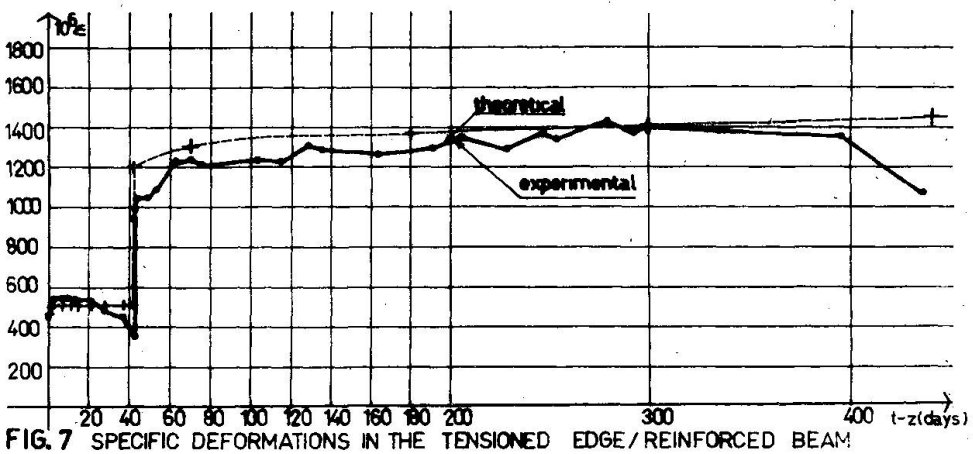

FIG. 7 SPECIFIC DEFORMATIONS IN THE TENSIONED EDGE / REINFORCED BEAM

In the case of fully prestressed concrete, the substitution of the reduced modulus in the conventional equations for concrete and cable stresses gives, together with the perfect bond condition between the cable and the surrounding concrete at all times, the wanted solution. Unfortunately, the cable eccentricity has also become a function of time so that a procedure of successive approximations has to be used. A computer program was written for these calculations. The same section shown in Fig. 5 was analysed and compared with the experimental results under way at the Institut du Genie Civil already mentioned earlier. Again a very good agreement was obtained between theoretical and experimental results (Figs. 8 and 9).

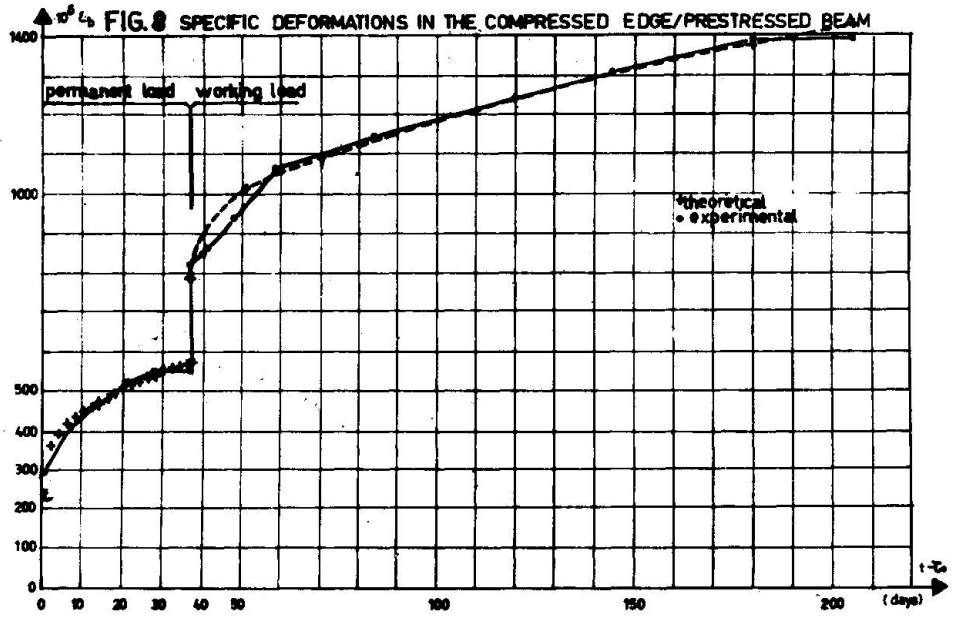

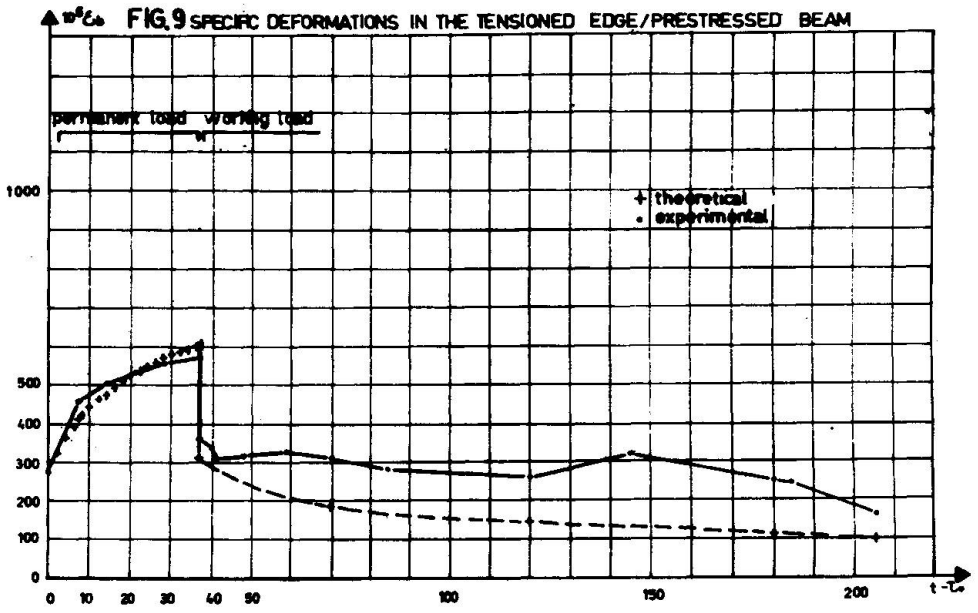

CONCLUSIONS:

The time dependant deformations of reinforced and prestressed concrete beams can be predicted with a good approximation by the reduced modulus concept or numerical integration of specific creep curves.

A previous creep history has a very small effect upon the flexural strength of reinforced concrete beams and the inheret variations of material properties make an experimental verification very difficult.

NOTATION:

E_b	secant modulus of concrete in compression
M	applied moment
M_r	failure moment
k_1	compressed area coefficient
k_2	coefficient for c. g. of compressed area
ε_b	concrete compressive strain in extreme fiber
$\bar{\varepsilon}_o$	specific creep strain
σ_b	compressive concrete stress in extreme fiber
ξ	neutral axis coefficient
σ_a	stress in steel reinforcement
τ	age
t	time

REFERENCES:

(1) A. Huber y R. Rasia "Investigación del comportamiento de vigas viscoelásticas armadas y sus cargas de roturas" .

XII Jornadas Sudamericanas de Ingeniería Estructural. III Simposio Panamericano de Estructuras, Caracas, 1967.

(2) S.K. Ghosh and M.Z. Cohn "Effect of creep on the flexural strength and deformation of structural concrete" .

Preliminary Publication, Symposium IABSE, Madrid, 1970.

(3) R. Rasia "Investigación del comportamiento de vigas simples de hormigón pretensado considerando retracción y fluencia lenta" .

IMAE, unpublished report, 1970.

(4) J.N. Distéfano "Base sperimentale per una teoria sul comportamento di strutture viscoelastiche lineari. Applicazione" .

La Ricerca Scientifica, N° 1, 1960.

SUMMARY

The effect of creep on the deformation and strength of statically determinate beams of rectangular and T-section of reinforced and prestressed concrete was studied both experimentally and theoretically. The effect of time-dependant deformation was introduced by both the reduced modulus concept and by numerical integration of specific creep curves.

The conclusion was made that a previous creep history has a very small effect on the flexural strength of reinforced concrete.

RESUME

On étudie de façon théorique et expérimentale l'influence du fluage sur la déformation et la résistance des poutres statiquement déterminées de section rectangulaire ou en T, en béton armé et en béton précontraint. L'effet du fluage a été introduit de deux manières: en utilisant le concept du module réduit et par intégration de la courbe de fluage spécifique.

On a pu conclure que l'histoire du fluage a une très petite influence sur la résistance à la flexion de la poutre armée.

ZUSAMMENFASSUNG

Der Einfluss des Kriechens auf statisch bestimmte Stahlbetonträger mit und ohne Vorspannung wird untersucht. Der Einfluss der zeitabhängigen Verformungen wurde mit Hilfe einer reduzierten Elastizitätskonstante und durch numerische Integrierung von spezifischen Kriechkurven berücksichtigt.

Es wurde die Schlussfolgerung gezogen, dass das vorhergehende Kriechen eine sehr kleine Auswirkung auf die Biegefestigkeit von Stahlbetonträgern hat.

II

Influence of Creep on Column Instability

Influence du fluage sur l'instabilité des colonnes

Der Kriecheinfluß auf das Knicken von Stützen

GUILLERMO J. CREUS
Institute of Applied Mechanics and Structures (IMAE)
Universidad Nacional de Rosario
Argentina

Whenever a structural element is required to resist compressive stresses, the possibility of failure due to instability has to be taken into account. Moreover, if the element is made of a visco-elastic material, the analysis should include the consideration of delayed instability phenomena (creep buckling).

Let's have a slightly bent concrete column under a constant compressive load. In the presence of creep, lateral deflexions increase with time, the action being triggered by the bending moments resulting from the simultaneous existence of initial deformation and end load. After a certain time, collapse may occur or, alternatively, the column may reach a new equilibrium position.

An usual definition states that a system in equilibrium is stable when, subjected to a small disturbance, it returns to its original position after the disturbance is removed. This definition is not of much use in the situations discussed in this work. A non-conservative system, when disturbed, may never return to its original position, but if a small disturbance causses only small displacement, it is for practical purposes as safe as a stable conserative system.

A stability concept introduced by Distéfano [1] seems more appropriate as a practical criterion: a column is considered stable if, for times $t \to \infty$ its deflexions approach a finite limit, that is

$$\lim_{t \to \infty} y(x,t) = y(x,\infty) < \infty$$

Naturally, the deflexions at $t=\infty$, although finite, could result larger than the material's allowable strain and stresses. In these circunstances, other considerations have to be used in addition to the stability criterion.

The simplest rigorous analysis of creep instability in concrete columns has been pionnered by the works of J. N. Distéfano. In the present discussion, the main results of this approach are outlined, and compared with Mr. Faessel's criteria and with other developments.

Linear case: the most general representation of linear viscoelastic behavior may be obtained with a stress-strain relation of the form

$$\varepsilon(t) = \frac{\sigma(t)}{E} + \int_0^t \sigma(\tau) f(t,\tau)\, d\tau \tag{1}$$

in which

$$f(t,\tau) = -\frac{\partial \varepsilon_0(t,\tau)}{\partial \tau} \tag{2}$$

and $\bar{\varepsilon}_0(t,\tau)$ is the specific creep strain function.

There are several different expressions currently used to represent the ageing of concrete. According to Aroutiounian [2] the specific deformation may be written:

$$\bar{\varepsilon}_0(t,\tau) = \left(\gamma_0 + \frac{c}{\tau}\right)\left(1 - e^{-\delta(t-\tau)}\right) \tag{3}$$

When the stress-strain relation (1) is introduced into the classical formulation for the equilibrium of a slightly bent bar, the following equation is obtained [1]:

$$\frac{\partial^2 y(x,t)}{\partial x^2} + \frac{M(x,t)}{E\,I} + \frac{1}{I}\int_0^t M(\tau) f(t,\tau)\, d\tau = 0 \tag{4}$$

In equation (4), $y(x,t)$ is the lateral deflexion, I the moment of inertia of the cross section and $M(t)$ the bending moment due to lateral loads and/or initial excentricity.

In adition to the terms present in the classical buckling analysis, equation (4) has the additional term representing the creep effects. Replacing equation (1) into the equation (4) the following integro-differential equation is obtained:

$$\frac{\partial^2 y(x,t)}{\partial x^2} + \frac{P}{E\,I}\, y(x,t) + \frac{P}{I}\int_0^t y(x,\tau)\, f(t,\tau)\, d\tau = \tag{5}$$

$$= -\frac{\chi(x,t)}{E\,I} - \frac{1}{I}\int_0^t \chi(x,t) f(t,\tau)\, d\tau$$

Equation (5) may be solved by expanding the functions $y(x,t)$ and $\chi(x,t)$ is series of orthogonal functions. Thus, the behavior of deflexions for times $t\to\infty$ may be analyzed. This analysis shows that deflexions remain bounded provided the axial load P satisfies the

inequality

$$P < \frac{P_E}{1 + E \gamma_o} = P^* \tag{6}$$

in which P_E is Euler's critical load and γ_o represents the asymptotic value of specific creep for the aged concrete. Similar results have been obtained by Ostlund [3] assuming expressions for the ageing for concrete other than (3).

It should be remarked at this point that, when Dischinger's formulation for ageing creep is considered, the asymptotic value of specific creep vanishes for aged concrete. Accordingly a limit loas is obtained which coincides with Euler's load [4] . Of course this result greatly overestimates the column's actual limit load.

Equation (6) applies to non-reinforced concrete elements. For reinforced members, this expression must be modified. In the particular case of a column with symmetrical cross section, the condition for asymptotic stability is written [5]

$$P < \frac{P_E}{1 + E_b \gamma_o} (1 + E_b \gamma_o n) \quad ; \quad n = \frac{E_e I_e}{E_b I_b} \tag{7}$$

in which I_b , E_b and I_e, E_e are respectively the moments of inertia and modulus of elasticity of concrete and steel.

References [1] and [5] give the exact expressions for the deflexions. A close approximation for the final values is obtained if a reduced modulus

$$\frac{E(\infty)}{1 + E(\infty) \gamma_o} \tag{8}$$

is used, together with the equations for instantaneous deflexions.

Non-linear case: when concrete stresses exceed 30-40 % of its compressive strength, non-linear behavior becomes important. In order to take into account non-linear creep effects, a procedure similar to that one used for the linear theory may be followed, provided some simplifying assumptions are made [6]

First, stress-strain relations are expressed in the form [2]

$$\varepsilon(t) = \frac{\sigma(t)}{E} + \int_0^t F(\sigma) f(t, \tau) d\tau \tag{9}$$

with

$$F(\sigma) = \sigma + \beta \sigma^2 \tag{10}$$

Second, the actual column cross section is replaced by an ideal I cross section.

The analysis indicates that asymptotic deflexions and buckling load are governed by a reduced modulus

$$\frac{E(\infty)}{1+E(\infty)\gamma_0(1+2\beta\sigma_0)} \tag{11}$$

in which

$$\sigma_0 = P/A \tag{12}$$

is the average stress on the cross section.

For the non-linear case, Mr. Faessel [14] proposes the use of a reduced modulus that in our notation may be written

$$\frac{E_t}{1+E_t\gamma_0} \tag{13}$$

E_t being the concrete tangent modulus which corresponds to the buckling stresses. This modulus applies to the case in which the same function represents the non-linear effect in both instantaneous and creep deformations, namely, when we may write

$$\varepsilon(t) = \frac{F(\sigma)}{E} + \int_0^t F(\sigma)\, f(t,\tau)\, d\tau \tag{14}$$

The above considerations show the great generality of stability criteria based on the concept of reduced modulus. As this concept has been greatly abused, it ought to be remarked that the mentioned results are <u>exact</u> under the assumed hypothesis and asymptotic behavior (i. E. for $t \to \infty$).

On the other hand, these conditions were found to be independent of excentricity or the existence of lateral loads. For practical cases, this appears to be not true, except for small excentricities and/or large slenderness ratios. The main reason for this discrepancy is the indefinitely elastic behavior assumed for the instantaneous strains. S nce elastic behavior is limited, it is; possible that for a given exentricity and a load $P<P^*$ the asymptotic deflexions predicted by the theory could never be reached because of premature plastic failure.

That is to say, a column whose material is characterized by a non-linear stress-strain curve for instantaneous loading, has a critical deflexion at which the applied load is the critical load. This critical deflexion can be calculated from the instantaneous material. This must be accompanied by a computation of the critical time necessary to reach the critical deflexion or, alternatively, the load which can be sustained during an infinite time; the latter approach being the more usual in concrete structures analysis [7]

Several works (besides the one under discussion) follow the

above mentioned approach. By using digital computers they are able to introduce close representations of actual material / characteristics, producing very reliable results. Mauch and Holley [8] for instance, perform an analysis similar to Naerlovic's [9] using experimental creep data. Warner and Thurlimann [7] consider the diminution in strength of concrete due to sustained load. Manuel and McGregor [10] introduce an analysis suitable for restrained / columns and frames.

A simplified procedure has been introduced in ref. [6]. In order to evaluate the actual limiting loads, the non-linear theory in combination with a suitable P-M interaction curve for the column cross section appears to be a reasonable approach.

Assume a given P-M interaction curve as shown in Fig. 1 and let $y(\infty, P, y_o)$ be the asymptotic deflexion. The resulting bending moment $P[y(\infty, P, y_o) + y_o]$ can be plotted and the load corresponding to the intersection of both curves will give the desired limit load. Deflexions may be calculated by using the reduced modulus (8).

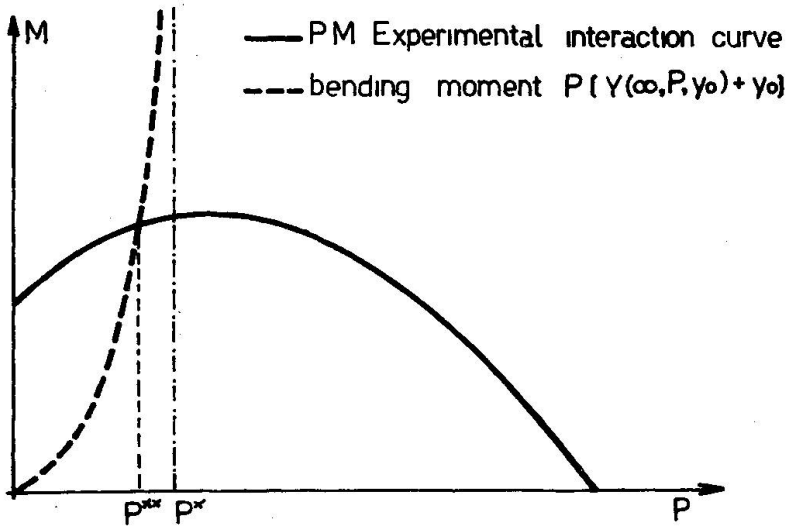

Fig. 1

Experimental results: an experimental program on plain and reinforced concrete columns has been carried out at I.M.A.E. in the period 1963-1965. A description of test procedures may be found in ref. [11]. Results have been published in refs. [12], [13].

The experiments were performed in a controlled environment with temperature 20°C ± 1°C, and humidity 50% ± 1%. Standard deviation in material properties were estimated in 5-6 %.

Columns with several different initial excentricities were tested in compression, under loads amounting to 0.95, 0.90, 0.85...

etc. of the instantaneous buckling value. The applied loads were maintained constant up to the columns failure; time dependent increments of deflexions and strains were registered.

A typical set of results, plotted as load versus critical

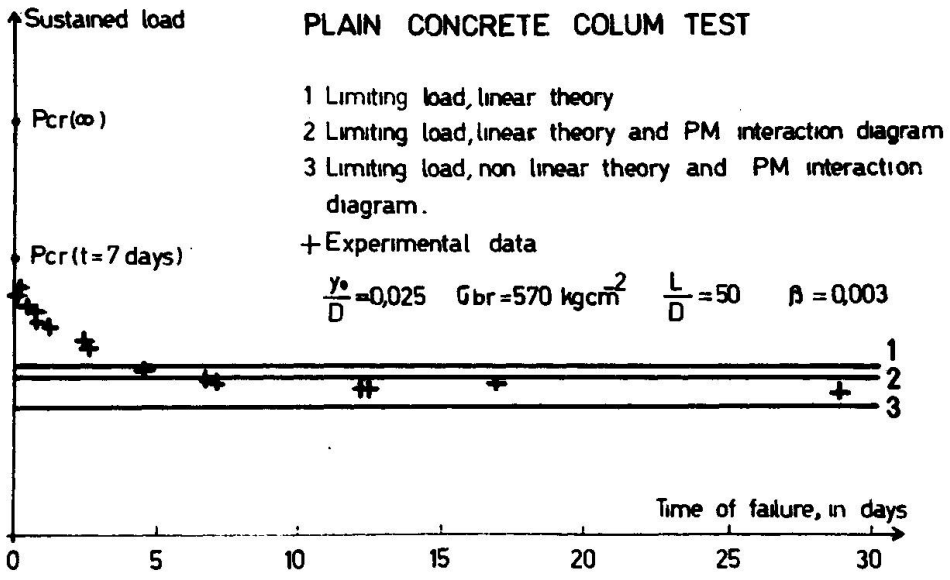

Fig. 2

time may be seen in Fig.2. The results are compared with some of the above mentioned theoretical conclusions. Line I indicates the

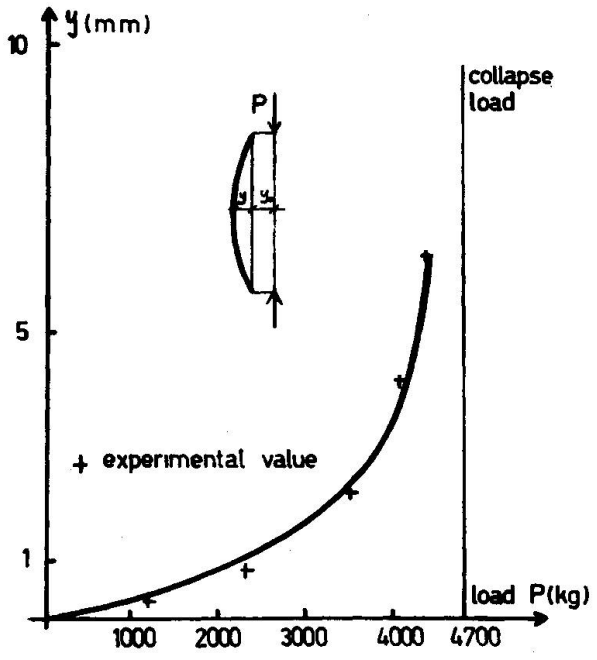

Fig.3

limit load predicted by the linear theory. Line 2 corresponds to the consideration of linear creep and the P-M interaction curve, and line 3 takes account of non-linear creep and the P-M curve.

Deflexions were calculated using the non-linear reduced modulus. In Fig. 3 a comparison between theoretical and experimental results for instantaneous deflexions may be seen.

Acknowledgment: some of the theoretical and all the experimental results were obtained in an investigation program partially supported by the C.N.I.C.T. (Consejo Nacional de Investigaciones Científicas y Técnicas).

References:

1 Distéfano J. N. "Sulla stabilitá in regime viscoelastico a comportamento lineare". Rendiconti, Accademia Nazionale dei Lincei, Rome, Italy, Fasc.5 y 6, Serie VIII, Vol.XXVII, 1959.

2 Aroutiounian N. Kh. "Applications de la theorie du fluage"Eyrolles, París, 1957.

3 Ostlund L. "Stability of Concrete Structures Submitted to Long Time Loads" Nordisk Betong, Vol.I, 1957

4 F. Levi et G. Pizzetti "Fluage - Plasticité - Precontraine, Dunond 1951.

5 Distéfano J. N. "Creep Deflexions in Concrete and Reinforced Concrete Columns" Publications, IABSE, Zurich, Vol. XXI, 1961.

6 Distéfano J. N. and G. J. Creus "Creep-Buckling of reinforced concrete Columns" (discussion) Journal ASCE, Vol.90, N° ST2, April 1964.

7 Warner R. F. and Thurlimann B. "Creep Failure of Reinforced Concrete Columns" Publications IABSE, Zurich, Vol.XXIII, 1963.

8 Mauch S. and Holley M. J. "Creep Buckling of Reinforced Concrete Columns" Journal ASCE, Vol.89 August 1963.

9 Naerlovic-Verljkovic, N. "Der Einfluss des Kriechens auf die Tragfähigkeit von Stahlbetonsäulen" Österreichisches Ingenieur Archiv, Vol.14 N° 2, June 1960.

10 Manuel R. F. and J. G. Mac Gregor "Analysis of Restrained Concrete

Columns Under Sustained Load". Journal ACI Vol.64 Jannuary 1967.

11 Distéfano J. N. and G. J. Creus "Equipment and Instruments for Creep and Creep-Buckling Test for Concrete" Bull.Rilem N° 22 March 1964.

12 Distéfano J. N. and G. J. Creus "Pandeo diferido de Columnas de Hormigón" IX Jornadas Sudamericanas de Ingeniería Estructural, Montevideo, Abril 1964.

13 Distéfano J. N. and G. J. Creus "Experiencias sobre pandeo de columnas esbeltas de hormigón simple". XI Jornadas Sudamericanas de Ingeniería Estructural, Sao Paulo, 966.

14 P. Faessel, "Influence du fluage sur les phénomenes d'instabilité. This Simposium,

SUMMARY

A short review of some simplified methods for the calculation of creep buckling loads is given.

Theoretical predictions are found in good agreement with experimental results.

RESUME

On donne un bref rappel des quelques méthodes simplifiées du calcul de la charge de flambement avec effet du fluage. Les résultats théoriques présentent un accord satisfaisant avec les valeurs expérimentales.

ZUSAMMENFASSUNG

Es wird ein kurzer Rückblick auf einige vereinfachte Verfahren zur Berechnung des Knickens beim Kriechen gegeben.

Theoretische Knicklasten stimmen gut mit Versuchsergebnissen überein.

II

Kriechknicken von Stahlbetonstützen

Creep Buckling of Reinforced Concrete Columns

Flambage des piliers en béton armé sous l'action du fluage

M. GRENACHER
dipl. Ing. ETH

B. THÜRLIMANN
Prof. Dr.

Institut für Baustatik an der
Eidg. Techn. Hochschule Zürich
Schweiz

Einleitung

Die Berechnung der Verformungen und der Nachweis der Knicksicherheit von Stahlbetontragwerken ist erschwert durch:

- nicht lineare Formänderungen des Stahles und hauptsächlich des Betons
- diskontinuierliches Formänderungsverhalten (Risse)
- Kriechen und Schwinden des Betons
- Streuungen der Festigkeits- und Querschnittswerte

Eine Berücksichtigung dieser Einflüsse in der Berechnung ist allgemein nur auf iterativem Wege möglich, wozu der Computer ein unentbehrliches Hilfsmittel ist. Um diese aufwendigen Berechnungen zu umgehen, werden in den entsprechenden Normen verschiedener Länder für die Bemessung von Stahlbetonstützen approximative Methoden angegeben, die zu unterschiedlichen und oft sogar unbekannten Sicherheiten führen. Die Schnittkräfte der Stützen werden mit den üblichen elastischen Methoden ermittelt. Die Bemessung wird dann mit Schnittkräften durchgeführt, die entsprechend der Schlankheit, des Armierungsgehaltes, der Dauerlast und der Lastexzentrizität modifiziert sind.

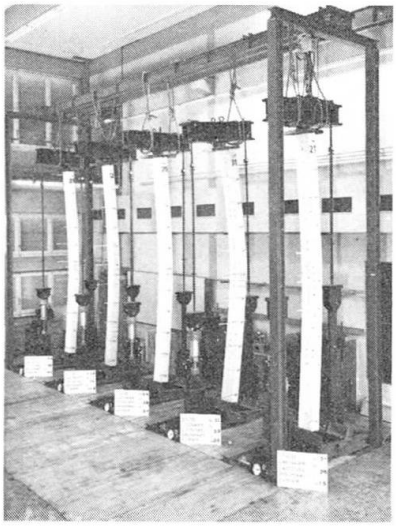

Bild 1: Versuchsanlage

Um bessere Grundlagen für eine zutreffendere Berechnungsweise zu schaffen, werden zur Zeit an verschiedenen Forschungsstellen umfassende Versuchsprogramme durchgeführt. Im Folgenden sollen ein paar Resultate von Versuchen,

die am Institut für Baustatik, ETH, Zürich, durchgeführt wurden, erläutert werden, [1] [2]. Es handelt sich um Versuche, in denen der Einfluss der Dauerlasten auf das Verformungsverhalten und die Traglast von gelenkig gelagerten Stahlbetonstützen untersucht wurde.

Bild 1 zeigt die Versuchsanlage [3], die es ermöglichte, gleichzeitig fünf Langzeitversuche mit individuell steuerbaren Lasten durchzuführen.

Nicht lineare Formänderungen

Das Verhalten von Stützen ist entscheidend beeinflusst durch deren Verformungen. Um etwas über Verformungen aussagen zu können, müssen die Spannungs- Dehnungs- Diagramme der Materialien bekannt sein. Diese sind sowohl für den Beton, wie auch für den kaltverformten Armierungsstahl nicht linear. Zudem ist besonders das Betondiagramm sehr stark von der Belastungsgeschwindigkeit und der Dauer der Belastung abhängig. Versuche zu seiner experimentellen Ermittlung müssen dehnungsgesteuert werden. Um den Einfluss der Belastungsgeschwindigkeit zu erfassen, müssen Dehnungshalte gemacht werden. Bei konstanter Dehnung sinken die Spannungen auf die sogenannten statischen Festigkeitswerte ab, wobei natürlich der Einfluss des Kriechens beim Beton nicht eliminiert werden kann. Unter dem Einfluss von Dauerlasten nehmen die Dehnungen um ein Mehrfaches der nicht linearen Kurzzeitdehnungen zu. Für verschieden lange Belastungszeiten müssen deshalb entsprechende Spannungs- Dehnungs-Diagramme verwendet werden. Die Verformungsberechnungen müssen also schrittweise für verschiedene aufeinanderfolgende Zeitintervalle durchgeführt und superponiert werden.

Diskontinuierliches Formänderungsverhalten

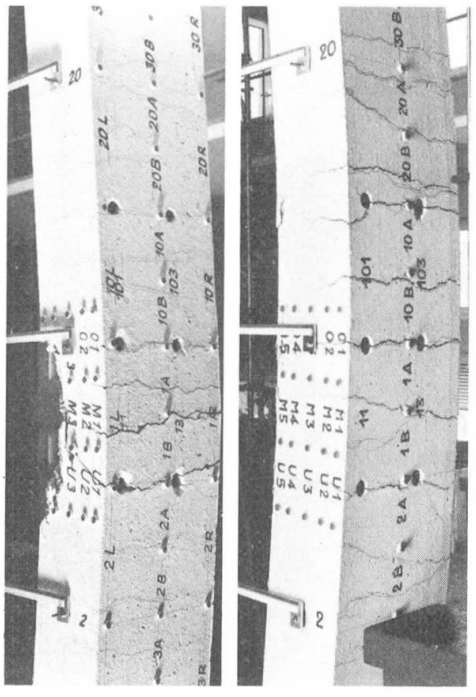

Bild 2: Rissebilder von zwei unterschiedlich beanspruchten Versuchsstützen

Das Formänderungsverhalten von Stahlbetonstützen ist beeinflusst durch die Risse und deren Verteilung über die Stützenlänge. Die Verteilung der Risse ist stark abhängig von der Dauerlast und deren Anfangsexzentrizität. Diese Abhängigkeit ist ersichtlich aus Bild 2. Die beiden Versuchsstützen sind 433 cm lang, haben einen Querschnitt von H = 15 cm und B = 25 cm, eine Schlankheit λ von 100 und einen Armierungsgehalt μ bezw. μ' auf der Zug- und auf der Druckseite von je 0,84 %. Die Stütze links wurde mit grosser Dauerlast und kleiner Anfangsexzentrizität belastet. Bei Belastungsbeginn wurden sowohl auf der Druckseite wie auch auf der späteren Zugseite Betonstauchungen gemessen. Bedingt durch das unterschiedliche Kriechen nahm im Laufe der Zeit die Krümmung der Stützensegmente zu. Mit den wachsenden Auslenkungen wurde auch die Biegebeanspruchung vergrössert. Im mittleren Stützenbereich wurden die Betonstauchungen auf der kon-

vexen Seite abgebaut. In einem beschränkten Bereich dehnte sich der Beton in der Folge, und die weiteren Verformungsvorgänge konzentrierten sich in diesem mittleren gerissenen Bereich. Die Stütze rechts im Bild 2 wurde mit kleiner Dauerlast und grosser Anfangsexzentrizität belastet. Sie dehnte sich auf der Zugseite unmittelbar nach der Belastung, und die Risse verteilten sich über die ganze Stützenlänge.

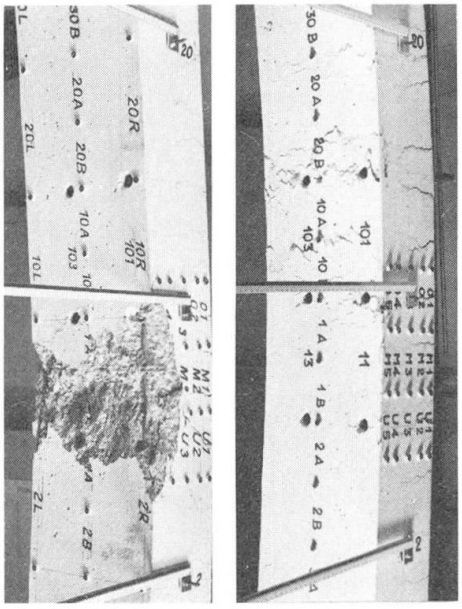

Bild 3: Bruchbilder von zwei unterschiedlich beanspruchten Versuchsstützen

Bild 3 zeigt die zu denselben Stützen gehörenden Bruchbilder. Bei der nur wenig exzentrisch mit grosser Dauerlast belasteten Stütze links im Bilde ist die Betondruckzone in einem sehr kleinen Bereich zerstört worden. Die Druckarmierung knickte aus. Bei der Stütze rechts im Bilde, die mit grosser Exzentrizität und kleiner Dauerlast belastet wurde, verteilt sich die Zerstörungszone über einen grossen Bereich. Der Beton wurde nicht abgesprengt.

Aus der Differenz der auf beiden Seiten gemessenen Betonverformungen und der Höhe des Querschnitts wurden die Krümmungen gerechnet. In Bild 4 sind die gemessenen Auslenkungen und Betonverformungen sowie die berechneten Krümmungen für eine Versuchsstütze dargestellt. Die ausgeprägten Krümmungsspitzen sind auf die Risse zurückzuführen. Auch hier lässt sich die starke Konzentration der Risse im mittleren Bereich der nur wenig exzentrisch belasteten Stütze erkennen.

Unabhängig von der Belastungsart traten die ersten Risse immer bei einer Dehnungszunahme gegenüber dem unbelasteten Zustand von $0.2 - 0.3 \cdot 10^{-3}$ auf. Der Ort der primären Risse war immer gegeben durch die Lage der Bügel. Waren einmal Risse entstanden, so konzentrierten sich die weiteren Verformungen auf die gerissenen Querschnitte. Die zwischen den Rissen liegenden Segmente wiesen nur noch eine geringe Zunahme der Verformungen auf. Bild 5 zeigt Dehnungsmessungen, die mit Strain Gages über eine Stützenlänge von 20 cm gemacht wurden.

Als Grundlage für die Verformungsberechnung dient die Beziehung zwischen Moment-Axiallast und Krümmung. Diese Beziehung darf nicht aus den lokalen Dehnungen berechnet werden, da die Dehnungen zu stark beeinflusst sind durch die Risse. Es muss deshalb eine nominelle Krümmung definiert werden, die aus Dehnungsmittelwerten über eine Länge mehrerer Rissabstände berechnet wird. Mit dieser nominellen Krümmung wurden die Auslenkungen aus den gemessenen Dehnungen berechnet und waren in sehr guter Uebereinstimmung mit den gemessenen Biegelinien.

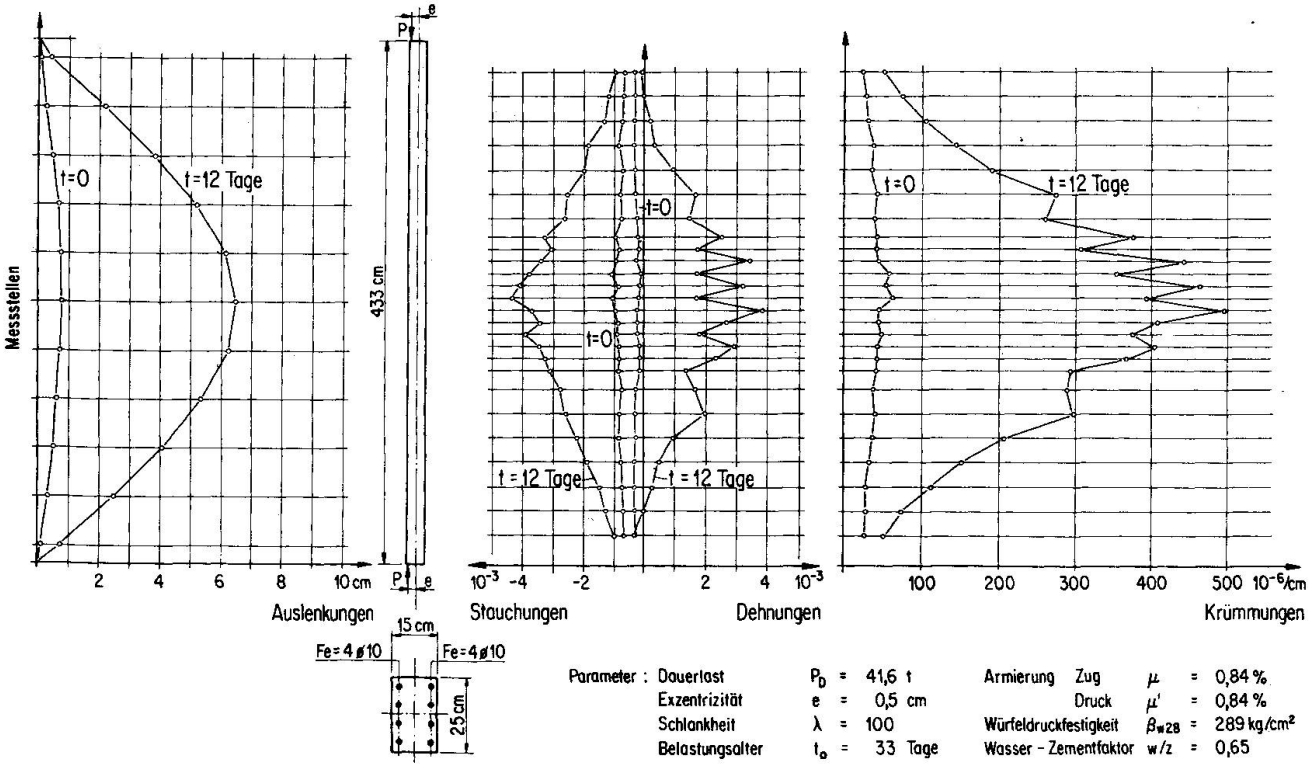

Bild 4 : Auslenkungen, Betonverformungen und Krümmungen einer Versuchsstütze

Einfluss des Kriechens auf die Auslenkung und die Knicksicherheit

Bedingt durch das Kriechen des Betons können die Stützenauslenkungen unter konstanter Dauerlast um ein Mehrfaches der Auslenkung unmittelbar nach Aufbringen der Last zunehmen. Bei der Bemessung muss diesen vergrösserten Auslenkungen und den davon linear abhängigen Momenten in irgend einer Form Rechnung getragen werden.

Die Auswertung der Versuche ergab drei grundsätzlich verschiedene Auslenkung - Zeit Kurventypen. Bild 6 zeigt oben eine Auslenkung - Zeit Kurve einer Stütze, die wenige Stunden oder Tage nach der Belastung infolge Kriechen versagt. Unten ist die Charakteristik einer Stütze gezeigt, bei der sich die Auslenkungen stabilisieren und die nicht zum Bruch kommt. Die Auslenkungskurve in der Mitte liegt zwischen den beiden erwähnten Grenzfällen. Die zusätzlichen Auslenkungen stabilisieren sich bis zu einem Wendepunkt. Nachher nehmen sie wieder vermehrt zu bis zum Bruch der Stütze.

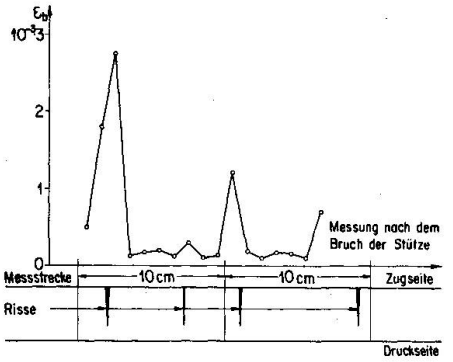

Bild 5 : Gemessenes Dehnungsverhalten des Betons zwischen Rissen

Das Auslenkung - Zeit Verhalten hängt von verschiedenen Parametern ab. In Bild 7 sind einige Versuchsresultate nach Parametern geordnet zusammengestellt. Der Einfluss der Dauerlast

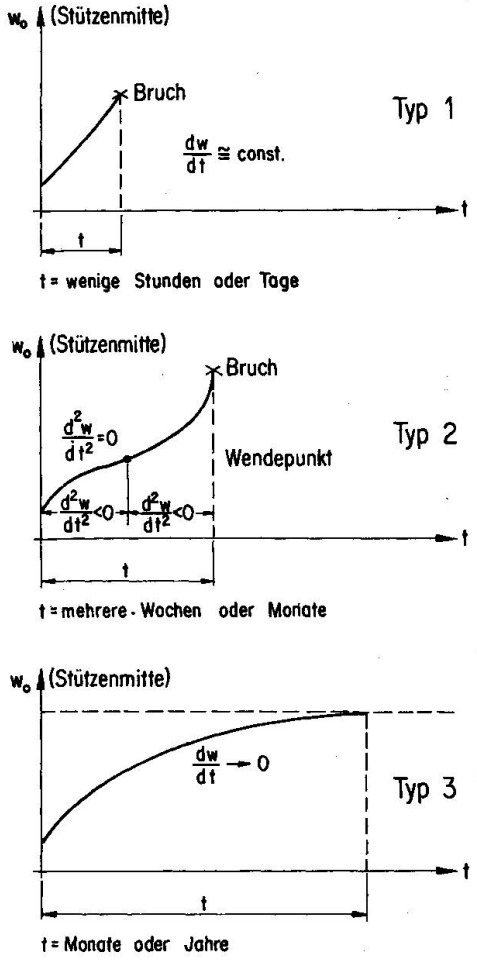

Bild 6: Auslenkung – Zeit Kurventypen

geht aus Bild 7a hervor. Die Exzentrizität e/H, der Armierungsgehalt μ, das Belastungsalter t_o und die Schlankheit λ wurden konstant gehalten. Die Stütze Nr. 12 mit der kleinsten Dauerlast kam nicht zum Bruch, während Stütze Nr. 16 mit höherer Dauerlast schon nach wenigen Tagen versagte.

Aus Bild 7b ist der Einfluss des Armierungsgehaltes ersichtlich. Alle anderen Parameter wurden konstant gehalten. Stütze Nr. 55 mit geringer Druckarmierung ($\mu' = 0.15$ %) versagte schon nach wenigen Stunden Belastungsdauer, während Stütze Nr. 64 mit starker Armierung ($\mu = \mu' = 2.15$ %) nicht zu Bruch kam. Aus diesem Verhalten der Versuchsstützen lässt sich ableiten, dass eine erhebliche Umlagerung der inneren Kräfte infolge des zeitlich bedingten Kriechens des Betons stattfinden muss. Durch Aenderung des Stahlquerschnittes wird die Aufnahmekapazität für Umlagerungskräfte und damit das Verformungs- und Tragverhalten einer Stütze entsprechend beeinflusst.

Bild 7c zeigt den Einfluss des Belastungsalters auf das Verformungsverhalten von Stahlbetonstützen. Es sind drei Auslenkungskurven gegeben, die zu Stützen gehören, die sich nur im Alter bei Belastungsbeginn voneinander unterscheiden. Die Stütze Nr. 54, die 16 Tage nach der Herstellung belastet wurde, versagte nach 26 Tagen, während die Stützen, die nach 28 Tagen bezw. 56 Tagen belastet wurden, nicht zum Bruch kamen.

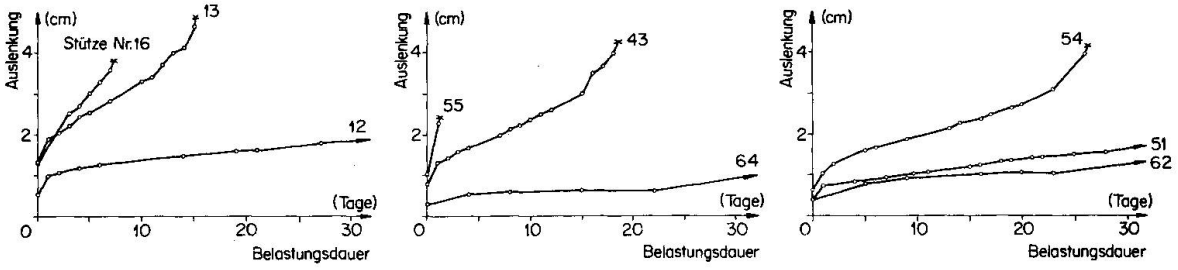

Stütze Nr.	16	13	12
P_D (t)	33,0	31,1	23,4
e/H	0,1		
μ, μ' (%)	0,84		
t_o (Tage)	28		
λ	100		

a) Einfluss der Belastung P_D

Stütze Nr.	55	43	64
P_D (t)	44		
e/H	0,033		
μ, μ' (%)	0,84/0,15	0,84	2,15
t_o (Tage)	28		
λ	100		

b) Einfluss des Armierungsgehaltes μ, μ'

Stütze Nr.	54	51	62
P_D (t)	44		
e/H	0,033		
μ, μ' (%)	0,84		
t_o (Tage)	16	28	56
λ	100		

c) Einfluss des Belastungsalters t_o

Bild 7: Gemessene Auslenkung – Zeit Kurven

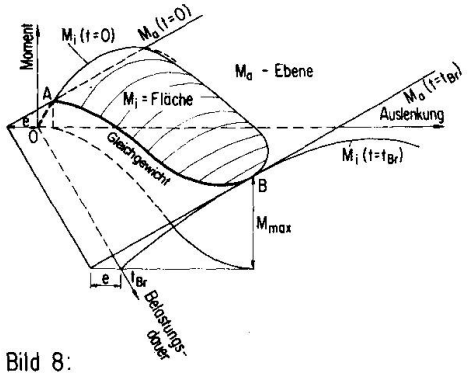

Bild 8:
Gleichgewichtslagen einer Stütze im Langzeitversuch

Mit den Kriechverformungen nehmen auch die Momente zu, die wiederum grössere elastische Auslenkungen zur Folge haben. Bild 8 zeigt in graphischer Darstellung das Verhalten einer Stütze bis zum Bruch im Langzeitversuch. Die Abhängigkeit der Momente M von der Auslenkung w ist in Funktion der Zeit t gezeigt. Der aus den inneren Spannungen berechnete Biegewiderstand M_i des Querschnittes ist abhängig von der Dauerlast P_D und der Belastungsdauer t. Das äussere Moment $M_a = P_D\,(e+w)$ ist linear abhängig von der Auslenkung w und stellt sich daher als Ebene dar. Die Durchdringungslinie der M_a - Ebene durch die M_i - Fläche ($M_a = M_i$) ergibt die Gleichgewichtslagen der Stütze. Punkt A stellt die Gleichgewichtslage unmittelbar nach der Belastung dar. Sie ist stabil, da die Zunahme des inneren Widerstandes dM_i/dw grösser ist als diejenige des äusseren Momentes dM_a/dw. Bei B ist die Stütze im labilen Gleichgewicht. Jede weitere Zunahme der Auslenkung und damit des äusseren Momentes führt zum Bruch. Die exzentrisch belastete Stütze versagt immer vor dem Erreichen des maximalen Biegewiderstandes. Das Verhältnis von maximal erreichbarem Moment M_{max} zum maximalen Biegewiderstand M_u des Querschnittes hängt von der Anfangsexzentrizität e der Last ab. Bei kleiner Exzentrizität e wird die Stütze instabil lange vor Erreichen des maximalen Biegewiderstandes M_u, währenddem für grosse Exzentrizität e der Querschnittswiderstand eher erreicht wird.

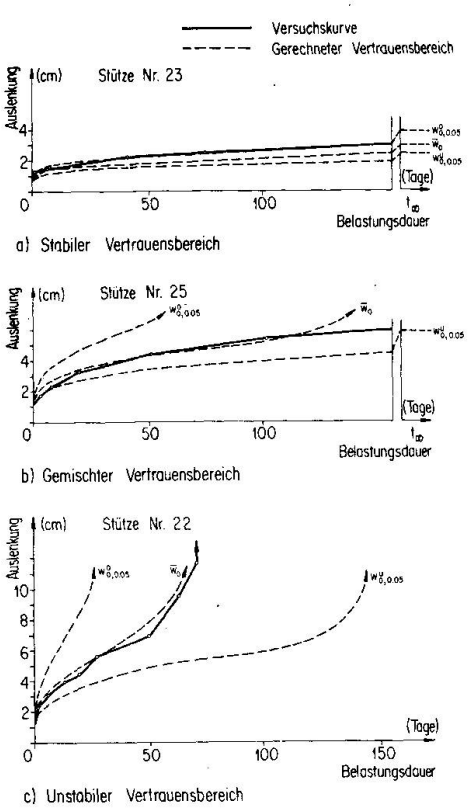

Bild 9 : Vertrauensbereich und gemessene Auslenkung – Zeit Kurven

Vertrauensbereiche für die Stabilität

Jede Berechnung von Tragwerken ist mit Unsicherheitsfaktoren behaftet. Die tatsächlich vorhandenen Lasten, Querschnittswerte und Materialeigenschaften können stark von den nominellen Grössen abweichen, die der Berechnung zugrunde gelegt werden. Schwankungen der Materialeigenschaften und Ungenauigkeiten der Abmessungen können als willkürliche Streuungen betrachtet werden und wurden in [4] mit Hilfe der Wahrscheinlichkeitstheorie statistisch untersucht. Der Einfluss dieser Streuungen auf die Momenten- Krümmungs-Beziehung und damit auf die Biegelinie einer Stütze kann ausschlaggebend werden für das Instabilwerden einer Stütze. Auf Grund der Streuungen der einzelnen Unsicherheitsfaktoren kann ein Vertrauensbereich für die Biegelinie berechnet werden. Bild 9 zeigt drei grundsätzlich verschiedene Vertrauensbereiche, wie sie sich aus der Berechnung zu den durchgeführten Versu-

chen ergaben. Die Wahrscheinlichkeit, dass die Biegelinie einer Versuchsstütze ausserhalb des Vertrauensbereiches liegt, wurde mit 5 % in Rechnung gestellt. Der obere sowie der untere Teil des Vertrauensbereiches für Stütze Nr. 23 (Bild 9a) ist stabil. Die Wahrscheinlichkeit, dass die Stütze stabil bleibt ist grösser als 95 %. Bild 9b zeigt einen gemischten Vertrauensbereich, dessen unterer Teil teilweise stabil und der obere Teil labil ist. Die Wahrscheinlichkeit, dass die Stütze Nr. 25 bis zur Zeit t_∞ stabil bleibt ist weniger als 50 %. Mit einer Wahrscheinlichkeit von mehr als 50 % wird die Stütze nach der Zeit von ca. 50 Tagen oder später instabil. Bild 9c zeigt den Vertrauensbereich für die Versuchsstütze Nr. 22. Sowohl der untere wie der obere Teil ist labil, d.h. in der Zeit zwischen 26 und 150 Tagen Belastungsdauer kommt die Stütze mit einer Wahrscheinlichkeit von 95 % zu Bruch. Die meisten gemessenen Auslenkungskurven lagen innerhalb des berechneten Vertrauensbereiches. Dieses gute Resultat bestätigt einerseits das Vorgehen in der theoretischen Untersuchung und erklärt andererseits die Streuungen der Versuchsresultate. Es wird eindeutig gezeigt, dass es nicht möglich ist, im gemischten Vertrauensbereich der Biegelinien (Bild 9b) eine verbindliche Aussage über die Stabilität der Stütze zu machen auf Grund von Einzelversuchen oder von Berechnungen ohne Berücksichtigung der Streuungen. Bei der Festlegung der Sicherheit gegen Knicken von Stahlbetonstützen müssen neben anderen Faktoren auch die Streuungen der Materialeigenschaften und der Querschnittsabmessungen berücksichtigt werden.

Literaturverzeichnis

[1] Ramu, P. / Grenacher, M. / Baumann, M. / Thürlimann, B.: Versuche an gelenkig gelagerten Stahlbetonstützen unter Dauerlast. Institut für Baustatik, ETH, Zürich, Versuchsbericht Nr. 6418-1

[2] Ramu, P.: Langzeitversuche an Stahlbetonstützen. Schweizerische Bauzeitung, 86. Jahrgang, Heft 13, März 1968

[3] Ramu, P. / Thürlimann, B.: Versuchsanlage zur Prüfung von Stützen unter Dauerlast. Schweizer Archiv 1968, Heft 9

[4] Oelhafen, U.: Formänderungen von Stahlbetonstützen unter exzentrischer Druckkraft. Institut für Baustatik, ETH, Zürich, Dissertation, erscheint 1970.

Bezeichnungen

B	Querschnittsbreite der Versuchsstütze
H	Querschnittshöhe der Versuchsstütze
F_e, F'_e	Querschnitt der Zug-,resp. der Druckarmierung
e	Exzentrizität der Last
w	Auslenkung der Versuchsstütze
w_o	Auslenkung der Versuchsstütze in Stützenmitte
$\bar{w}_o$	Mittlere, theoretische Auslenkung in Stützenmitte
$w^o_{o,0.05}$	Obere Vertrauensgrenze (5 %) für die Auslenkung in Stützenmitte

$w^u_{o,o.o5}$	Untere Vertrauensgrenze (5 %) für die Auslenkung in Stützenmitte
P_D	Mittlere experimentelle Dauerlast
M_a	Aeusseres Moment
M_i	Innerer Biegewiderstand
M_u	Biegewiderstand des Querschnittes
β_{w28}	Würfeldruckfestigkeit nach 28 Tagen
μ	= Fe/BH
μ'	= Fe'/BH
λ	= Schlankheit
t	= Belastungsdauer
t_o	= Belastungsalter der Stütze

ZUSAMMENFASSUNG

Es werden Resultate von Langzeitversuchen an gelenkig gelagerten Stahlbetonstützen erläutert. Speziell wird auf das Problem der diskontinuierlichen Formänderungen und der Risseverteilung über die Stützenlänge hingewiesen. Der Einfluss verschiedener Parameter auf die Auslenkung wird untersucht. Theoretische Vertrauensbereiche für die Biegelinien werden mit Versuchsresultaten verglichen. Es wird gezeigt, dass Unsicherheitsfaktoren bezüglich Materialfestigkeiten und Geometrie einen ausschlaggebenden Einfluss auf das Instabilwerden der Stützen haben können.

SUMMARY

Results of tests on hinged reinforced concrete columns under sustained loads are discussed. Special emphasis is given to the discontinuous change of deformations and the distribution of the cracks over the length of the column. The influence of several parameters on the deflections is investigated. Theoretical limits of confidence for the deflections are compared with test results. It is shown that uncertainties concerning material properties and geometry are very important when considering column stability.

RESUME

On présente quelques résultats d'essais de longue durée effectués sur des piliers à appuis articulés. Il est spécialement fait allusion au problème du comportement discontinu de la déformation et de la répartition des fissures le long du pilier. On examine l'influence sur la déformation de différents paramètres. On compare les résultats des essais avec les limites théoriques de confiance pour les lignes élastiques, et on démontre que les facteurs d'insécurité des proprietés des matériaux et de la géometrie peuvent être déterminants pour l'instabilité des piliers.

II

Magnitude of Creep and Shrinkage for Design of Light-Weight Concrete Structures

Importance du fluage et du retrait pour le calcul des structures en béton léger

Die Größe des Kriechens und Schwindens für die Bemessung von Bauwerken aus Leichtbeton

MASATANE KOKUBU
Professor

HAJIME OKAMURA
Associate Professor

University of Tokyo
Japan

Introduction

The advantage of using artificial light-weight aggregates, which is to decrease the weight of the structural members, is of course significant in structures with long span members, but in many cases it is also very significant in structures where the base ground is of low bearing power. Since large cities in Japan such as Tokyo, Osaka and Yokohama are generally built on weak ground, the use of light-weight aggregate concrete has been intensively studied. For example, light-weight prestressed concrete railway bridges were constructed on two sites of the outskirts of Tokyo, and the result have been economically satisfactorily.[1) 2)] On one site light-weight concrete was used not only in the super structures but also in the rigid frame piers.[1)]

In designing various prestressed concrete structures using light-weight concrete, it is necessary to investigate carefully the magnitude of creep and shrinkage to be considered in the design. Concerning the shrinkage and creep of light-weight aggregate concrete, Tertea et al[3)] and Okada et al[4)] also discussed them in the preliminary publication. The magnitudes of creep and shrinkage to be considered in the design of light-weight concrete structures are naturally dependent on the qualities of the light-weight aggregates, especially on their water absorption, mix proportion and age of concrete and so forth. In addition, the variation of magnitudes of creep and shrinkage due to the difference of the cross sectional dimensions and moisture conditions of a member makes the deduction of the magnitudes considerably complicated. That is, creep and shrinkage strains obtained from laboratory tests with small specimens are apt to differ greatly with those in actual structures.

This report discusses the magnitudes of creep and shrinkage to be considered in designing light-weight concrete structures, based on the results of measurements of laboratory tests specimens and of actual structures.

Measurements of creep and shrinkage in laboratory

Creep and shrinkage strains were measured for two years on concrete using four brands of typical structural light-weight aggregates now marketed in Japan (denoted by X, O, P and R) and the results were discussed comparing them with those of normal weight concrete.[5)]

(a) Concrete

Light-weight fine and coarse aggregates were used in the saturated surface-dry state. The amount of water absorption of aggregates at the time was almost equal to that of the 24 hours' absorption. The specific gravity, fineness modulus and absorption are shown in Table 1. The amount of absorption of the aggregates varied from 3.5% to 17.5% when used according to the brands of the aggregate. Maximum size of coarse aggregates was 15mm.

High early strength portland cement was used in concrete and the water cement ratio was maintained at 0.45. Mix proportions of concrete were determined to yield a concrete of slump about 4 cm and air content about 3% . Compressive strengths of 10 × 20 cm cylinder specimens cured in water of 21°C at the age of 7 days, 28 days and 1 year are shown in Table 2. Strengths of light-weight concrete using river sand as fine aggregate regardless of the difference in coarse aggregates were very similar to that of concrete using river gravel and sand. This tendency is recognized at later ages when the compressive strength reaches 600 kg/cm^2. The reason seems to be that light-weight coarse aggregate particles do not crush until the failure of mortar occurs and that the bond strength between mortar and coarse aggregate particles is larger in light-weight aggregates, than in river aggregates. However the strength of concrete using light-weight aggregate as both coarse and fine aggregates are about 10% less than that of concrete using river aggregates. This seems to be due to the considerably large effect of the quality of fine aggregate particles on the strength of mortar.

(b) Drying shrinkage

Concrete specimens of 10 × 10 × 42 cm were placed in a condition controlled room of 21°C and 60% RH and measurements of shrinkage strain were carried out periodically for 2 years, using contact type strain gages of 20 cm length. The strains shown in Fig. 1 is believed to indicate the shrinkage strains along the axis of specimens, as gage points were embedded deep in concrete and shrinkage strains shown is the mean value of the measured values on two opposite faces.

Normal concrete NN using river coarse and fine aggregates shows rapid increase of shrinkage at early age of drying, the amount of shrinkage for the first 28 days being 490×10^{-6}. On the other hand, Concrete XX using light-weight coarse and fine aggregates with large water absorption shows very small shrinkage at early age of drying, the amount of shrinkage being only 110×10^{-6} for the first 28 days, which is only about 20% of that of normal concrete. Shrinkage strains of light-weight concrete increase during the first 18 months at a constant rate, but the magnitude of shrinkage is still smaller than that of normal concrete. This is due to the difference of water absorption in aggregate particles. Dried concrete absorbs moisture at high humidity, and the degree of absorption is remarkably larger in light-weight concrete. Therefore, in the design of prestressed concrete structures exposed to weather, the magnitude of shrinkage for light-weight concrete may be considerably smaller than for normal concrete.

(c) Effect on properties of light-weight concrete due to drying

Drying shrinkage of light-weight concrete, as a whole, is smaller than that of normal concrete as described in section (b). In general the inner part of light-weight concrete is more wet than normal concrete, therefore the undesirable effect of surface drying is much larger in light-weight concrete. The degree of this effect is not simple, being affected by water absorption of aggregate, mix proportion and age of concrete, dimension of member, drying speed and degree of drying.

Fig. 2 shows a comparison of the compressive strengths of concrete specimens cured in water of 21°C for 7 days and after that dried in a room of 21°C and 60% RH. Compressive strength increases with increase of age for all specimens, but the degree of increase is larger in light-weight concrete. It is believed that this is because the hydration of cement continued by the large amount of water absorbed in light-weight aggregate particles. In usual structures, concrete is not dried as much as in room, being affected by weather and more increase of strength at later ages can be expected for light-weight concrete, than normal concrete.

On the other hand, in tensile and bending strength, adverse effect of drying appears in light-weight concrete. Table 3 shows the results of tensile and bending strength of concrete cured in water for 10 or 8 days and after that dried in a room of 21°C and 50% RH for 20 days and 14 days respectively. Tensile and bending strength of light-weight concrete decrease with drying, and the decrease becomes remarkably large in case of using highly water absorbed aggregates. This is due to the larger moisture gradient between the surface and the inner part of concrete existing in light-weight concrete. It was ascertained by experiments that the strength recovered remarkably if dried concrete was moistened again.

(d) Creep

For environments of the creep tests, three cases, which were a condition controlled room of 21°C and 60% RH, immersion in water of 21°C and natural condition in courtyard were selected. In case of outdoors, specimens of 15 × 15 × 55 cm were used in addition to those of 10 × 10 × 42 cm, since the influence of environment varies with the dimensions of specimens. Specimens were cured in water and stressed at the age of 7 days then placed in the

TABLE 1. PROPERTIES OF AGGREGATES

Type				Specific Gravity	Absorption %	Fineness Modulus
Coarse aggregate	River Gravel		N	2.66	1.1	6.50
	Light-weight aggregate	Expanded Shale	X	1.46	16.1	6.43
		〃	O	1.50	10.5	6.50
		〃	P	1.45	3.9	6.49
		Fly-ash	R	1.55	5.1	6.44
Fine aggregate	River Sand		N	2.63	1.9	3.05
	Light-weight aggregate		X	1.88	17.5	2.84

TABLE 2. PROPERTIES OF CONCRETE

Aggregate		Water Content, kg/m³	Air Content %	Unit Weight, t/m³	Comp. Strength, kg/cm²		
Coarse	Fine				7d	28d	1y
N	N	158	2.7	2.39	402	491	574
P	N	161	3.8	1.90	406	491	570
R	N	160	2.9	1.95	385	479	596
O	N	159	3.2	1.92	408	472	544
X	N	162	2.9	1.92	383	444	556
X	X	178	2.7	1.70	357	439	524

Remarks:
(1) Water cement ratio was 0.45; sand percentage was 40; slump was 4 cm.

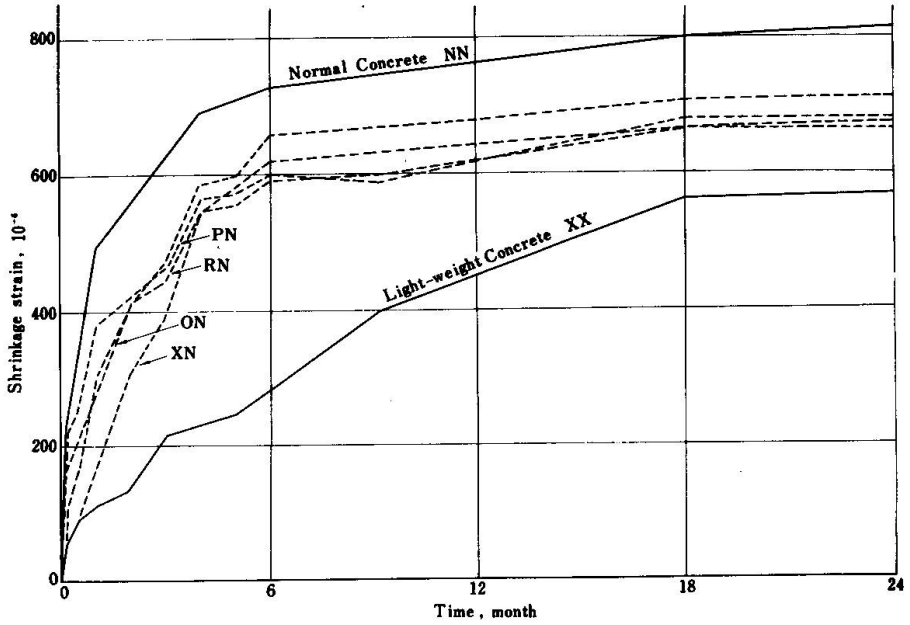

Fig. 1 Shrinkage strain of concrete specimens

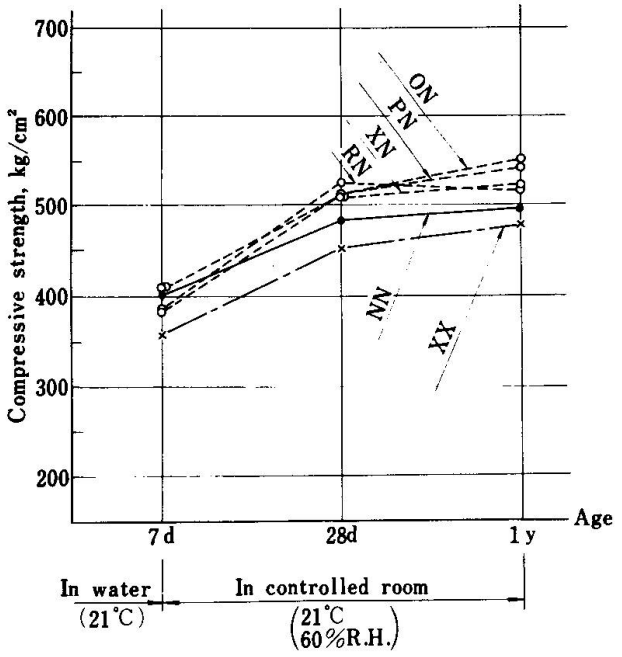

Fig. 2 Compressive strength of concrete specimens

pre-determined environment immediately after stressing. Compressive strengths at the age of 7 days were approximately 400 kg/cm^2. Creep tests by measuring the strain on a total of 60 kinds of specimens consisting of 6 combinations of aggregates, 3 kinds of environmental conditions and 5 levels of stress on concrete; were conducted for 2 years.

The concrete specimen was stressed by stretching a high-tensile steel bar placed through a sheath embedded in the center of section and anchored to anchor plates with ample rigidity at both ends of the specimen. Load applied on concrete was controlled through the measurements of two wire strain gages on the bar. Strains on the surfaces of specimens were measured by contact type strain meter with gage length of 20 cm. In this test method, since the strain of bar decreases as the creep and shrinkage of concrete increases stress of concrete gradualiy decreases with the increase of loading time. Therefore, in order to obtain creep values under constant stress condition from this kind of test, creep per unit stress should be calculated based on such assumptions as that creep is in proportion to applied stress. Accordingly, increase of creep strain per unit stress was assumed to be the quotient of the increment of difference in strain between loaded specimens and that of unloaded specimens divided by the stress at the time. This creep strain increase at loading time was added and the creep per unit stress was determined.

Creep per unit stress of light-weight concrete determined by the aforementioned method are shown in Table 4. When strength and other conditions are similar, creep of various kinds of light-weight concrete is very similar with each other during two years, regardless of the differences of the brands of aggregates. Furthermore, whether in controlled room or in water or in outdoors, large differences were not recognized between typical light-weight aggregate concrete and normal concrete. Creep of specimens in condition controlled room of 60% RH were twice as much as that in water and 1.7 times as much as that in out-doors, that is, effects of environmental conditions on creep of light-weight concrete are very similar to that of normal concrete. The reason of a little larger creep strain of light-weight concrete XX seems to be due to its lower strength.

These resuits indicate that creep phenomenon in concrete with artificial light-weight aggregates is essentially the same as that in normal concrete and influence of the difference in absorption and elastic modulus of aggregates on creep of concrete is negligible. However, creep coefficient of light-weight concrete differs greatly according to the kinds of light-weight aggregates because the elastic modulus of concrete differs greatly according to the different kinds of light-weight aggregates. Therefore, it is not proper that magnitude of creep of light-weight prestressed concrete to be used in design is calculated based on a creep coefficient as in the case of normal concrete, but it may be proper for example to specify a certain creep per unit stress according to the compressive strength of the concrete.

Measurements of creep and shrinkage in an actual bridge

Measurements of delayed deformation in Kanamayam Railway Bridge made of light-weight prestressed concrete girders were conducted by Japanese National Railways. This bridge (completed in 1965) is the first light-weight prestressed concrete bridge in Japan. The bridge has six tracks each of them being composed of three simply-supported post-tensioned prestressed concrete girders, which span length was 15.8 m as shown in Fig. 3.[2] Mix proportion of concrete used in this bridge is shown in Table 5. Compressive strength at 28 days was 565 kg/cm^2, and unit weight was 1.9 t/m^3. Light-weight aggregate was used for the size of coarse aggregate smaller than 10mm, and for 10mm to 20mm crushed stone was used. This was adopted in order to ensure good durability.

Strains were measured by Carlson type strain gages embedded in the middle of web and upper and lower flanges of girders. For comparison, measurements of strain were conducted in normal concrete girders with the same cross sections constructed in parallel to the light-weight girders. The results are shown in Table 6. Total delayed deformations for 200 days in light-weight concrete girders were very small compared to that of normal concrete. Especially during 10 days after prestressing rapid increase of deformations are recognized in the girder of normal concrete. On the other hand, the increase of strain during the same period is not very great in light-weight concrete girders. This seems to be due to the extremely smaller shrinkage of light-weight concrete compared to that of normal concrete, and the points of argument described in the preceding chapter seems to be conformed by the case of the actual bridge. However, the number of measured data in actual bridges are so few that more data of measurements of creep and shrinkage in actual light-weight prestressed concrete bridges are still desired hereafter.

TABLE 3. EFFECTS OF DRYING ON TENSILE AND FLEXURAL STRENGTH OF LIGHT-WEIGHT CONCRETE

Coarse Aggregate[2]		Tens. Strength, kg/cm²		F_{td}/F_{tw}	Flex. Strength, kg/cm²		F_{bd}/F_{bw}
		F_{tw}[3]	F_{td}[4]		F_{bw}[5]	F_{bd}[6]	
River gravel	N	34.6	35.6	1.03			
Light-weight	O	27.2	22.5	0.83	46.8	30.0	0.64
〃	X	25.4	18.6	0.73			

Remarks:
(1) Water cement ratio was 0.50.
(2) River sand was used.
(3) Cured in water for 10 days.
(4) Dried in air for 20 days after 10 days' curing in water.
(5) Cured in water for 8 days.
(6) Dried in air for 14 days after 8 days' curing in water.

TABLE 4. RESULTS OF CREEP TESTS

Condition	Aggregate	Elastic Strain, ε_e, $\times 10^{-6}$/kg/cm²	Creep Strain, ε_c, 10^{-6}/kg/cm²			Ratio of ε_c at 2_y	$\varepsilon_c/\varepsilon_e$ at 2_y
			28d	6m	2_y		
In air (21°C 60%RH)	NN	3.49	4.10	7.22	8.10	1	2.32
	PN	3.61	3.17	5.40	6.75	0.83	1.87
	RN	3.54	3.31	5.53	6.79	0.84	1.92
	ON	4.13	3.11	5.50	6.63	0.82	1.60
	XN	4.29	3.45	5.75	7.03	0.87	1.64
	XX	6.81	4.57	8.08	9.86	1.22	1.45
Out-door	NN	3.54	3.66	5.10	6.40	1	1.80
	PN	3.70	2.61	4.43	5.21	0.81	1.41
	XN	4.82	3.40	5.68	—	—	—
	XX	6.58	3.82	5.90	6.76	1.06	1.03
In water (21°C)	NN	3.58	1.80	3.26	3.45	1	0.96
	PN	3.60	1.37	2.48	2.84	0.82	0.79
	XN	4.01	1.61	2.49	3.67	1.06	0.91
	XX	7.01	1.88	3.68	4.32	1.25	0.62

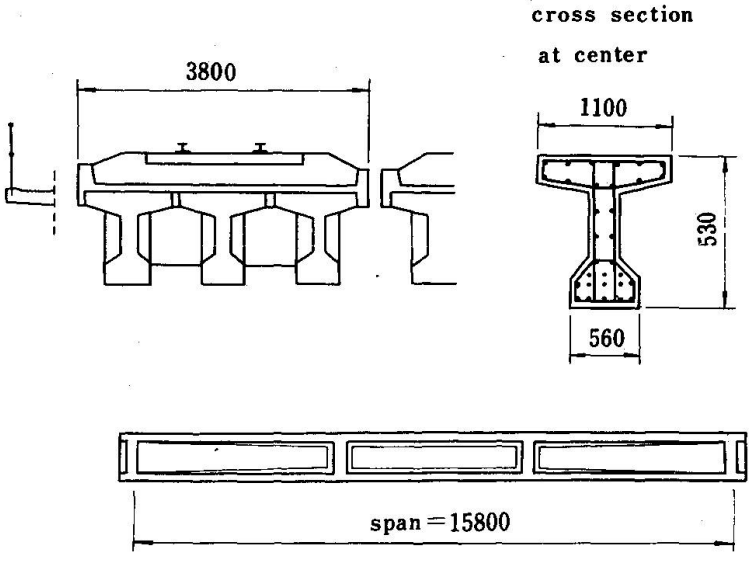

Fig. 3 Sections of Kanayama Railway Bridge

TABLE 5. PROPERTIES OF CONCRETE

Aggregate		Water Content, kg/m³	Air Content, %	Unit Weight, t/m³	Compressive Strength, kg/cm²		
25–10 mm	Under 10mm				3d	7d	28d
N	X	179	4.9	1.92	377	519	565

Remarks:

(1) High early portland cement wasused; water cement ratio was 0.38; sand percentage was 37; slump was 3.5 cm.

TABLE 6. RESULTS OF MEASUREMENT IN KANAYAMA RAILWAY BRIDGE

Measured Position	Concrete	Elastic Strain at Prestressing,(1) 10^{-6}	Delayed Deformation, 10^{-6}		
			28d	6m	2y
Lower flange	Normal	410	390	500	—
	Light-weight	630	100	130	220
Web	Normal	210	210	290	—
	Light-weight	220	80	120	160
Upper flange	Normal	0	130	130	—
	Light-weight	−30	40	100	130

Remarks:

(1) Prestressed at 5 days' age

Conclusion

The following can be said within the limits of the investigations regarding concrete using structural artificial light-weight aggregates now marketed in Japan.

(1) Shrinkage strain along the axis of concrete members made of concrete using light-weight aggregates with high water absorption is extremely smaller than that of normal aggregate concrete. Therefore, magnitude of shrinkage to be considered in design of statically indeterminate structures or prestressed concrete members may be considerably smaller for light-weight concrete.

Concrete used in usual structural members can not dry like small specimens in laboratory. Therefore, undesirable effect of drying on tensile strength of light-weight concrete is quite reduced in actual members, and a little amount of shrinkage reinforcement is enough to cope with the danger of cracking by drying.

(2) Amount of creep strain of light-weight concrete, when the stress and age at loading are the same, were recognized to be almost the same as that of normal concrete with the same compressive strength regardless of the kinds of light-weight aggregates used. However, creep coefficient of light-weight concrete is different according to the kinds of light-weight aggregates because of the large difference of elastic modulus between the kinds of light-weight concrete. Therefore, it is not proper to use a constant creep coefficient regardless of the kind of aggregate used in the design of prestressed concrete. It seems to be a practical method at this stage that a certain creep per unit stress be specified according to the compressive strength of concrete.

It is quite natural that careful investigation should be taken whether or not the above conclusions can be applied to concrete with light-weight aggregate of different quality from those investigated in this experiment. However, the above conclusions seem to be able to be applied to considerably wide range of light-weight concrete, since light-weight aggregates used in this investigation include those with extremely different water absorptions.

Acknowledgements

The authors owe their profound appreciation to the efforts of the many engineers of the Concrete Laboratory of University of Tokyo and the Japanese National Railways who participated in the investigation and research. They are also grateful to Mr. Akira Tada of Onoda Cement Co., Associate Professor Noriaki Nishizawa of Chuo University, and Mr. Sukenobu Momoshima of Kajima Corporation for their valuable assistance in the preparation of the manuscript.

References

1) S. Koike, Y. Takamatsu, N. Miyasaka and Y. Ikeda; "Design and Construction of Arakawa Higashi Elevated Railway Bridge—Construction of Prestressed Concrete Elevated Railway Bridge by Block Method Using Artificial Light-weight Aggregate," Concrete Journal, Vol. 6, No. 6, June 1968, pp. 27–40 (in Japanese).
2) S. Koike; "Application of Light-weight Concrete to Prestressed Concrete Bridges," Civil Construction Engineering, Vol. 3, No. 1, Jan. 1970, pp. 91–97 (in Japanese).
3) I. Terţea, T. Onet and M. Beuran; "Influence of Creep and Shrinkage upon Cracking and Deflection of Lightweight Reinforced Concrete Beams," Preliminary Publication of 1970 IABSE Symposium in Madrid, pp. 125–132.
4) K. Okada, W. Koyanagi and Y. Yoshioka; "Study on the Differential Shrinkage of Composite Prestressed Concrete Beam," Preliminary Publication of 1970 IABSE Symposium in Madrid, pp. 45–54.
5) M. Kokubu, M. Kobayashi, H. Okamura and Y. Yamamoto; "Some Problems on Light-weight Aggregate Concrete," Concrete Library, Japan Soc. Civil Eng., Vol. 24, Oct. 1969, pp. 1–13 (in Japanese).

SUMMARY

Magnitude of creep and shrinkage to be considered in designing light-weight concrete structures is discussed based on the results of measurement in laboratory tests specimens and in actual structures. The results on concrete using artificial light-weight aggregates of good quality are as follows, so long as those produced in Japan are concerned: (1) magnitude of shrinkage can be made smaller than that of normal weight aggregate concrete, (2) creep may have the same magnitude as that of normal weight concrete.

RESUME

On applique les résultats des essais effectués en laboratoire et sur le chantier au calcul des structures en béton léger. On a obtenu les résultats suivants pour l'examen du béton contenant des agrégats légers produits couramment au Japon: (1) le coefficient du retrait peut être inférieur à celui pour le béton normal, (2) celui du fluage peut être égal à celui du béton normal.

ZUSAMMENFASSUNG

Die Grösse des Kriechens und Schwindens, die bei der Bemessung der Bauwerke aus Leichtbeton berücksichtigt werden soll, wird unter Zugrundlegung der Messergebnisse von Laborversuchen und an bestehenden Bauwerken diskutiert. Die Ergebnisse für Beton mit künstlichen Leichtstoffzuschlägen guter Qualität sind die folgenden, sofern die Herstellung in Japan berücksichtigt wird: (1) Das Schwindmass kann gegenüber jenem für Normalbeton verringert und (2) das Kriechmass in der gleichen Grössenordnung wie für Normalbeton gehalten werden.

Leere Seite
Blank page
Page vide

II

Non-Linear Creep in Concrete Columns

Fluage non-linéaire des colonnes en béton armé

Nichtlineares Kriechen in Betonstützen

R.F. WARNER
Australia

The constitutive relation for concrete proposed by Gamble [4] takes into account non-linear effects at high stress, as well as effects of limited creep recovery and varying ambient conditions. Gamble's work is an interesting generalization of the superposition equation,

$$\epsilon_c(t) = \int_{t_o}^{t} c(t, \tau)\, d\sigma(\tau) \qquad (1)$$

Although the integral formulation has proved to be useful in theoretical studies of viscoelastic behaviour, a differential formulation is often found to be convenient when practical calculations have to be made for the analysis of structural behaviour [5] .

Details of a differential equation of state which also takes into account effects of non-linearity, limited creep recovery and time-varying ambient conditions are herein presented. The equation is, essentially, an extension of the well known Dischinger creep equation. It is at present being used by the writer in a study of creep effects in reinforced concrete columns.

A concrete fibre subjected to a stress history σ (t) is considered, and it is assumed that concrete creep is made up of three components,

$$\epsilon_c = \epsilon_d + \epsilon_v + \epsilon_n \qquad (2)$$

The first component, ϵ_d , is time-hardening and non-recoverable and is similar in all essentials to Dischinger creep. The strain rate $\dot{\epsilon}_d$ may thus be expressed as

$$\dot{\epsilon}_d(t) = \epsilon_{el}(t)\,\dot{\varphi}_d(t) = \epsilon_{el}(t)\,[\,\varphi_d^{*} - \varphi_d(t)\,]\,\frac{1}{T_d} \qquad (3)$$

in which $\varphi_d(t)$ is a creep function of the form

$$\varphi_d(t) = \varphi_d^* (1 - e^{-t/T_d}) \qquad (4)$$

The second component, ϵ_v, is non-hardening and recoverable. The strain rate $\dot{\epsilon}_v$ can be expressed as

$$\dot{\epsilon}_v(t) = (\epsilon_v^*(t) - \epsilon_v(t)) \frac{1}{T_v} \qquad (5)$$

in which the end strain $\epsilon_v^*(t)$ is fixed by the instantaneous stress [2], ie

$$\epsilon_v^*(t) = \epsilon_{el}(t)\ \varphi_v^* \qquad (6)$$

Depending on the relative magnitudes of $\epsilon_v^*(t)$ and $\epsilon_v(t)$, $\dot{\epsilon}_v(t)$ can be either positive or negative.

It will be noted that the two terms ϵ_d and ϵ_v are linear with respect to the stress, and that the total end creep value φ_n (obtained from a creep test at constant low level stress, $\varphi_n = \epsilon_c(\infty) / \epsilon_{el}$) is separated into two components which correspond to irrecoverable and recoverable creep, respectively;

$$\varphi_d^* = \alpha_d\ \varphi_n, \qquad \alpha_d < 1{\cdot}0 \qquad (7)$$

$$\varphi_v^* = (1 - \alpha_d)\ \varphi_n \qquad (8)$$

In Eqs. 3 and 5 the time coefficients T_d and T_v have been assumed to be constant. If greater flexibility is desired, these can be allowed to increase gradually with time : $T_d(t)$, $T_v(t)$.

The strain rate of the third creep component, ϵ_n, is assumed to be zero whenever the stress σ is less than a critical value σ_c. For $\sigma > \sigma_c$, a power function of stress is used to evaluate $\dot{\epsilon}_n$. A convenient expression for $\dot{\epsilon}_n$ is

$$\dot{\epsilon}_n(t) = (\dot{\epsilon}_d(t) + \dot{\epsilon}_v(t)) \cdot f(\sigma) \qquad (9)$$

in which

$$\sigma \leq \sigma_c : \quad f(\sigma) = 0$$

$$\sigma_c \leq \sigma \leq \sigma_u : \quad f(\sigma) = \alpha_n \left[\frac{\sigma - \sigma_c}{\sigma_u - \sigma_c} \right]^n \qquad (10)$$

In the above relations σ_u is the ultimate strength of the concrete and α_n and n are open parameters defining the function $f(\sigma)$. Values of α_n and n must be obtained using available test data.

The total creep strain rate at time t thus becomes

$$\dot{\epsilon}_c = (\dot{\epsilon}_d + \dot{\epsilon}_v)(1 + f(\sigma)) \qquad (11)$$

with $\dot{\epsilon}_d$ and $\dot{\epsilon}_v$ and $f(\sigma)$ being given by Eqs. 3, 5, and 10, respectively. An advantage of this incremental formulation is that use has not been made of the superposition principle for stresses in the non-linear range, as is the case in many integral formulations [1]. For practical calculation purposes the above Equations can be written in difference form and used in a finite step-by-step procedure for evaluating structural behaviour.

Although Eq. 11 applies only to the case of time-varying stress under constant ambient conditions, variations in relative humidity, etc., can be taken into account by regarding the "target" values φ_d^* and φ_v^* as time varying functions of the ambient history, rather than constants chosen to suit average conditions. Thus, for a sequence of varying ambient conditions $H_0, H_1, \ldots H_i, \ldots$, one can write in finite form

$$\varphi_d^*(k) = g_d [\alpha_0^d H_0, \alpha_1^d H_1, \ldots \alpha_i^d H_i, \ldots \alpha_i^d H_k] \qquad (12)$$

$$\varphi_v^*(k) = g_v [\alpha_0^v H_0, \alpha_1^v H_1, \ldots \alpha_i^v H_i, \ldots \alpha_k^v H_k] \qquad (13)$$

in which α_i^d and α_i^v are weighting factors representing the relative importance of the i-th stage of the ambient history.

It is interesting to note in passing that the formulation used in Eqs. 12 and 13 can be extended to produce a discrete memory process model in place of the conventional state model, as represented by Eq. 11. Memory functions similar to Eqs. 12 and 13 can be introduced for stress increments, ambient conditions and strains

$$g_\sigma [\alpha_0^\sigma \Delta\sigma_0, \alpha_1^\sigma \Delta\sigma_1, \ldots \alpha_i^\sigma \Delta\sigma_i, \ldots \alpha_k^\sigma \Delta\sigma_k] \qquad (14)$$

$$g_h [\alpha_0^h H_0, \alpha_1^h H_1, \ldots \alpha_i^h H_i, \ldots \alpha_k^h H_k] \qquad (15)$$

$$g_\epsilon [\alpha_0^\epsilon \epsilon_0, \alpha_1^\epsilon \epsilon_1, \ldots \alpha_i^\epsilon \epsilon_i, \ldots \alpha_k^\epsilon \epsilon_k] \qquad (16)$$

and expressions for either the total strain or the strain increment can be developed in terms of the memory functions,

$$\epsilon(k) = G_1 [g_\sigma, g_h, g_\epsilon] \qquad (17)$$

$$\Delta\epsilon(k) = G_2 [g_\sigma, g_h, g_\epsilon] \qquad (18)$$

As pointed out by Gamble and others, conditions in the early stages of the process ($i = 0,1,2$) and in the immediate past ($i = k - 1,\ k - 2$) tend to be of prime importance. Thus, provided repeated cycling of stress and of ambient conditions does not occur, the weighting factors might well be expected to approach zero for $0 << i << k$. If the ambient conditions are assumed to be constant, a suitable choice of weighting factors, together with a simple summation form for G_1, leads to a difference equation which is equivalent to Eq. 1.

Returning to the differential formulation, we note that the total strain rate in the concrete fibre is obtained by adding to $\dot{\epsilon}_c$ the elastic and shrinkage strain rates,

$$\dot{\epsilon} = \dot{\epsilon}_c + \dot{\epsilon}_{el} + \dot{\epsilon}_s \qquad (19)$$

In order to obtain an equation of state involving the total strain rate, Eq. 19 is first differentiated. After substitution and rearrangement one obtains a non-linear second order equation

$$b_2(\sigma)\,\ddot{\sigma} + b_1(\sigma, t)\,\dot{\sigma} + b_0(\sigma, t)\,\sigma + c(\sigma)\,\dot{\sigma}\,\dot{\epsilon} = a_2\,\ddot{\epsilon} + a_1\,\dot{\epsilon} - \epsilon_s^*\,s(t) \qquad (20)$$

in which the coefficients b_1 and b_0 are functions of time, b_2 and c are functions of stress, and a_2 and a_1 are constants. The final term on the right hand side accounts for shrinkage : ϵ_s^* is the end shrinkage strain and s is a known function of time.

When $\sigma < \sigma_c$, Eq. 20 simplifies to a linear equation with time-varying coefficients,

$$\ddot{\sigma} + b_1(t)\,\dot{\sigma} + b_0(t)\,\sigma = a_2\,\ddot{\epsilon} + a_1\,\dot{\epsilon} - \epsilon_s^*\,s(t) \qquad (21)$$

For comparison purposes it is noted that the equation of the standard Burger's body can be expressed as [5]

$$\ddot{\sigma} + c_1\,\dot{\sigma} + c_0\,\sigma = d_2\,\ddot{\epsilon} + d_1\,\dot{\epsilon} \qquad (22)$$

in which the coefficients are constants. Eq. 22 has been described as " the simplest differential constitutive relation capable of describing complex material behaviour " [5].

If now only large values of time t are considered, the coefficient b_1 in Eq. 21 approaches a constant non-zero value, while b_0 and s approach zero, so that

$$\ddot{\sigma} + b_1\,\dot{\sigma} = a_2\,\ddot{\epsilon} + a_1\,\dot{\epsilon} \qquad (23)$$

Integration of Eq. 23 yields the standard equation for a Spring-Kelvin Body system in series

$$\dot{\sigma} + b_1\,\sigma = a_2\,\dot{\epsilon} + a_1\,\epsilon$$

If now α_d is set equal to unity in Eqs. 7 and 8, Eq. 21 reduces to the Dischinger equation

$$\dot{\epsilon} = \frac{\dot{\sigma}}{E} + \dot{\varphi}_d \frac{\sigma}{E} + \dot{\epsilon}_s \qquad (25)$$

which is, of course, frequently used in many practical calculations. The simplifying assumption implied in Eq. 25 is that the component ϵ_v is similar in form to ϵ_d. An alternative simplification has been suggested by Nielsen [6], which has much to recommend it. Nielsen proposes that ϵ_v be regarded, for approximate calculations, as an immediate elastic strain. The strain ϵ_v is thus grouped with ϵ_{el} to give

$$\dot{\epsilon} = \frac{\dot{\sigma}}{E'} + \dot{\varphi}_d \frac{\sigma}{E'} + \dot{\epsilon}_s \qquad (26)$$

in which the effective modulus is $E' = E/(1 + \varphi_v^*)$

It is of interest, finally, to inspect the non-linear character of the creep strain rate in Eq. 11. Typical values which have been used for the coefficients in Eq. 10 are :

$$\alpha_n = 10, \quad n = 3, \quad \sigma_c = 0{\cdot}4\,\sigma_u.$$

At a constant stress level $S = \sigma/\sigma_u = 0{\cdot}7$, these values produce a non-linearity factor of

$$N = 1 + f(\sigma) = 2{\cdot}25$$

which is comparable to the value of 2·0 quoted by Gamble. (A value of $N = 1{\cdot}0$ represents linearity.) At a stress level of $S = 0{\cdot}6$, the non-linearity factor becomes 1·37, which is in fair agreement with data presented by Freudenthal and Roll [3].

At high stress, eg $S = 0{\cdot}85$, Eqs. 9 and 10 predict bounded creep behaviour. This may well be in error. However, until more detailed test data become available for this final creep phase just prior to failure, a more accurate treatment is hardly warranted.

In this respect, it should be noted that a precise treatment of concrete at very high stress will not always necessarily be a prerequisite for an accurate study of creep failure in structural concrete. In preliminary calculations made by the writer for several columns failing under sustained loading, concrete compressive stresses were found to remain surprisingly small, up until a short time before failure. This was caused by the "brakeing" action of the compressive steel reinforcement. The redistribution of compressive force from the concrete to the steel was found, in these calculations, to be more than sufficient to compensate for the natural increase in stress corresponding to increased moments caused by increased deflections. Thus, only when the compressive steel had yielded was there a relatively sudden and significant increase in concrete stress. The nett result was that the concrete was subjected to high stress only in the last, late phase of the loading history. Rather large errors in predicted creep rates in this final, short phase do not affect significantly the predicted life of the element.

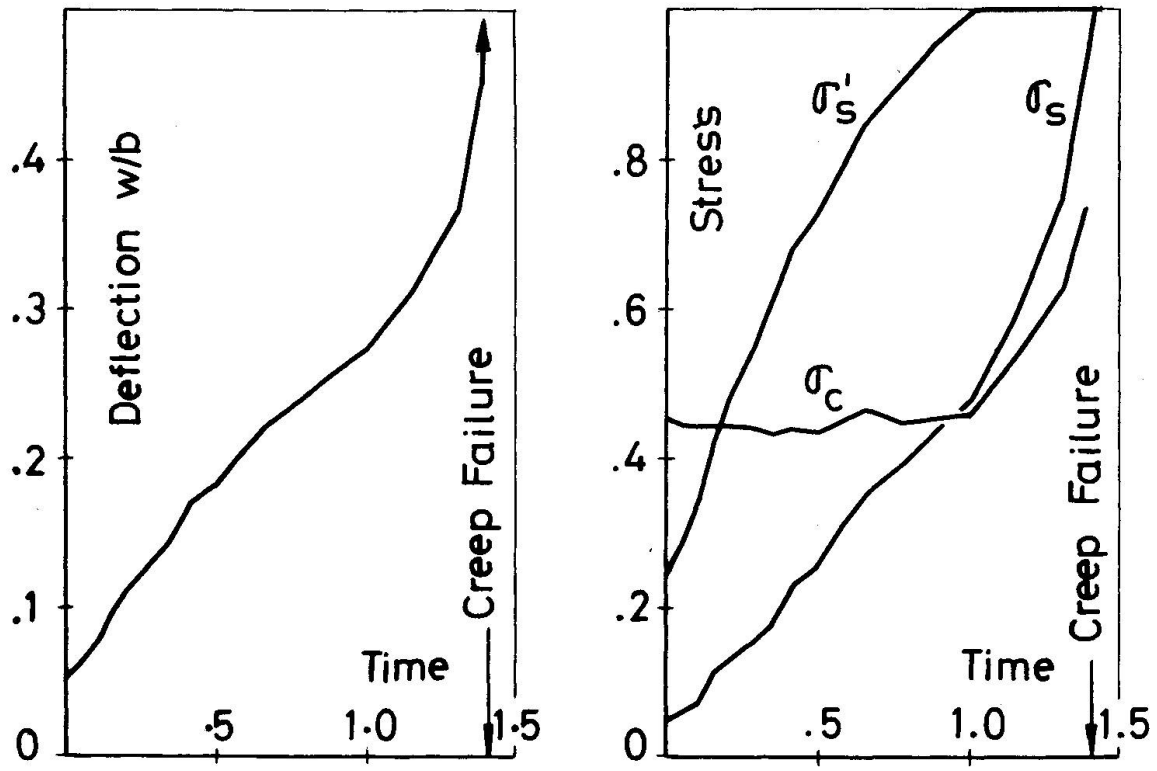

Owing to space limitations, details of the column calculations cannot be given here. However, typical calculated variations in mid-length deflection w, in maximum concrete compressive stress σ_c, and in the tensile steel stress σ_s and compressive steel stress σ'_s are shown in the above Figures for a pin-ended column failing under an eccentric sustained loading. Deflection is plotted as a proportion of the section width b, while stresses are plotted non-dimensionally as proportions of the ultimate or yield stress. The time unit is T_d.

Acknowledgment

The initial phase of this work was carried out in the School of Civil Engineering, University of New South Wales, under the sponsorship of the Building Research Division of the CSIRO.

The auther wishes to express his thanks to the Alexander von Humboldt Foundation for a research stipendium, which has enabled the work to be continued during 1970 at the Institute for Reinforced Concrete Structures, Technical University, Braunschweig.

References

1. Arutyunyan, N. Kh., "Some Problems in the Theory of Creep", Translated by H. E. Nowottny, Pergamon Press, 1966.

2. Flügge, W., "Viscoelasticity", Blaisdell Publishing Co., Waltham, Mass. 1967.

3. Freudenthal, A. M., Roll, F., "Creep and Creep Recovery of Concrete under High Compressive Stress", Journal, American Concrete Institute, Proc. Vol. 54, June 1958.

4. Gamble, Bruce R., "A Constitutive Relationship for Maturing Concrete " Paper 10, Theme I, Preliminary Publication, IABSE Creep Symposium, Madrid, 1970.

5. Lubliner, J., Sackman, J. L., "On Ageing Viscoelastic Materials ", J. Mech. Phys. Solids, Vol. 14, pp 25 - 32, Pergamon Press, 1966.

6. Nielsen, L. Fuglsang, " Effects of Creep in Uncracked Composite Structures of Steel and Concrete ", Bygningsstatiske Meddelelser, Vol. 38, No. 3, 1967.

SUMMARY

A non-linear equation of state for the study of creep failure of reinforced concrete columns is described. Typical variations in concrete and steel stresses with time, up to the instant of failure, are shown for a reinforced concrete column under sustained loading.

RESUME

On décrit une relation non-linéaire pour l'analyse théorique de l'influence du fluage sur la résistance des colonnes en béton armé et on discute des variations caractéristiques des tensions de l'acier et du béton en fonction du temps pour la cas des poteaux soumis à une charge excentrique et permanente.

On donne les variations caractéristiques jusqu'à la ruine des tensions de l'acier et du béton en fonction du temps, pour les colonnes soumises à une charge permanente excentrique.

ZUSAMMENFASSUNG

Ein nicht-lineares Kriechgesetz für die Untersuchung des Versagens von Stahlbetonstützen infolge Kriechens wird beschrieben. Der typische zeitliche Verlauf der Stahl- und Betonspannungen bis zum Zeitpunkt des Bruches wird für eine unter konstanter Dauerlast beanspruchte Stahlbetonstütze dargestellt.